Correlation Sonar Using Pseudo-random Noise Codes

George A. May[1]

George A. May & Associates, Ltd.
R.R. 1, East Sooke Road
Sooke, B.C. V0S 1N0, Canada

Institute of Ocean Sciences
Department of Fisheries and Oceans
Sidney, B.C. V8L 4B2

1983

Canadian Contractor Report of Hydrography and Ocean Sciences No. 14

Fisheries and Oceans Pêches et Océans

Canada

Canadian Contractor Report of Hydrography and Ocean Sciences

These reports are unedited final reports from scientific and technical projects contracted by the Ocean Science and Surveys (OSS) sector of the Department of Fisheries and Oceans.

The contents of the reports are the responsibility of the contractor and do not necessarily reflect the official policies of the Department of Fisheries and Oceans.

If warranted, Contractor Reports may be rewritten for other publications series of the Department, or for publication outside the government.

Contractor Reports are produced regionally but are numbered and indexed nationally. Requests for individual reports will be fulfilled by the issuing establishment listed on the front cover and title page. Out of stock reports will be supplied for a fee by commercial agents.

Regional and headquarters establishments of Ocean Science and Surveys ceased publication of their various report series as of December 1981. A complete listing of these publications and the last number issued under each title are published in the *Canadian Journal of Fisheries and Aquatic Sciences*, Volume 38: Index to Publications 1981. The current series began with Report Number 1 in January 1982.

Rapport canadien des entrepreneurs sur l'hydrographie et les sciences océaniques

Cette série se compose des rapports non publiés réalisés dans le cadre des projets scientifiques et techniques par des entrepreneurs travaillant pour le service des Sciences et Levés océaniques (SLO) du ministère des Pêches et des Océans.

Le contenu des rapports traduit les opinions de l'entrepreneur et ne reflète pas nécessairement la politique officielle du ministère des Pêches et des Océans.

Le cas échéant, certains rapports peuvent être rédigés à nouveau de façon à être publiés dans une autre série du Ministère, ou à l'extérieur du Gouvernement.

Les rapports des entrepreneurs sont produits à l'échelon régional mais sont numérotés et placés dans l'index à l'échelon national. Les demandes de rapports seront satisfaites par l'établissement auteur dont le nom figure sur la couverture et la page de titre. Les rapports épuisés seront fournis contre rétribution par des agents commerciaux.

Les établissements des Sciences et Levés océaniques dans les régions et à l'administration centrale ont cessé de publier leurs diverses séries de rapports depuis décembre 1981. Vous trouverez dans l'index des publications du volume 38 du *Journal canadien des sciences halieutiques et aquatiques*, la liste de ces publications ainsi que le dernier numéro paru dans chaque catégorie. La nouvelle série a commencé avec la publication du Rapport n° 1 en janvier 1982.

CANADIAN CONTRACTOR REPORT OF HYDROGRAPHY AND OCEAN SCIENCES No. 14

1983

CORRELATION SONAR USING PSEUDO-RANDOM NOISE CODES

by

George A. May[1]

[1]George A. May & Associates, Ltd.

R.R.1, East Sooke Road, Sooke, B.C., VOS 1NO, Canada

Institute of Ocean Sciences
Department of Fisheries and Oceans
Sidney, B.C. V8L 4B2

Cat. No. Fs 97-17/14 ISSN 0711-6748

Correct citation for this publication:

May, G.A. 1983. Correlation Sonar Using Pseudo-Random Noise Codes.
Can. Contract. Rep. Hydrogr. Ocean Sci: 14: 134 p.

DISCLAIMER

The work described in this report was done under contract and the contents of the report are the responsibility of the contractor.

CONTENTS

FIGURES (continued)

APPENDICES

ABSTRACT

May, G.A. 1983. Correlation Sonar Using Pseudo-Random Noise Codes. Can. Contract. Rep. Hydrogr. Ocean Sci: 14: 134 p.

This paper consists of an analysis of the use of pseudo random noise codes (PRN) for correlation sonar measurements of velocity in the ocean. Both the problem of back-scatter from the sea-floor and also that of volume-scatter are treated. A theoretical analysis demonstrates the advantages and limitations of the technique for each type of measurement. A new approach to correlation sonar is proposed whereby pulses are "labelled" with a unique PRN code. A succession of such labelled pulses can be used for the correlation calculation thus making available a succession of different correlation lags. The variety of correlation lags takes the place of a variety of spatial separations in the original concept, thus permitting, in principle, the use of only two hydrophones along each axis. Even with more than two hydrophones the labelled pulse approach confers a special advantage by increasing the data set available for calculation of the correlation function. In general, very substantial gains are possible in the signal-to-noise ratio by using the PRN approach whenever environmental noise degrades the return. The advantage diminishes for very strong echoes, but will always produce at least as good a result as the "2 ping" approach in such cases and allows very great improvement for weak returns. Since the signal-to-noise ratio ultimately determines the range of the sonar for given system parameters, the techniques described here are most relevant to the problem of extending the useful range of the sonar. Smearing of the pulse (a finite beam-width effect) and cross-correlation effects both between a pulse and itself and between neighbouring pulses, is also examined. A set of field data has been very thoroughly examined and compared with the theory. Where comparisons are possible, the theory is borne out by the data. In particular, good speed measurements are obtained from bottom echoes using the labelled pulse approach with two transducers. Noise in all but one of the preamplifiers prevented the acquisition of good volume echo returns. However, for the one good channel excellent decoding was obtained from the volume scatter, demonstrating the viability of the PRN approach to correlation measurements in the water column as well as from the bottom echoes.

Key words: correlation, sonar, pseudo random noise codes.

ABSTRACT

May, G.A. 1983. Correlation Sonar Using Pseudo-Random Noise Codes. Can. Contract. Rep. Hydrogr. Ocean Sci: 14: 134 p.

Dans le présent article, on analyse l'utilisation de codes de bruit pseudo-aléatoires (BPA) pour des mesures de vélocité dans l'ocean en se servant de la méthode de corrélation par sonar. On y traite du problème de rétrodiffusion à partir du fond marin de même que de celui de la diffusion. Une analyse théorique démontre les avantages et les limites de la technique pour chaque type de mesure. On propose une nouvelle méthode de corrélation par sonar où les impulsions sont "marquées" à l'aide d'un seul code de BPA. Une série de telles impulsions marquées peut être utilisée pour le calcul des corrélations, ce qui fournirait une série de décalages différents de corrélation. La variété de décalages de corrélation remplace une variété de séparations spatiales dans le concept original, ce qui permet en principe d'utiliser seulement deux hydrophones le long de chaque axe. Même avec plus de deux hydrophones, la méthode des impulsions marquées confère un avantage particulier en accroissant la série de données disponibles pour le calcul de la fonction de corrélation. De façon générale, des gains très appréciables sont possibles dans le rapport signal/bruit lorsqu'on utilise la méthode des BPA chaque fois que le bruit de l'environnement affaiblit l'écho. L'avantage est moindre pour des échos très forts mais, dans ces cas, le résultat sera toujours au moins aussi bon qu'avec la méthode des 2 impulsions et l'amélioration sera très marquée pour des échos faibles. Etant donné que le rapport signal/bruit détermine en dernière analyse la portée du sonar pour certains paramètres du système, les techniques décrites ici sont liées pour la plupart au problème d'étendre la portée utile du sonar. L'étalement de l'impulsion (un effet fini à la largeur du faisceau) et les effets de corrélation croisée à la fois entre une impulsion et cette dernière et entre des impulsions voisines sont également étudiés. On a examiné très soigneusement une série de données recueillies sur le terrain et on les a comparées avec la théorie. Lorsque les comparaisons sont possibles, les données confirment la théorie. En particulier, on obtient de bonnes mesures de vitesse à partir d'échos du fond en utilisant la méthode des impulsions marquées au moyen de deux transducteurs. Le bruit dans tous les préamplificateurs, sauf un, a empêché d'obtenir des retours d'écho suffisamment puissants. Cependant, un excellent décodage a été obtenu à partir de la diffusion pour le seul canal fiable, ce qui démontre la viabilité de la méthode des BPA utilisée pour les mesures de corrélation dans la collonne d'eau de même qu'à partir des échos du fond.

Mots-clés: correlation, sonar, codes de bruit pseudo-aléatoires.

CORRELATION SONAR USING PSEUDO-RANDOM NOISE CODES

Introduction

When attempting to obtain information from deep sea floors, or weak scatterers, or in a noisy environment, signal to noise ratio is the limiting factor. To increase signal to noise ratio (S/N) one can increase the transmitted pulse power and/or the pulse length. However, there is a practical limit to the peak-power a transducer can withstand and to the cost of the transducer and power amplifier. Increasing the pulse length allows more integration time but at the cost of lowered spatial resolution. It is possible to 'sweep' the carrier frequency during the pulse transmission, and have a long transmitted pulse and then to use dispersive receive filters to compress the long pulse to a short spike, thus retaining the time resolution, yet obtaining an improved S/N. Due to the increased integration time the gain in S/N is approximately the compression ratio. This method is known as the 'CHIRP' (SONAR). It is also possible to amplitude or phase modulate a long pulse with Pseudo-Random Noise Codes (PRN), then to use correlation methods to obtain 'correlation gain'; the gain in S/N (amplitude) obtainable is approximately equal to 'N' the number of bits in the PRN sequence. This approach, more versatile and easier to implement than the 'CHIRP' method, will be detailed below.

PROPERTIES OF PRN CODES

Use of Random Binary Sequences

Figure 1 shows a random sequence of '1's and '0's, (i.e. '1' and '0' occur with equal probability and chosen by chance) of length N_S bits. If we define any subsequence length $N_T<N_S$ in the sequence N_S as a 'template' and then form a correlation of the sequence and the template, we get a value of N_T when the template coincides in position with the identical subsequence in the random sequence, whereas for any other position the expected RMS amplitude is $\sim\sqrt{N_T}$. (The definition of correlation in this case is the number of agreements minus the number of disagreements.) Note that any of the

subsequences or more than one of the subsequences may be used as template sequences; each result is a one bit wide correlation peak only at the matching location. From this we see that multiple labelled pulses in effect may be transmitted and the return signals received, i.e. using one template for each pulse. This results in improved signal to noise over a simple two pulse system. Also, this approach permits a simpler version of correlation sonar requiring only three receiving transducers, and with four transducers, gives redundancy, as described in more detail later.

Estimates of S/N for PRN Code Systems and 2-Pulse Systems

S/N Ratio Using Double Pulse

Referring to Figure 2 assume a single pulse of period τ_B is transmitted, and the receiver is range gated at $(t, t + \tau_B)$; this means the beginning of the pulse is scattered in the layer of water from depth $Ct/2$ to $C(t + \tau_B)/2$ and the last part of the pulse from layer depths $C(t - \tau_B)/2$ to $Ct/2$. Most of the return per unit depth is from $Ct/2$ (Figure 3); three-quarters of the return comes from the layer $C(t/2 \pm \tau_B/4)$. It is convenient to think of the returns from a layer $C\tau_B/2$ thick at depth Ct_1.

Consider the double pulse case. The pulses are separated by τ; each pulse width $= \tau_B$. Assume we want the signal from a layer at depth $Ct/2$. Using a range gate of $(t, t + \tau_B)$ for the expected return from the first pulse transmitted. We see the signal returned from the layer $Ct/2$ as before, but in addition, we also see the signal returned from the second pulse transmitted time τ later, and returned from depth $C(t-\tau)/2$. And similarly for the expected signal from the second pulse returned from the same layer, depth $Ct/2$, using a range gate of $(t + \tau, t + \tau + \tau_B)$. In addition to the pulse 2 signal we also see a return from the first pulse from depth $C(t + \tau)/2$. Assuming approximately uniform average return signal amplitude per bit period pulse from the layers is equal to S and the averaged environmental RMS noise amplitude during the pulse period is N_E, then the signal to noise amplitude ratio is given by:

(1) $$(S/N)_{AMPL.} = S/(S^2 + N_E{}^2)^{1/2} = (1 + (N_E/S)^2)^{-1/2}$$

Volume

Referring to Figure 4, a PRN sequence of modulated sound is propagated into the water. The sequence is shown subdivided into T_1, T_2, T_3, as an example. Assume we are interested in the returns from the layer of water at depth A, from the signals resulting from subsequence T_3. The duration of the subsequences are chosen to be 'τ' each and the propagation time to A is t. Thus the required range-gate is $(t, t + \tau)$. During this period we receive signals from layer A of thickness $C/(2N_T) = C\tau_B$, where C is the speed of sound, N_T is the number of bits in the sequence. During this period we also receive signals scattered by other layers and by other parts of the PRN sequence. The total number of layers with the same thickness as A from which the signal is received, is $N_S + N_T$, where N_S is the total number of bits in the sequence (i.e. number of subsequences times number of bits per sequence). Referring to Figure 4, we see the signal contributions resulting from the different layers, for the range-gated period $(t, t + \tau)$. For simplicity the figure shows three subsequences used, $N_T = 7$. The correlation of the received signal with T_2 is the sum of all signal contributions to the i^{th} bit period times the i^{th} bit polarity of template T_2, summed for all $i = 1$ to N_T. Thus the correlation is equal to the sum of correlation of contributions of signal from each layer with T_2. (The starting $[N_T - 1]$ layers and the ending $[N_T - 1]$ layers do not contribute signal during the whole period.) The layer A at depth $Ct/2$ to $C(t + \tau_B)/2$ returns signal which exactly matches the template T_2. Assuming the scattering strength did not change over the period, and the average scattered signal amplitude per bit period is S; then the contribution from this layer is:

(2) Signal amplitude = $N_T S$

Because of the pseudo-random nature of the code and the template, the contributions from the other layers and bit periods to the correlation sum may be regarded as random. Assuming on the average the scattered amplitude per bit period is S, then the RMS amplitude of the contribution from signal scattered from layers other than A is:

(3) $$S(N_S\ N_T)^{1/2} = S\ m^{1/2}\ N_T$$

since $N_S = mN_T$ where m is the number of subsequences.

If the environmental noise contribution per bit period is N_E, then over the correlation period the squared noise amplitude contribution is $N_T N_E^2$; (because of the random nature of the noise and the template).

Summing the noise from the undesired signal returns and the environmental noise we get:

(4) $$\text{RMS noise amplitude} = (m\ N_T^2\ S^2 + N_T\ N_E^2)^{1/2}$$

The signal to noise ratio[1] is then:

(5) $$(S/N)_{AMPL.} = N_T S/(N_T S(m + (N_E/S)^2/N_T)$$
$$= (m + (N_E/S)^2/N_T)^{-1/2})$$

We have used the random nature of the PRN code to derive the above equation. It is possible to derive a more exact answer numerically using the actual PRN code to calculate the noise contributions from the signal scattering. Assuming the average scattering amplitude contribution per bit period per layer is approximately uniform, the total undesirable signal amplitude is:

(6) $$N_{SIG} \approx S(\sum_{j,k} R_{i,j,k} - R_{i,i,o})$$

where i is the template number
j is the subsequence number, $(1, \ldots, m)$
k is the bit shift number , $(0, \ldots, N_T - 1)$,

----

1. We included cross-correlation contributions as noise.

and where R_i, i, 0 is the desired signal from layer A. S is the amplitude of the signal. Subtracting the desired signal from the total signal leaves the undesired part. If the subsequences are linear maximal sequences, the auto correlation properties result in:

$$R_1,i,k = -1 \quad \text{for } k \neq 0;$$

thus these terms do not contribute to the noise fluctuations. Assuming the remainder are random then we get:

$$(7) \qquad S/N_{AMPL.} = (m-1 + (N_E/S)^2/N_T)^{-1/2}$$

Note that we have given the signal to RMS noise amplitude in (7). For signal power to noise power ratio, the result is:

$$(8) \qquad (S/N)_{PWR} = (m-1 + (N_E/S)^2/N_T)^{-1}$$

Interpretation

From equation 1 we see that for the double pulse the effective signal to noise ratio can never be greater than 1, even for a perfect situation with no environmental noise (i.e.$(N_E/S) = 0$). From equation 7 with m = 2, i.e. two subsequences used, (maximal linear code PRN) with $(N_E/S) = 0$, the maximum signal to noise ratio is also 1. However, when (N_E/S) becomes significant, the signal to noise ratio using PRN sequences deteriorates at a much slower rate. (Refer to Figure 5A,B, for graphical plots).

$$(9)\qquad \frac{(S/N)_{AMPL,PRN}}{(S/N)_{AMPL},\ \text{2-PULSE}} = \left[\frac{(m-1 + (N_E/S)^2/N_T)_{-1/2}}{(1 + (N_E/S)^2)}\right]$$

it is easy to see that when $(N_E/S)^2 \gg 1$

Equation (9) $\approx N_T^{1/2}$ For $m = 2$

that is, the signal to noise amplitude ratio is enhanced by $\sqrt{N_T}$ if PRN coding is used in a noisy environment.

When using more than two subsequences, signals may be derived from more than one pair of sequences and the results may be averaged to improve the signal to noise ratio. Thus if K pairs can be used then deriving the signal to noise amplitude ratio as above:

Signal ampl. = $KS\ N_T$

Cross-correlation RMS amplitude = $S\ M_T(K(m-1))^{1/2}$

Environmental noise RMS ampl. = $(KN_T\ N_E{}^2)^{1/2}$

Thus:

$$(10)\quad (S/N)_{AMPL.} = KSN_T/(S^2N_T{}^2(m-1)\ K + KN_T\ N_E{}^2)^{1/2}$$
$$= ((m-1)/K + (N_E/S)^2/KN_T))^{-1/2}$$

For example if $m = 5$ and adjacent subsequence pairs are used, then the available number of pairs for averaging the signal is $K = 4$, equation 10 then gives:

$$(11)\quad (S/N)_{AMPL.} = (1 + (N_E/S)^2/KN_T)^{-1/2}$$

i.e. S/N is not worse if the signal averaging is used, in fact the environmental noise term is reduced by a factor of K.

From the above it is clear that the PRN code approach can obtain usable signals from very weak scatterers or in noisy environments or both, and for the case $N_T = 127$, $m = 2$, it can be $\gtrsim 10$ times better for the same pulse width and resolution. i.e. the power ratio is of order 100 times better than in the two pulse approach.

SIGNAL TO NOISE RATIO CONSIDERATIONS

S/N Single Pulse, Single Scatterer

Assuming the received signal strength over the bit period τ_B is S, and the environmental noise amplitude is N_E, then:

(12) $$(S/N)_{AMPL.} = S/N_E$$

S/N PRN Sequences for Single Target Scattering

Assuming signal amplitude is uniform and equal to S over the period, and the environmental noise amplitude is equal to N_E, then:

(13) $$(S/N)_{AMPL.} = N_T S/(N_T S^2 + N_T N_E^2)^{1/2} = N_T^{1/2}/(1 + (N_E/S)^2)^{1/2}$$

The $N_T S^2$ term results from cross correlation between preceding and following subsequences with the template of the target subsequence, amplitude $= \sqrt{N_T} S$. The $N_T N_E^2$ term results from the correlation of environmental noise with the reference template giving an RMS amplitude of $\sqrt{N_T}\, N_E$. Summing the power and taking the square root we get the expected total noise amplitude. The desired subsequence on the match gives a correlation output amplitude of N_T, thus equation (13). The expected S/N amplitude ratio is plotted in Figure 6.

Bottom Signal Returns

Referring to Figure 7A as the wavefront meets the bottom in the interval dt a ring of width dy reflects the signal. Assuming diffuse scattering the signal returned is proportional to the solid angle subtended by the ring of width dy and radius y. Thus the signal energy returned in time dt is proportional to:

(14) $2\pi y dy \cos\theta / R^2$

$$= dt(dx/dt)(dy/dx)2\pi y/R^2$$

$$= dt(\pi)(C)2D/(D + x)^2 \approx dt(2C/D)\pi \quad \text{For } x \ll D$$

where D is the water depth.

Note that x is small compared to D for small beam widths, thus the expected signal power returned from a flat bottom for diffused scattering from a single pulse is nearly uniform. If the bottom is rugged then the depth fluctuations result in a further broadening of the signal return peak.

Figure 7B shows the wave front of a pulse meeting the bottom and reflecting. The transmitting transducer and receiving transducer combination results in a half beam width of θ. It is clear that signal returns occur during a period of $2x_m/C$ where x_m is the maximum value of x. By geometry we get:

(15) $x_m = D(\sec\theta - 1)$

that is to say the pulse is smeared over this interval.

Bottom Returns S/N Ratio

For a single pulse signal, the effect of bottom smearing results in a widened pulse but still the same S/N.

For the PRN sequence case, if the smearing is over N_{SM} bit periods, then the result is the super-positioning of N_{SM} returned, PRN signal sequences. This, in turn, after correlating with the reference template results in N_{SM} superposed correlated sequences (Figure 7C). The correlation peaks are displaced, so on addition, the amplitude of the peak does not change; however the cross correlation noise surrounding the peak is added, thus the cross correlation noise component amplitude increases by $\sqrt{N_{SM}}$. The resulting signal to noise amplitude ratio is thus:

(16) $$(S/N)_{AMPL.} = N_T S/(N_T N_{SM} S^2 + N_T N_E{}^2)^{1/2}$$

$$= N_T{}^{1/2}(N_{SM} + (N_E/S)^2)^{1/2}$$

Interpretation of S/N Results

(17) For small (N_E/S) the expected S/N amplitude $= \sqrt{N_T/N_{SM}}$

The cross correlation contributions completely determine the S/N ratio. It is also clear the N_{SM} must be small, i.e. the bottom smear must be small for a good S/N ratio since $N_{SM} = 2x_m/C\tau_B$ we must have a small x_m; thus for greater depths, the beam width angle must be smaller. The improved time resolution with PRN results in a finer structure in the signal for correlation even for a smaller beam angle.

For (N_E/S) large:

(18) $$(S/N)_{AMPL.} = (N_T S/N_E)^{1/2}$$

thus the signal to noise ratio is improved by a factor of $\sqrt{N_T}$ for noisy or low signal to noise conditions by using PRN coding in spite of smearing effects.

Numerical estimates of S/N for 1271 ping 4

The environmental noise contribution for this 'ping' is very low, thus the processed signal to noise amplitude is given by equation (17).

(19) $$N_{SM} = 2x_m/C\tau_B = 21.45$$

$$(S/N)_{AMPL.} = (N_T/N_{SM})^{1/2} = 2.43$$

$\theta = 10^0$
$D = 104.3$ meters
$x_m = 1.609$ meters

Thus the expected value is 2.43 but we can also obtain an estimated value from the correlated output of this ping for transducer 1, pattern 1, of 2.57. This is a good estimate, with the uncertainty of bottom type roughness and beam angle. With signal averaging from the five subsequences actually used the S/N ratio should improve by $\sqrt{5}$, the expected S/N is thus ≈ 5.5.

The test condition does not show the advantages of the PRN coding as can be seen in equation (16); the processed signal to noise ratio goes down very slowly resulting in useful signals even in very poor S/N ratio conditions.

Calculation of Bottom and Volume Velocities

The above theoretical analysis showed that PRN coding improves S/N ratio in poor conditions. We now calculate velocity over the bottom and volume velocities with available data.

AVAILABLE DATA (Pseudo random code data) taken on SQUAMISH

Total data collected. Source = CE PHASE 1 REPORT

Tape	Line	Tape Counter	Frequency	Data	Array	Speed	
1062-SE-11 30IPS	I263	1763	102 KHz	volume*1	large	-0 KT	
EOT 1062-SE-11 30IPS	I264	2071	102 KHz	bottom*2	large	-0 KT	
1062-SE-12 30IPS	I271	1569	102 KHz	volume*3	large	1.5 KT est	
EOT 1062-SE-12 30IPS	I272	1830	102 KHz	bottom*4	large	1.5 KT est	
I062-SE-14	I300	1316	102 KHz	volume	small	3 KT est	
I062-SE-14	I301	1707	102 KHz	bottom	small	3 KT est	not available as digitized tape
EOT I062-SE-14	I302	1983	102 KHz	bottom	small	4 KT est	
EOT I062-SE-16 60IPS	I322	1596	102 KHz	?	large useless data	2 KT est	

*1, 2, 3, 4. Based on the window delay and window values given, I263 is volume data, I264 is bottom data, I271 is bottom data, and I272 is volume data. The actual plot of raw data and correlation results confirmed this. (The original specification of bottom and volume is reversed for I271 and I272.)

Digitized Data Available

Line	Window**	Window Delay**	Ping**
I263	250.0 ms	140.0 ms	4
"	"	"	5
"	"	"	6
"	"	"	7
I264	180.0 ms	460.0 ms	4
"	"	"	5
"	"	"	6
"	"	"	7
I271	190.0 ms	490.0 ms	4
"	"	"	5
"	"	"	6
"	"	"	7
I272	300.0 ms	150.0 ms	4
"	"	"	5
"	"	"	6
"	"	"	7

Comments on Data Collected

** Window and window delays are specified with original tape running at 1/4 actual speeds. The numbers given are four times the actual real time value.

Note that data were collected for the large array at 0 knots and at 1.5 knots estimated, whereas data were collected at 3 knots for the small array, just the reverse of the desired state. At 1.5 knots the expected interference pattern merely shifts one transducer spacing of 7.6 cm at the maximum equivalent pulse spacing available of 4 pattern lengths is 50.8ms. Since the decorrelation time for volume scatterers is expected to be 20 ms, correlation is lost at 50 ms and the data are not suitable for volume velocity estimates. The small transducer array data would be useful if available.

EXPERIMENTAL-DATA PROCESSING

Introduction

The signals picked up by six transducers in the transducer array resulting from a P.R.C. amplitude-modulated acoustical pulse ('ping' for short) was recorded on analog tape. The tape was then played back at 1/4 speed, the signal's amplitude detected and the resulting waveforms digitized and stored on digital tape. Four samples per 'bit' period were taken (sample interval = 0.025 ms) and four digitized runs were available. (See table on pages 89 & 90). Briefly:

I264 pings 4,5,6,7 were recorded for bottom signals, platform drifting.

I271 pings 4,5,6,7 were recorded for bottom signals, velocity = '1.5 Kt est.'

I263 pings 4,5,6,7 were recorded for volume signals, platform drifting

I272 pings 4,5,6,7 were recorded for volulme signals, velocity = '1.5 Kt est.'

The quoted speeds were estimated by the field crew and are at best rough approximations.

First Correlations

The digitized signals are raw data. Since five subsequence codes were transmitted sequentially, (M(7,1), M(7,2), M(7,3,2,1), M(7,4,3,2), M(7,6,4,2)) we can derive signal returns from five equivalent 'labelled' pulses by calculating the correlation function of the raw data with each of the five subsequences as templates. As a result we should get five 'patterns' from each transducer for each ping. To calculate the correlation functions we must derive the A.C. component of the raw data, by subtracting a running average of the absolute amplitude over eight bit periods (32 sample points). We use eight bits because the maximum runs of '1's in M7 codes is seven, and maximum runs of '0's are six (bit periods). In the actual correlation calculation, we add or subtract the A.C. signal amplitude to the correlation sum (of a point) if the corresponding point on the template sequence is 1 or 0 respectively, for each point of the template sequence, for one data point on the correlation function. The template is then moved forward by one data point relative to the raw data and the above is repeated for following data points until the range of interest has been covered. The above is repeated for other template sequences for the remaining patterns. The result of the above calculations gives us five patterns, each is the equivalent to the signal returned from an acoustical pulse of duration one bit period, transmitted at the start of each subsequence PRC. The calculations are repeated for each transducer (T_1 to T_6) and each ping (ping 4 to ping 7) and each run.

Observations

The raw data for I264 ping 4,5,6,7, I271 ping 4,5,6,7 transducer 1, and I264 ping 4, I271 ping 4 transducer 4 are shown in Figures I1-D10. Comparing T_1 and T_4 data we note that T_1 data has an oscillatory component which probably originated in the associated preamp-filter. The same problem occurs in all other channels except T_4.

The results of first correlations are shown in Figures I11-I34 and I43-D66. From these figures; for example, Figure I14 (I264, ping 4, T_4), it is clear that signals from 'labelled pulses' may be derived by correlation from the raw data received from a PRC sequence transmission. T_4 signals for all pings and runs give mostly good S/N because of a better preamp-filter. The $(S/N)_{AMPL.}$ is consistent with theory including bottom pulse smearing effect.

Note that pattern 5 for all runs, pings and transducers does not show any signals; this probably resulted from only four instead of the five subsequences being transmitted. All M7 codes were used to test for presence of the fifth subsequence in case some other subsequence than the planned M7 code was used; no signal could be detected. The missing fifth subsequence and consequent absence of signal clearly shows the validity of the signals in the other patterns.

The data values of the patterns go negative as well as the expected positive correlation. This effect can result from amplitude modulated envelope waveform inversion due to the presence of another carrier, close in frequency to the original, adding to and inverting the phase of the original carrier associated with the signal side-bands. (See APPENDIX D.) This new 'carrier' frequency energy can result from local electronic defect, or less probably, mechanical-acoustical coupling of vibrations (noise) or received signal.

Detailed Examinations of Data

Zero Velocity, Bottom Signal. (I264, ping 4,5,6,7)

If the platform is at rest relative to the bottom, the acoustical fringe pattern does not shift relative to the receiving transducer array. Thus successive patterns, the equivalent responses from successive labelled pulses, should be the same. The trisponder data shows that the actual velocity relative to the bottom is about 0.185 m/s slow enough for successive patterns on the same transducers to be nearly the same.

I264, ping 4, (Figures I11-I16)

Transducer 4 gives the best S/N for the reasons given above, and in addition it is not in an acoustical interference null area. We can see the strong resemblance between successive patterns. T_3, T_5 signals are also good but S/N is worse because of the previously mentioned probable preamp-filter problem. T_1, T_6 signal is visible but worse again, due to lower signal strength.

Normalized correlation functions are calculated from pattern 1 with itself and successive patterns over 80 data points bracketing the bottom return pulse peak, for relative shifts of ± 10 data points. (four data points = one bit period Figure I35) The results are shown in Figures I35-I38. As expected from looking at the patterns the correlation is best for T_4 patterns, good for T_2, T_3, T_5, and poor for T_1, T_6. Also of interest is the shape of the normalized correlation functions. For T_4, the zero-crossing of the curves spans approximately 13 points, and the negative excursions are small. For T_2 the span at zero-crossing ~ 7 points, and the negative excursions are much greater. This resulted from the interference present in the preamp-filter and consequent oscillatory signals.

I264, ping 5

Transducer 1 S/N is good, shows strong resemblance from pattern to pattern, and the pattern shows interference effects. S/N decreases for the T_2, T_3 patterns. T_4 still shows a good S/N ratio due to better preamp-filter operation. For T_5 and T_6 the S/N ratio degrades further. Going from T_1 to T_6, the transducer array extends from a stronger signal zone towards a signal null in the acoustical diffraction fringes.

As in ping 4, correlation functions are calculated (Figure I36). The correlation for T_1 signal is very good and as before for this channel we see the effect of interference. The zero-crossing points are ± 4.5 indicating a strong oscillatory component from interference. Correlation peak values drop in T_2, T_3, T_5, T_6 progressively. However the T_4 signal is very good with peak values of $\sim$0.8; this reflects the near absence of interference effect on this channel.

I264, ping 6

(See Figures I23-28, I37, I41.) Good signals are received on transducers 1,2,3,4 and 6. Transducer 5 signals are very poor, possibly due to a combination of interference and being located in a weak signal zone. The T_4 signal is good though it is probably also in a weak signal region, due to reduced interference.

The correlation function curves reflect the above. The T_1 correlation function curve shows high correlation peak values and zero-crossing occurs at $\sim\pm$ 8 data points, probably because the signal strength is high enough to overcome the interference effects. The T_2 and T_3 signals still give good correlation peaks but it is clear that the interference effects are becoming more important; the zero-crossing is $\sim\pm$ 4 data points. For T_4 signals the correlation peak values are high and the zero-crossing is $\sim\pm$ 8 points indicating lower interference effects. No significant correlation is seen in T_5 signals, because of poor signal strength. For T_6 significant correlation is seen and zero-crossing is at $\sim\pm$ 4 data points, indicating interference effects.

I264, ping 7

(See Figures I29-I34, I38, I42.) The low signal zone (null) for this ping appears to be located near T_2, T_3, T_5, which show weak but recognizable signals. Good signals are received on T_1, T_4, T_6. T_4 signals are good because of low interference.

The correlation function curves reflect the relative signal strength and interference; correlation peaks are high for T_1, T_4, T_6. Again the zero-crossing of the curves reflect the significance of the interference.

Summary of I264 Analysis

Because of the low drift velocity of the platform the successive patterns from equivalent labelled pulses clearly show similarities as expected. T_4 signals show the least interference effects, resulting in good signals even in a low signal strength zone. The plotted correlation function curves clearly show the similarities of successive first correlation curves. The zero-crossing of the correlation function occurs at $\pm$ 4 data points for cases where interference is significant and $\pm$ 8 data points for cases where interference effects are negligible.

Improvements in transducer preamp-filter should clear up the interference problems and real time crystal-clock controlled digitization of received data should remove digitization clock error problems such as offset of the correlation peaks, and degradation of the S/N ratio.

'1.5 Kt' estimated Velocity, Bottom Signal, I271, ping 4,5,6,7.

(Figures I43-I66, I67-I71.) The actual platform velocity was determined by a plot of the trisponder data to average 1.272 m/s or 2.47 Kt average. Good bottom returns are seen in pings 4,5 and 6. The signal is very poor for ping 7 for unknown reasons. As expected, the pattern waveform evolves with time since the platform is moving, causing the acoustical platform to move along the array at twice the platform velocity. We can calculate the platform velocity relative to the bottom in two ways; the variable pulse separation method and the spatial correlation method.

Velocity Calculation Using 2 Transducer Variable Pulse Separation Method

In this approach, as the transducer array moves across the acoustical pattern generated by a pulse, a signal is received by the leading transducer; if, during the inter-pulse interval, the second transducer moves to the corresponding position in the acoustical pattern to receive the signal from the second pulse then the same signal pattern is expected on the second transducer (lagging). Thus if a number of labelled pulses are sequentially sent, and we correlate the first pattern received by the first (leading) transducer, with the succeeding patterns received by the second (lagging) transducer, the correlation peak value should reach a maximum at the pulse separation which gives the time required for the pattern to move from transducer 1 to transducer 2. This gives the pattern-velocity which is twice the platform velocity.

For I271, ping 4, four PRN subsequences are actually transmitted (instead of the planned five) and transducer 6 is the leading transducer. Thus for each ping cross-correlation, functions are calculated for signals of adjacent transducers as follows:

$T_2P_1 : T_1P_x$ x = 1,2,3,4,5. (5 not usable)

$T_3P_1 : T_2P_x$

$T_4P_1 : T_3P_x$

$T_5P_1 : T_4P_x$

$T_6P_1 : T_5P_x$

note: the x = 1 cross-correlations are always high because of finite fringe widths of the acoustical pattern. They are therefore not used in the estimate for the correlation peak.

We thus use three data points from each pair of transducers for each ping to estimate the maximum correlation peak location.

Signal Analysis

<u>I271, ping 4</u> (Figures I43-I46) Good patterns occur for T_1, T_2, T_3 and T_4. Successive patterns clearly resemble each other and evolve continuously due to platform motion, but the interference can be seen here as well. The T_4 signals are quite different from the others, as previously described. The peak value of the cross-correlation function between $T_2P_1 : T_1P_x$ shows a peak between x = 3 and 4.

Cross correlation between $T_3P_1 : T_2P_x$ shows similar results. $T_4P_1 : T_3P_x$, and $T_5P_1 : T_4P_x$ cross correlation functions are not usable probably due to the large interference effects (compared to signal strength) causing significant differences in the patterns.

Cross correlation between $T_6P_1 : T_5P_x$ is not as good as the first two and is excluded from the data for velocity calculations.

I271,ping 5 (Figures I49-I54) Good patterns are obtained for T_1, T_2, T_3, T_4, T_5, T_6 as in Ping 4. Cross correlations including T_4 show definite asymmetry, due to the interference problems with the other channels. Cross correlation data including T_4 are therefore not used.

I271, ping 6 (Figures I55-I60) Signals are only fair and for I271, ping 7 signals are poor; this is reflected in the corresponding cross-correlation functions. This data is not included in the velocity calculations.

Platform Velocity Calculations

A parabolic interpolation is used with the sets of three data points. The peak location is calculated as shown in APPENDIX G.

The following set of data points is used to calculate the correlation peak location:

I271, ping 4	y	x (ms)	x max
$T_2P_1 : T_1P_2$	0.7428	12.468	
$: T_1P_3$	0.9477	24.936	30.39
$: T_1P_4$	0.9395	37.404	
$T_3P_1 : T_2P_2$	0.8088	12.468	
$: T_2P_3$	0.8858	24.936	25.11
$: T_2P_4$	0.8129	37.404	
$T_4P_1 : T_3P_2$	0.5636	12.468	
$: T_3P_3$	0.7064	24.936	25.59
$: T_3P_4$	0.5909	37.404	

I271, ping 5		y	x (ms)	x max
T_2P_1	: T_1P_2	0.7501	12.468	
	: T_1P_3	0.9144	24.936	28.593
	: T_1P_4	0.8716	37.404	
T_3P_1	: T_2P_1	0.5791	12.468	
	: T_2P_3	0.7652	24.936	29.434
	: T_2P_4	0.7351	37.404	
T_6P_1	: T_5P_2	0.7302	12.468	
	: T_5P_3	0.8273	24.936	23.94
	: T_5P_4	0.6933	39.404	

where y is the correlation peak value, x is the effective pulse separation in milliseconds and x max is the pulse separation for the maximum correlation peak value.

mean transit time = $\overline{\text{x max}}$ = 27.23 ms

$\therefore$ mean pattern velocity relative to the array

$$= \frac{\text{transducer separation}}{\text{transit time}}$$

$$= \frac{0.0762 \text{ meter}}{0.02723 \text{ sec.}}$$

$$= 2.799 \text{ m/s}$$

$\therefore$platform velocity = 1/2 pattern velocity = 1.399 m/s
(2.72 Kt)

$\sigma v \cong 0.127$ m/s

This is quite different from the ship-board estimate of 1.5 Kt.

The standard deviation for the calculated transit time is 2.47 ms.

$$\frac{\sigma x\ \max}{(\overline{x\ \max})} = \frac{\sigma V}{|\bar{V}|} = 0.0908$$

this gives a measure of the precision of the data, 9%.

The trisponder position data were translated to xy coordinates and plotted and the corresponding velocities calculated.

For I271 the trisponder derived platform velocity was

$V = 1.272$ m/s = 2.47 Kt, $\sigma = 0.238$ m/s

$$\frac{\sigma V}{|\bar{V}|} = 0.187$$

The trisponder data are less precise than the sonar data and the sonar mean velocity value lies within $\sigma/2$ of the trisponder mean velocity.

The above shows that platform velocity relative to the transducer array can be determined using only one pair of transducers with the "variable pulse separation" method being the PRN code sequence. Platform velocity can also be determined using the usual spatial correlation method using one pair of patterns from all the transducers. (Code of patterns represents the signal received from an equivalent labelled pulse) These calculations will be carried out at a later date, perhaps with better data.

Volume Data

I263, pings 4,5,6,7 are recorded with the platform drifting (at 0.18 m/s). The amplifier gains are set high for the expected weak volume signal returns and the signal window was set to include only the volume signal. As before, transducer channels 1,2,3,5,6 give oscillatory raw data due to a probable preamp-filter defect. (Figures I72-I77 show plotted raw data from sample points 500 to 3000.) T_4, as before, is better but the signal amplitude is very low. Because of the expected low level of the signal and the noted interference effect only ping 4 is analyzed in detail to see if volume signal information is present. The first correlation is performed to extract the five patterns from each transducer as before. (Figures I78-I83 show data from range 1250-2250.0 Next, correlations are formed between adjacent patterns over 160 data points (40 bit periods) at ten data point intervals (Figures I84-I89). This gives a set of correlation coefficient profiles, which in theory, since the platform is stationary relative to the water, should be similar. The maximum correlation for volume scattering (without large targets) should be 0.5 if the layer of water is stationary relative to the transducer array. To give a measure of the confidence level of the correlation coefficient profiles, the products of the root mean square amplitude over 160 data points of the adjacent patterns are calculated and plotted (Figures I90-I95). The larger the amplitude the more significant is the corresponding point on the correlation plot (i.e. higher signal amplitudes on both patterns).

(Figures I78-I83) P_5 contains no information; the corresponding RMS product profile is low for the P_4, P_5 correlation profile. This is also true for other transducers.

T_5, and T_6 show roughly similar correlation coefficient profiles, which seem to indicate there is a stationary layer of water relative to the transducer. T_1, P_1P_2 profile also shows a similar region. However, due to the presence of interference in these channels the correlation can be due to the interfering signals. The T_4 channel did not show significant interference with the bottom signal, but with increased gain for volume signal recording there is uncertainty on the stability. The T_4, P_1P_2 profile does show correlation over the water column. T_4, P_2P_3 profile is similar to P_1P_2 for the first half. We can conclude that a volume signal is probably observed but must be verified with better instrumentation and measurements.

<u>I272, pings 4,5,6,7</u> Due to the large transducer spacing and low platform velocity, the pattern shift is not significant before the expected decorrelation time; new data is required.

CONCLUSIONS

The PRN code approach works and labelled pulses are observable; in particular PRN AM modulated acoustical pulses were transmitted and labelled signals recovered using subsequences as templates. Using the labelled pulse effect, two transducer measurements of bottom velocity using variable pulse separation is successful. Back-scattered correlations from targets within the water column are observed for the stationary case but due to instrumentation problems (preamplifier interference), further observations are required to verify the results.

FUTURE WORK

The success of the variable pulse separation approach suggests development of a simple low power four transducer (vector) velocity measuring correlation sonar. (Phase Shift Keying) PSK modulation in theory should give at least three db improvement in (S/N) power and should be tested.

Direct drive of a broad band transducer with PRN code should bring improved performance, eliminate null zones and simplify electronics. This approach requires the availabilty of a broad band transducer; the PVDF piezoelectric plastic transducer is probably suitable.

ACKNOWLEDGEMENT

Thanks are due to Jim Galloway and Jim Mattock for collection of the sonar data, to Don Booth for helpful advice, and to Grace Kamitakahara-King for carry out extensive computations and curve plots, and to Netta Delacretaz for typing my unreadable manuscript and revisions. Finally a very special thanks to Dave Farmer for encouragement in my work and patient help in the editing and preparation of this report. Final word processing, editing and preparation of figures and tables in a form suitable for publication was carried out by Diana Rowles of Copy Right Services.

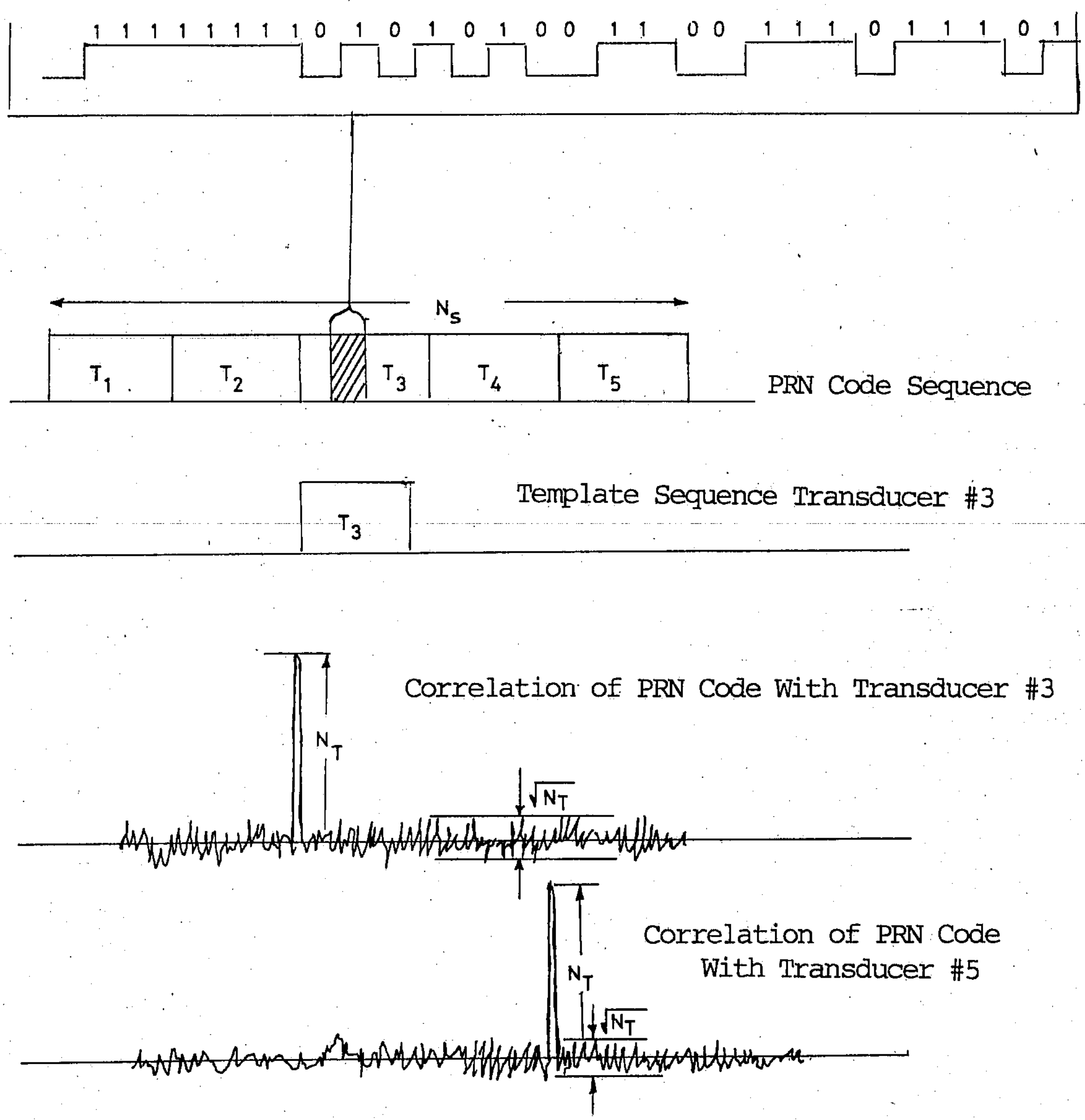

FIGURE 1 CORRELATION PROPERTIES OF PSEUDORANDOM CODE WITH SUBSEQUENCES

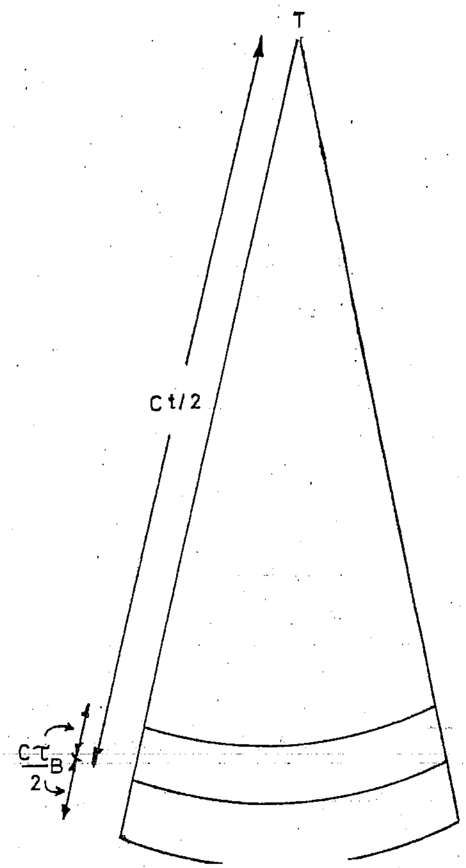

FIGURE 2 VOLUME-SCATTERED SIGNAL FROM SINGLE PULSE WIDTH τ_B RANGE GATED $(T, T + \tau_B)$

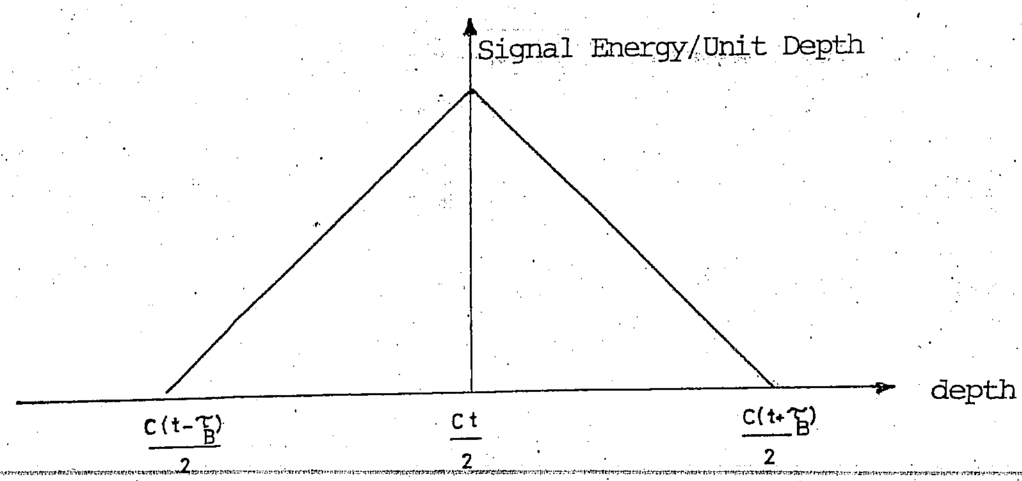

FIGURE 3 SIGNAL-ENERGY CONTRIBUTION INSIDE RANGE GATE $(t, t + \tau_B)$ FROM DIFFERENT DEPTHS

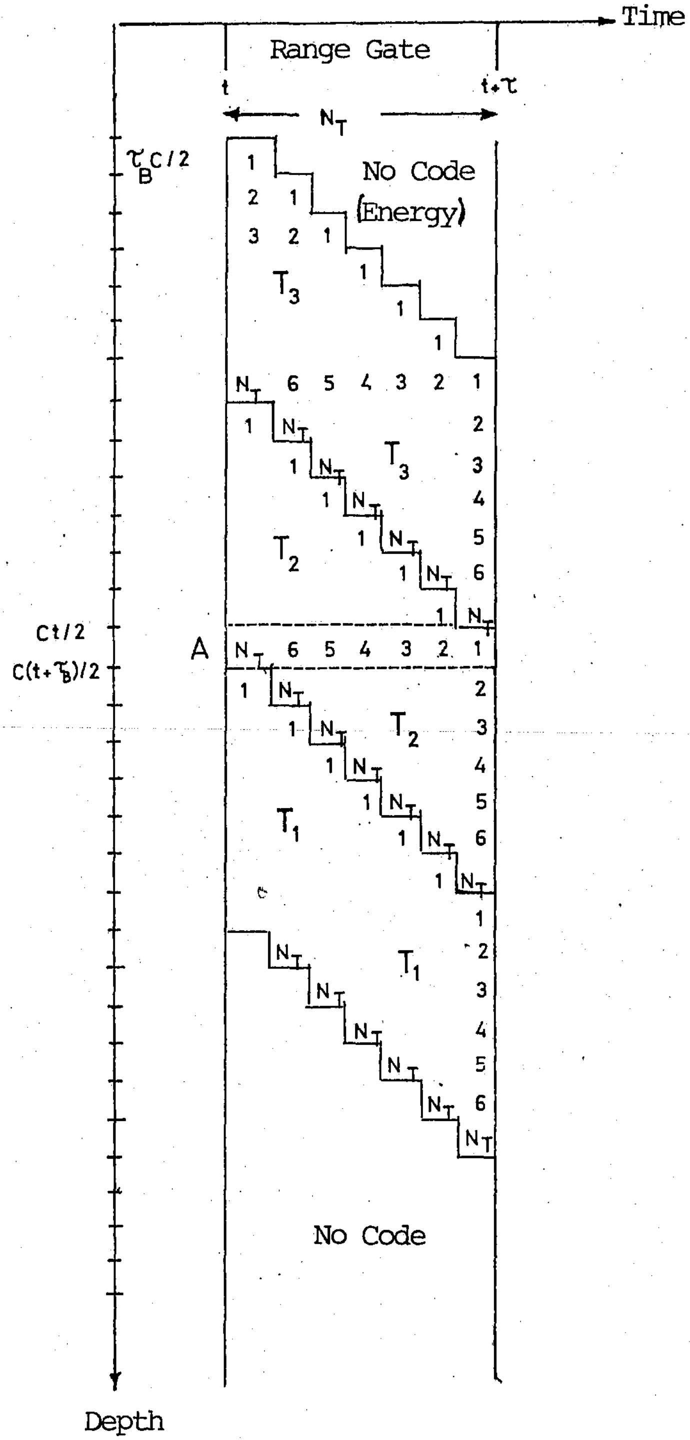

FIGURE 4 VOLUME SIGNAL RETURNED FROM PRN CODE TRANSMISSION

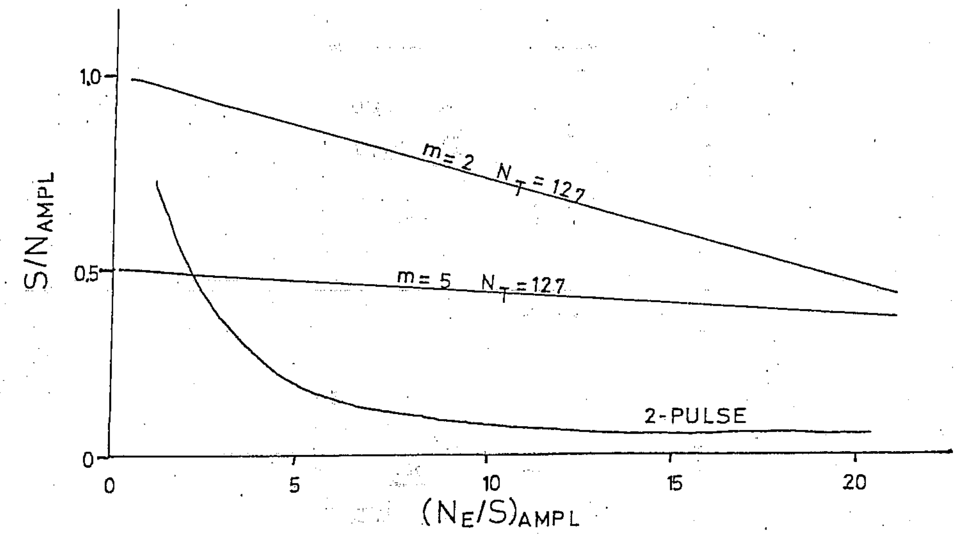

FIGURE 5A EFFECTIVE $(S/N)_{AMPL.}$ VOLUME SIGNAL RETURN

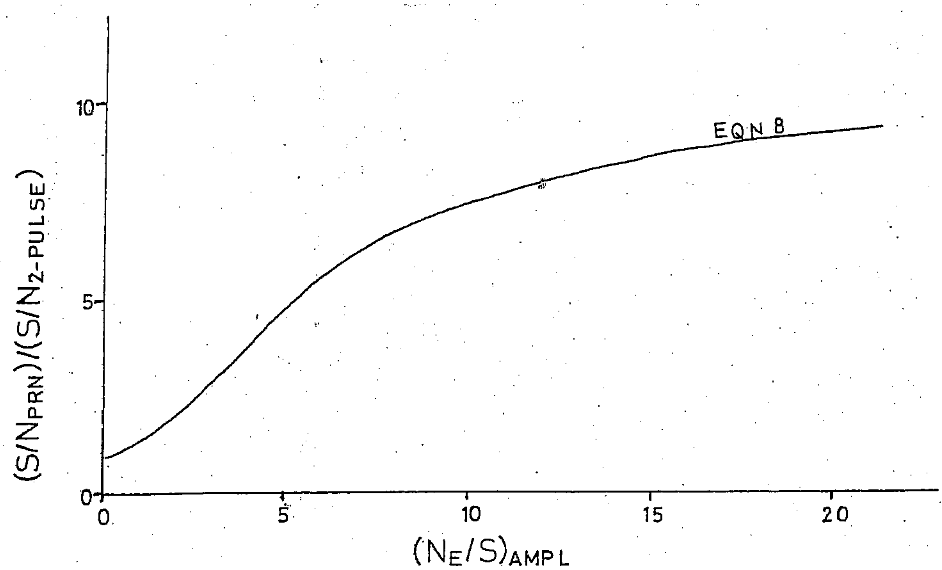

FIGURE 5B $\frac{(S/N)\ PRN\ M = 2\ \ N_T = 127}{(S/N)\ 2\ PULSE}$

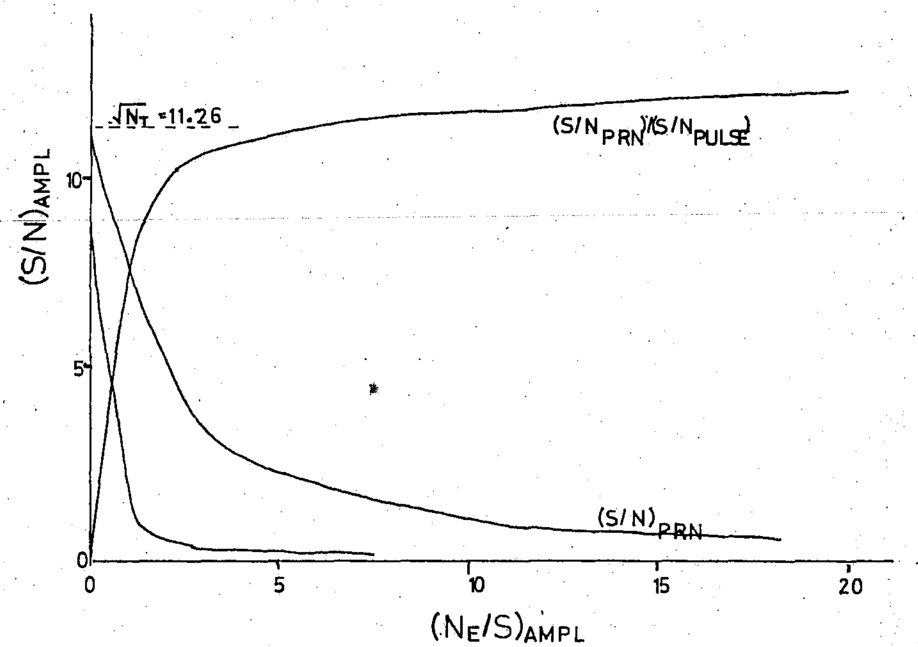

FIGURE 6 (S/N) AMPL. FOR SINGLE TARGET SCATTERING

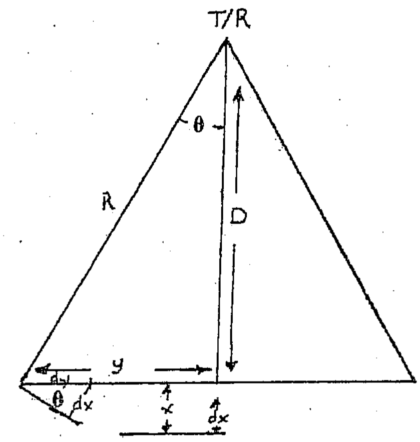

FIGURE 7A PULSE INTERCEPTING SEA BOTTOM

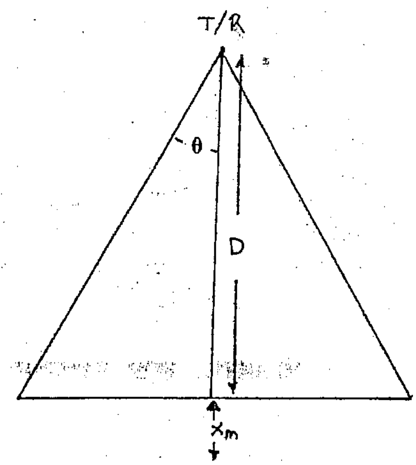

FIGURE 7B BEAM WIDTH LIMIT OF T/R TRANSDUCER COMBINATION

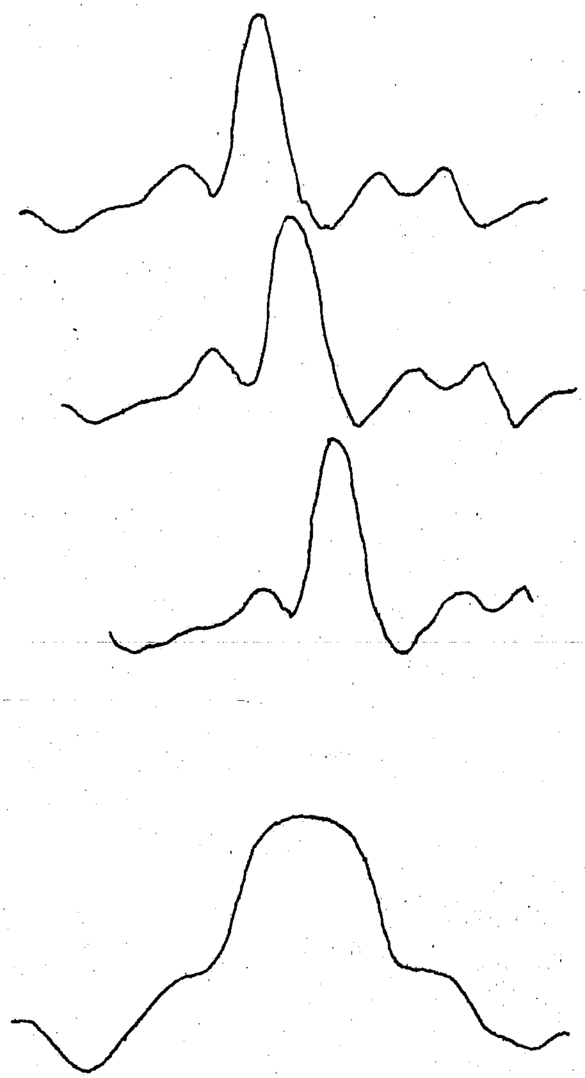

FIGURE 7C BOTTOM PULSE STREAMING EFFECT

APPENDIX A

Math Details of PRN Code Approach

We define a 'BOX CAR' function:

(A.1) $D(t_k,\tau,t) = H(t-t_k) - H(t-t_k-\tau)$

where $H(t-t_k)$ is a Heaviside function = 0 for negative argument and = 1 for positive argument, same for $H(t-t_k-\tau)$.

Assume a 'UNIT AMPLITUDE transmitted pulse width τ is scattered by k point-scatterers, the k^{th} scatterer returning a signal at time t_k, amplitude A_k, then the total response seen at the receiver is given by

(A.2)

$$S_o = \sum_{k=o}^{k} A_k D(t_k,\tau,t)$$

where $t_k = \frac{2R_k}{C}$, R_k = distance to k scatter

A_k = scattering strength from k^{th} scatterer.

When a PRN sequence $B(\ell)$ is transmitted with bit width τ_B, ie. $B(\ell) = 1$ or 0 corresponding to the ℓ^{th} bit of the sequence, the response received is:

(A.3)

$$S_1(t) = \sum_{k+0}^{K} A_k \sum_{\ell=0}^{L} D(t_k + \ell\tau_B,\tau_B,t)\ B(\ell)$$

The A.C. COMPONENT of the RESPONSE is:

(A.4) $$S_2(t) = \sum_{k=0}^{K} A_k \sum_{\ell=0}^{L} D(t_k + \ell\tau_B,\tau_B,t)\ (B(\ell)-1/2)$$

Since $B(\ell)$ is a PSEUDO-random noise code, the average amplitude is 1/2. Removing the average amplitude leaves the A.C. component.

Correlating the response (A.4) with the template $2(B(\ell)-1/2)$

(A.5)
$$C(\tau^*) = \sum_{k=0}^{K} A_K \int_{o}^{L\tau_B} \sum_{\ell=0}^{L} D(t_k+\ell\tau_B, \tau_B, t+\tau^*)(B(\ell)-1/2)$$
$$\sum_{\ell'=0}^{L} D(\ell'\tau_B, \tau_B, t)(B(\ell')-1/2)\, dt$$

τ: is the relative separation from the incoming data and the reference pattern. DEFINING $D^*(t_K,\tau,t)$ as Figure A.O and by algebraic operations detailed in the following pages we get:

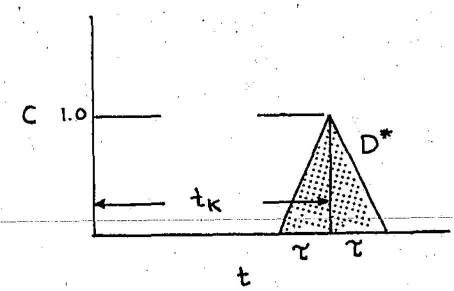

FIGURE AO

(A.6)
$$C(\tau^*) = L \sum_{k=0}^{K} A_k D^*(t_k, \tau_B, \tau^*) + \delta(\tau^*)$$

then equation (A.6) is very similar to equation (A.2). It is in fact equation (A.2) with rise and fall slope limited and equation (A.6) is L times larger.

The term δ is the sum of terms resulting from non-zero partial auto-correlation (correlation noise), and is a function of the code used.

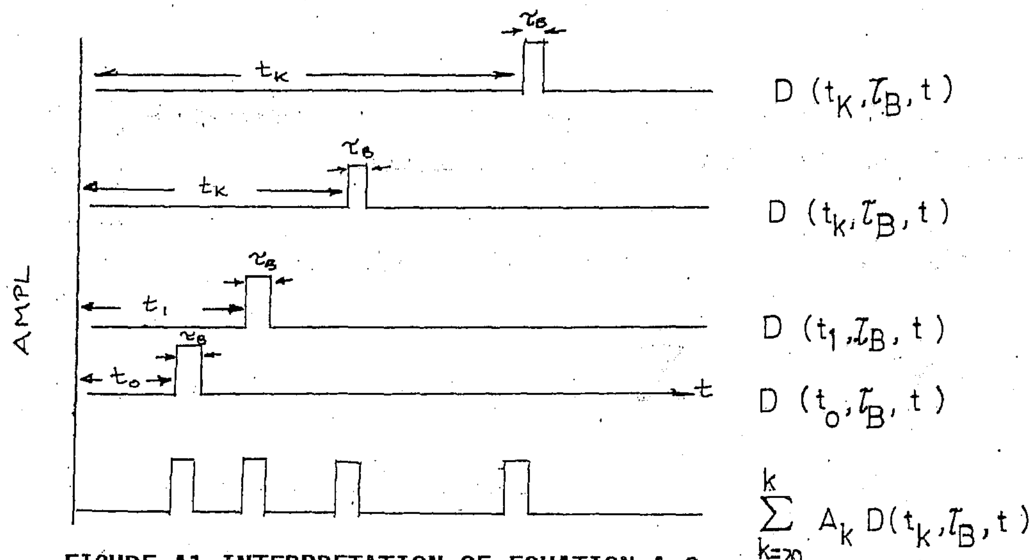

FIGURE A1 INTERPRETATION OF EQUATION A.2

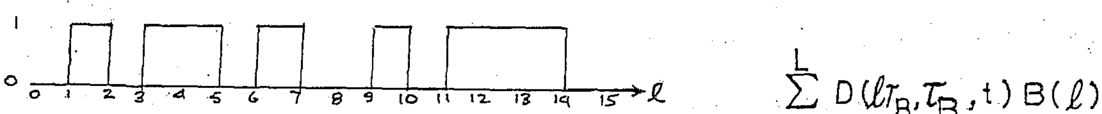

FIGURE A2 INTERPRETATION OF B[ℓ]

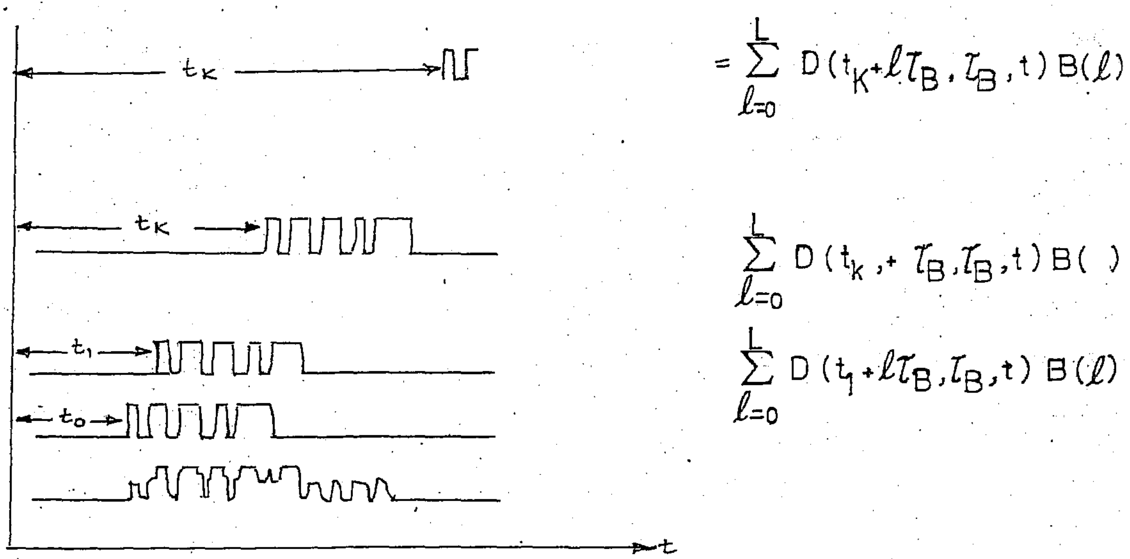

FIGURE A3 INTERPRETATION OF EQUATION A.3

Details of Correlation of PRN Template with Equation (A.4)

Correlation of $S_2(t)$ with PRN template is equivalent to the sum of the correlation of each term of $S_2(t)$ in the summation over k with the PRN template. Thus we first get the correlation of:

(A.7)

$$P(t) = A_k \sum_{\ell=0}^{L} D(t_k + \ell\,\tau_B, \tau_B, t)(B(\ell)-1/2) \text{ SIGNAL TERM}$$

with

(A.8)

$$R(t) = 2 \sum_{\ell'}^{L} D(\ell'\,\tau_B, \tau_B, t)(B(\ell)-1/2) \text{ PRN REFERENCE TEMPLATE}$$

From Figures (A.2) and (A.3) it is evident that for each term we simply have the usual sliding autocorrelation of the PRN code with itself. This results in a maximum at t_k, amplitude = L

FIGURE A4

(A.9)

$$\int_0^{L\tau_B} P(t+\tau)\ R(t)\ dt\ =$$

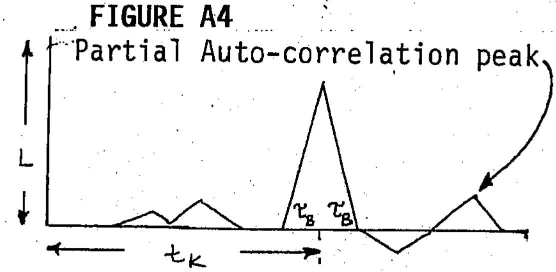

and depending on the code used, different amplitudes for partial autocorrelation peaks. For actual M prime 127 bit codes used (L = 127) false correlation peaks of amplitude $<+ 21, -9$ (for (7, 6, 3, 1) code). This is a worst case. This gives a signal peak power to noise peak power ratio of 36.6 or correlation noise power is 2.7% of peak signal power in the worst case.

NUMERICAL CALCULATION DETAILS

(A-10)
$$C(\tau^*) = \int_0^{L\tau_B} \Big(\sum_{k=0}^{K} A_K \sum_{l=0}^{L} D(t_K + l\tau_B, \tau_B, t+\tau^*)(B(l)-\tfrac{1}{2})\Big(2\sum_{l'=0}^{L} D(l'\tau_B, \tau_B, t)(B(l)-\tfrac{1}{2})\, dt$$

$$= \int_0^{L\tau_B} \Big(\sum_{k=0}^{K} A_K \sum_{l=0}^{L} D(t_K + l\tau_B, \tau_B, t+\tau^*)\, B(l) \cdot \Big(2\sum_{l'=0}^{L} D(l'\tau_B, \tau_B, t)(B(l')-\tfrac{1}{2})\, dt$$

$$= -\frac{1}{2}\int_0^{L\tau_B} \sum_{k=0}^{K} A_K \sum_{l=0}^{L} D(t_K + l\tau_B, \tau_B, t+\tau^*\,) \cdot \Big(2\sum_{l'=0}^{L} D(l'\tau_B, \tau_B, t)(B(l')-\tfrac{1}{2})\, dt$$

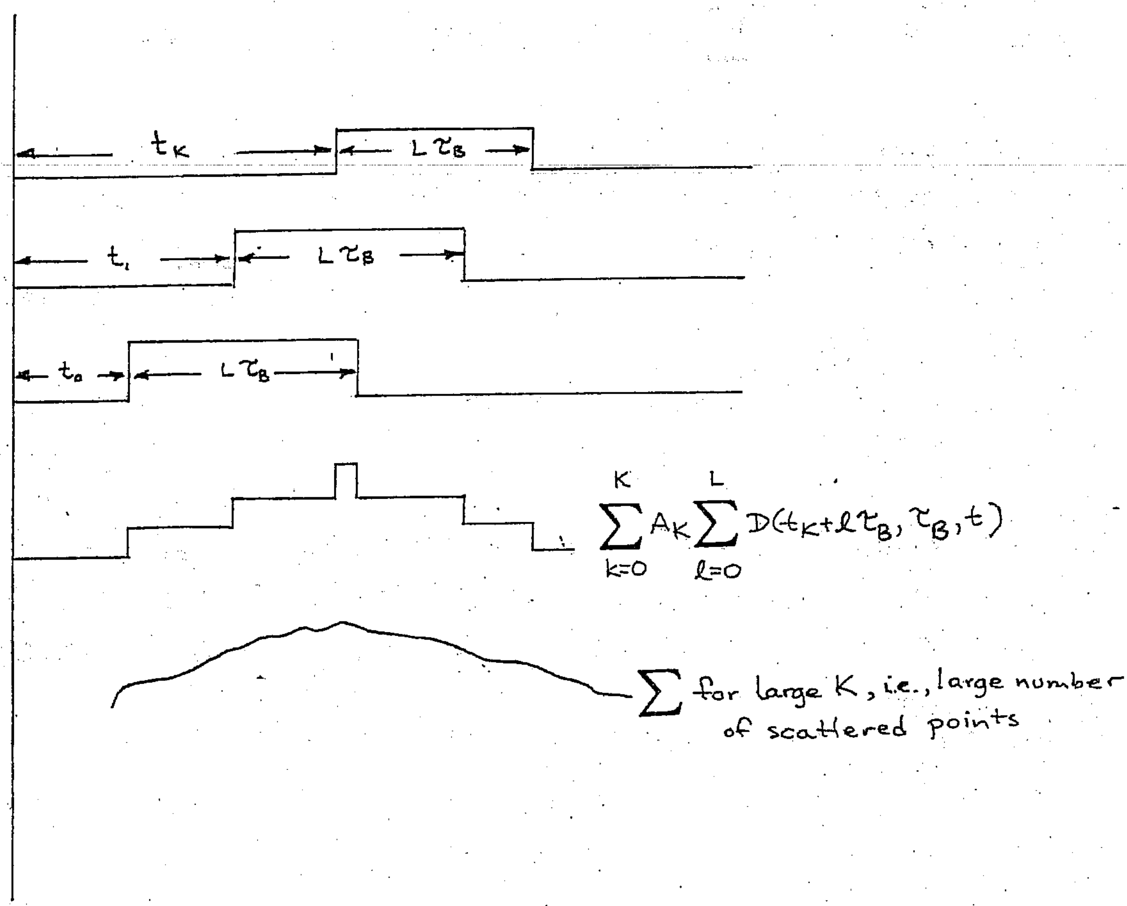

FIGURE A5 INTERPRETATION OF TERM 1A OF EQUATION A.10

Best Estimate for Term (2)A

Term (2)A is the RMS amplitude from the kth scatterer and is not individually available. Since only the sum of all these terms is required, the best estimate is by the 'instantaneous' RMS amplitude.

Discussion

Instantaneous Amplitude

Since the purpose of subtracting 1/2 the instantaneous RMS amplitude is to remove the DC component before the correlation process, for the PRN sequence used, the maximum sequence of '1's are seven and of '0's are six. Thus a good estimate is a running eight bit period average. Term (1)A - (2)A is the AC component of the envelope of the received signal amplitude.

Calculations of (1)A

(1)A is simply our received signal S(t), i.e. equation (A.3). This is the measured or recorded quantity.

Calculation of (1)B or (2)B

These are our PRN code templates which we need for matching. The -1/2 simply shifts the template from (1, 0) to (+1/2, - 1/2), and the factor 2 defines a template with ±1 values.

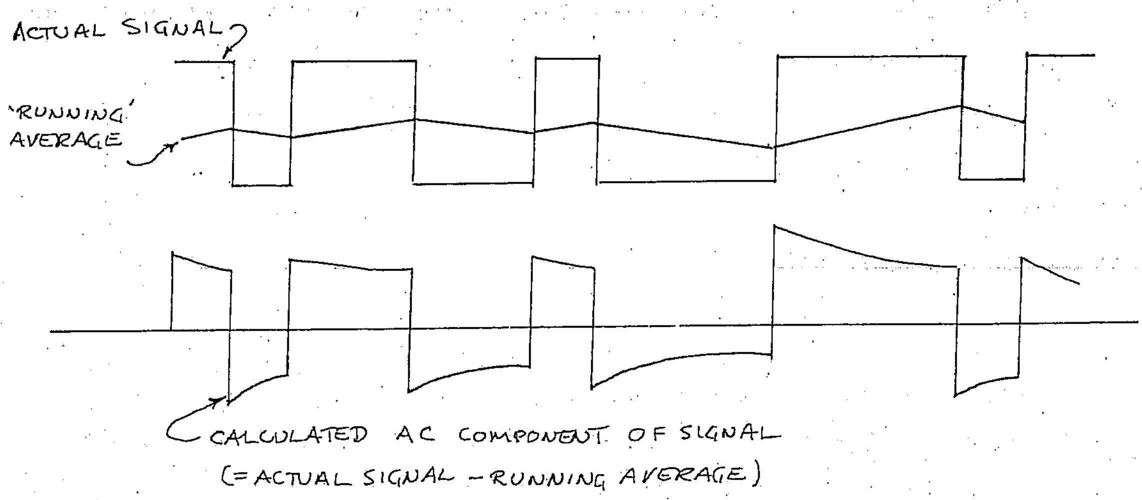

FIGURE A6 DERIVATION OF THE AC COMPONENT OF THE RECEIVED SIGNAL

APPENDIX B

DEPENDENCE OF MAXIMUM CORRELATION COEFFICIENT ON SIGNAL TO NOISE RATIO

Strings of data points x_i, y_i, may be represented by Vectors x, y. Thus the correlation coefficient of two strings of data points may be written as:

(B.1) $R(\vec{x},\vec{y}) = \vec{x}\bullet\vec{y}/|\vec{x}|\bullet|\vec{y}|$

let $\vec{x} = (\vec{S}_1 + \vec{N}_1)$ = Received signal_1 + noise components

$\vec{y} = (\vec{S}_2 + \vec{N}_2)$ = Received signal_2 + noise components

(B.2) $\vec{x}\bullet\vec{y} = \vec{S}_1 \bullet \vec{S}_2 = \vec{N}_1\vec{N}_2 + \vec{S}_1 \bullet \vec{N}_2 + \vec{S}_2 \bullet \vec{N}_1$

(B.3) thus $E(\vec{x}\bullet\vec{y}) = MS^2 = \sqrt{M}(N^2 + SN + SN)$

where M = number of data points correlated

S = average signal amplitude contribution per data point interval.

N = average noise amplitude contribution per data point interval.

$E(\vec{x},\vec{y})$ is the probable value of $\vec{x}\bullet\vec{y}$.

(B.4) and $E|\vec{x}|\bullet|\vec{y}| = MS^2 + MN^2 + 2\sqrt{M}\bullet S\bullet N$

From (B.3) (B.4),

we get the probable value of $R(x,y) = \dfrac{E(\vec{x}\bullet\vec{y})}{E(|\vec{x}|\bullet|\vec{y}|)}$

(B.5) $$= \frac{1 + ((N/S)^2 + (N/S))/\sqrt{M}}{1 + (N/S^2 + 2(N/S)/\sqrt{M}}$$

Two-Pulse Case, Volume-Scattering

For this case it was shown in the main text that the N/S is given by:

(B.6) $$(N/S)_{AMPL.} = (1 + (NE/S)^2)^{1/2}$$

thus for NE = 0, that is, no environmental noise, (N/S) = 1

and we get, using (B.5):

(B.7) $$E(R(\vec{x}\bullet\vec{y})) = \frac{1 + 3/\sqrt{M}}{2 + 2/\sqrt{M}} \approx 0.5 \text{ for } M \gg 1$$

for large (NE/S), (N/S) ≈ (NE/S)

(B.8) $$E(R(\vec{x}\bullet\vec{y})) \approx \left(\frac{S}{NE}\right)^2 + \frac{1}{\sqrt{M}}$$

PRN Code Case, Volume Scattering

For this case it was shown in the main text that the (N/S) is given by:

(B.9) $$(N/S)_{AMPL.} = (m-1 + (NE/S)^2/N_T)^{1/2}$$

for m = 2 (m = number of subsequences with N_T bite each)

and NE = 0

(B.10) $$(N/S) = E(R(\vec{x}.\vec{y})) = 0.5 \text{ for } M \gg 1$$

as in (B.7) for the two-pulse case.

From (B.9) and (B.6) it is obvious that for the PRN case the (N/S) increases much more slowly with increasing (NE/S).

For large (NE/S), $(N/S) \approx (NE/S)/\sqrt{N_T}$

(B.11) $$E(R(\vec{x}.\vec{y})) \approx N_T(S/NE)^2 = 1\sqrt{M}$$

In both cases above with $(S/N) \rightarrow 0$ i.e. insignificant signal, compare to noise

(B.12) $$E(R(\vec{x}.\vec{y})) \approx 1/\sqrt{M},$$

we are left with the purely random fluctuations.

ERROR ESTIMATES of $R(\vec{x}.\vec{y})$

Using (B.7) and (B.12)

$$\Delta = \frac{E(R(\vec{x}.\vec{y}))\ \text{no signal}}{E(R(\vec{x}.\vec{y}))\ \text{ideal signal}} = \frac{1/\sqrt{M}}{\dfrac{1+3/\sqrt{M}}{2+2/\sqrt{M}}} = \frac{2}{\sqrt{M}}\left\{\frac{1+\sqrt{M}}{3+\sqrt{M}}\right\} \qquad \text{(B.13)}$$

for $M = 80$ number of data points used in numerical calculation of correlation coefficients in the present experiment. Thus the number of data points must not be too small or the fluctuations can be a significant portion of the result, and fluctuation can be confused with signal.

$\Delta = 0.186$

APPENDIX C

MAXIMUM USABLE CODE SEQUENCE FOR VOLUME VELOCITY MEASUREMENT

Reference Figure C.1.

We assume a code sequence transmitted by T, scattered at different depths x and received by receivers R. Since the receiver can get the signal only after the transmission is complete, the maximum duration of signal received from a depth x is 2x/c where c is the velocity of sound. This is shown by the line (A) of Figure C.2. Because the echo from the bottom is very strong, it would drown out the signal from volume scattering if simultaneously present. Thus, near the bottom, a shorter usable sequence results; in fact the bottom signal results in 2(D - x)/c length (maximum) of the signal from depth x. This results in a maximum sequence length of D/c for the return from x = D/2. If a code sequence shorter than the maximum is used then the actual length of the code sequence also imposes a limit on the received signal duration. The received signal duration should be maximized because, using correlation methods on the received signal, the processing gain is proportional to the length of the received sequence.

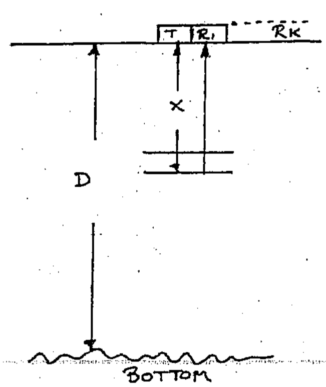

FIGURE C1

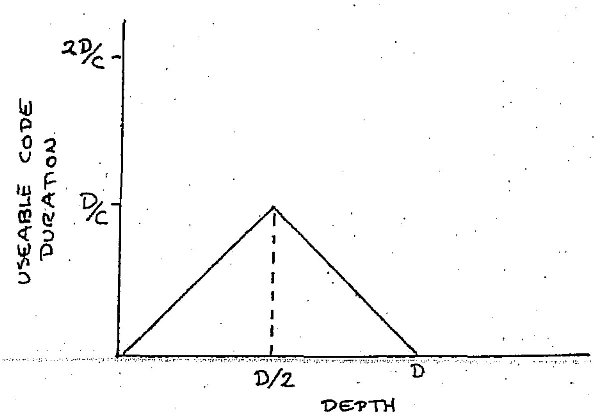

FIGURE C2

APPENDIX D

INTERFERENCE EFFECTS

Envelope Inversion of A.M. Waveforms

In the first correlation calculations, where a template was correlated with the raw signal (the envelope of the received signal), positive as well as negative peaks occur. Theoretically only positive peaks can occur unless the envelope is inverted. The envelope waveform can be inverted if an interfering signal at or near the carrier frequency is present. The following is a simple example:-

Consider a sinusoid modulated carrier given by:

(D.1) $(1 + \cos\omega_A t)\ \sin\omega_c t$

If a carrier of $-2\ \sin\omega_c t$ is added to (D.1)

we get:

(D.2) $+(1 - \cos\omega_A t)\ \sin(-\omega_c t)$

Thus the envelope of the carrier is inverted.

If the interfering signal is near but not at the carrier frequency then a 'beat' signal can occur resulting in periodic envelope inversion, and if the signal is strong, can fade out the desired AM signal.

If the interfering signal is at the carrier frequency, and is continuous, then signals returned at progressively later times will get into and out of phase with the interfering signal, thus the envelopes are periodically inverted at later times, causing periodic negative values in the first correlation results. This phenomenon is actually observed for T_1, T_2, T_3, T_5, T_6 transducer channels, and to a lesser extent in T_4.

APPENDIX E

SOFTWARE CORRECTION OF DIGITIZATION/CORRELATION PROGRAM ERROR

Correlation Sonar Using PRN Codes

Modulation and template matching

In our present AM modulator, bit rate is exactly 1/10 of carrier frequency, ie.e. one bit period is exactly 10 cycles of carrier. When the received signal is demodulated (envelope detected) the analog signal is digitized at four samples per bit period and stored. The template is 127 bits long (and therefore 508 data points, four points per bit), the correlation functions of the template with the received signal is computed to derive the expected correlation gain of 127, and time resolution of one bit period.

Sources of error in program used for computing correlation function

The actual carrier frequency used was 102 KHz, thus the bit rate is 10.2 K Bit/s. The demodulated signal was digitized at ~ 40 KHz, this resulted in less than four sample points per bit. The program used for the computation of the correlation assumed exactly four sample points per bit period, whereas we actually have 3.92 points per bit period. Consequently, over the template period, we have an error of 2.54 bits, or one bit slip every 50 bits. This results in two effects on the correlation output:-

1. Since there is one bit slip every 50 bits, the correlation peak is attenuated and spread out over ~ 2.5 bits, i.e. amplitude is 2.5 times lower and time resolution is 2.5 times worse. The results from only part of the template correlated with the code at any time,l (i.e. 25 bits contribute for every 1/2 bit shift).

2. Since only part of the code is effectively contributing to the correlation at any time the accidental cross-correlation is not as calculated and is probably worse due to the effectively smaller code

length.

The cure is as follows:-

From the signal sampled at 40 KHz derive, by interpolation, the expected signal sampled at 40.8 KHz, i.e. at four samples per bit period. Then calculate correlation function as before.

APPENDIX F

FAST ALGORITHM FOR CORRELATION CALCULATIONS USING MC68000 OR EQUIVALENT

Correlation Calculations Using Log Data

1. A⟶D analog to digital conversion (two alternatives):

   A. analog to linear binary, then use lookup table to convert magnitude to "$LOG_2|X|$" i.e. convert linear value to $\log_2$ value, sign bit stored as most significant bit(MSB).

   B. analog to $\log_2|X|$ in one step. Sign bit stored as MSB e.g. $LOG_2|X| = (L_7, L_6, L_5, L_4, L_3, L_2, L_1, L_0)$

If amplifier is gain-controlled digitally such that $GAIN = 2^N$ where N is the input binary value to the gain control input,

$(N = (N_3, N_2, N_1, N_0)$ for example,

then the data is represented as

$(S, N_3, N_2, N_1, N_0, L_7, L_6, L_5, L_4, L_3, L_2, L_1, L_0)$ S = sign

- 'S' may be placed in bit 15 position in a 16 bit word.
- if less precision is required then an eight bit word may be used: $(S, N_2, N_1, N_0, L_3, L_2, L_1, L_0)$.

2. Correlation calculations

Define: $$C_{ij}(n_0T) = \sum_{n=1}^{M} A_{i,n}\, B_{j\,(n+no)}$$

$$= \sum_{n=1}^{M} SGN_{i,n},\ SGN_{j,n+no}\left[ANTILOG_2\ (LOG_2 A_{i,n} + LOG_2 B_{j,n+no})\right]$$

SGN = sign bit

Procedure in words:

A. obtain ($SGN_{i,n} \log_2 A_{i,n}$), ($SGN_{j},(n+no)\ \log_2 B_{j},(n+no)$) from memory (using indexed addressing) into registers, (auto increment to next n values) use test and clear instruction to test and clear $SGN_{i,n}$, $SGN_{j},(n+no)$, (branch accordingly) SUM $LOG_2 A_{i,n}$,$LOG_2 B_{j,(n+no)}$, and get antilog using the sum as an index register to reference the antilog table.

B. depending on the branch taken on tests of SGNs, if SGNs are the same, add the antilogged value to $\sum$, if different, subtract.

C. repeat for other 'n's until finished.

APPENDIX G

PARABOLIC CURVE FIT WITH THREE DATA POINTS AND LOCATION OF MAXIMA

(G.1) A parabolic curve can be represented by: $y = Ax^2 + Bx + C$

Thus $dy/dx = 2Ax + B$

(G.2) and location of maxima (or minima) is $x\ max = \frac{-B}{2A}$

A set of three data points completely specifies a parabolic curve if the data points are given by (x_1y_1, x_2y_2, x_3y_3) then using (G.1) we get:

(G.3)
$$x_1^2A + x_1B + 1C = y_1$$
$$x_2^2A + x_2B + 1C = y_2$$
$$x_3^2A + x_3B + 1C = y_3$$

Solving the linear equations and using (G.2) we get:

(G.4)
$$x\ max = -1/2\left\{\frac{x_1^2(y_2-y_3) + y_1(x_3^2-x_2^2) + (x_2^2y_3-y_2x_3^2)}{y_1(x_2-x_3) + x_1(x_3-y_2) + (y_2x_3-x_2y_3)}\right\}$$

Numerical Data and Calculation of x Max Using (G.4)

1271 Ping 5

T_2P_1 : T_1P_2 x_1 = 12.468, y_1 = 0.7501
: T_1P_3 x_2 = 24.936, y_2 = 0.9144/x max = 28.593 ms
: T_1P_4 x_3 = 37.404, y_3 = 0.8716

T_3P_1 : T_2P_2 x_1 = 12.468, y_1 = 0.5791
: T_2P_3 x_2 = 24.936, y_2 = 0.7652/x max = 29.434 ms
: T_2P_4 x_3 = 39.404, y_3 = 0.7351

T_6P_1 : T_5P_2 x_1 = 12.468, y_1 = 0.7302
: T_5P_3 x_2 = 24.936, y_2 = 0.8273/x max = 23.940 ms
: T_5P_4 x_3 = 37.404

1271, Ping 4

T_2P_1 : T_1P_2 x_1 = 12.468, y_1 = 0.7428
: T_1P_3 x_2 = 24.936, y_2 = 0.9477/x max = 30.69 ms
: T_1P_4 x_3 = 37.404, y_3 = 0.9395

T_3P_1 : T_2P_2 x_1 = 12.468, y_1 =0.8088
: T_2P_3 x_2 = 24.936, y_2 = 0.8858.x max = 25.11 ms
: T_2P_4 x_3 = 37.404, y_3 = 0.8129

T_4P_1 : T_3P_2 x_1 = 12.468, y_1 = 0.5636
: T_3P_3 x_2 = 24.936, y_2 = 0.7064/x max = 25.59 ms
: T_3P_4 x_3 = 37.404, y_3 = 0.5909

APPENDIX H

TRISPONDER DATA AND VELOCITY CALCULATIONS

Range-range data is used to calculate the x, y, data. The origin is set at the Institute of Ocean Sciences wharf. Coal Point is the second reference point with coordinates x_s = -2595 meters, y_s = 2601.2 meters.

The x, y coordinates are calculated using equations supplied by Jim Galloway:

(H.1) $$L = R_1^2 - R_2^2 + x_s^2 + y_s^2/2y_s$$

(H.2) $$M = x_s/y_s = (-2595/2601)$$

(H.3) $$x = \frac{ML - \left[R_1^2(1 + M^2) - L^2\right]^{1/2}}{1 + M^2}$$

(H.4) $$y = -Mx + L$$

I271 Coordinate sample rate = 10 seconds

Range 1	Range 2	x	y	δ	$\lvert\bar{V}\rvert$
3374 m	4217	-2970.93	-1599.20	11.2	1.20 m/s
3385	4220	-2982.35	-1601.10	10.0	1.00
3395	4229	-2989.19	-1609.59	10.8	1.08
3406	4235	-2998.93	-1614.69	17.0	1.07
3423	4242	-3015.30	-1620.13	13.4*	1.34
3437¶	4256¶	-3024.10	-1633.31	13.4*	1.34
3450	4256	-3039.75	-1631.70	12.0	1.20
3462	4262	-3050.75	-1636.56	16.1	1.61
3478	4272	-3064.31	-1645.14	9.8	0.98
3488	4277	-3073.51	-1649.15		

3511¶	4284¶	-3097.29	-1653.45

δ = distance between successive coordinate points. V = speed.

On plotting the resulting (x, y) two data points appear to be in error; these are marked '¶' in the above tabulation. These points are excluded from the velocity calculations. Because one point is excluded in the middle of the set of coordinate points, the distance between coordinate points shown is half that between the preceding and succeeding cordinate points (marked*).

The mean speed is 1.272 m/s

and the standard deviation is 0.238 m/s for 1271 data.

I263

R_1	R_2	x	y
1922	3605	-1772.64	-908.75
1992	3606	-1772.17	-909.67
1993	3608	-1772.23	-911.73
1992	3609	-1770.75	-912.42
1992	3611	-1769.81	-914.25
1992	3613	-1768.86	-916.08
1991	3615	-1766.90	-917.68
1991	3616	-1766.42	-918.59
1991	3618	-1765.48	-920.42
1991	3620	-1764.52	-922.25
1991	3622	-1763.56	-924.08

APPENDIX I

LIST OF TITLES

I.1 I264 PING # 4 BOTTOM RAW DATA (500-3000) TRANSDUCER # 4

I.2 I264 PING # 4 BOTTOM RAW DATA (500-3000) TRANSDUCER # 1

I.3 I264 PING # 5 BOTTOM RAW DATA (500-3000) TRANSDUCER # 1

I.4 I264 PING # 6 BOTTOM RAW DATA (500-3000) TRANSDUCER # 1

I.5 I264 PING # 7 BOTTOM RAW DATA (500-3000) TRANSDUCER # 1

I.6 I264 PING # 4 BOTTOM RAW DATA (500-3000) TRANSDUCER # 4

I.7 I264 PING # 4 BOTTOM RAW DATA (500-3000) TRANSDUCER # 1

I.8 I264 PING # 5 BOTTOM RAW DATA (500-3000) TRANSDUCER # 1

I.9 I264 PING # 6 BOTTOM RAW DATA (500-3000) TRANSDUCER # 1

I.10 I264 PING # 7 BOTTOM RAW DATA (500-3000) TRANSDUCER # 1

I.11 I264 PING # 4 BOTTOM DATA TRANSDUCER # 1 CONSTANT = 1.0164

I.12 I264 PING # 4 BOTTOM DATA TRANSDUCER # 2 CONSTANT = 1.0164

I.13 I264 PING # 4 BOTTOM DATA TRANSDUCER # 3 CONSTANT = 1.0164

I.14 I264 PING # 4 BOTTOM DATA TRANSDUCER # 4 CONSTANT = 1.0164

I.15 I264 PING # 4 BOTTOM DATA TRANSDUCER # 5 CONSTANT = 1.0164

I.16 I264 PING # 4 BOTTOM DATA TRANSDUCER # 6 CONSTANT = 1.0164

I.17 I264 PING # 5 BOTTOM DATA TRANSDUCER # 1 CONSTANT = 1.0164

I.18 I264 PING # 5 BOTTOM DATA TRANSDUCER # 2 CONSTANT = 1.0164

I.19 I264 PING # 5 BOTTOM DATA TRANSDUCER # 3 CONSTANT = 1.0164

I.20 I264 PING # 5 BOTTOM DATA TRANSDUCER # 4 CONSTANT = 1.0164

I.21 I264 PING # 5 BOTTOM DATA TRANSDUCER # 5 CONSTANT = 1.0164

I.22 I264 PING # 5 BOTTOM DATA TRANSDUCER # 6 CONSTANT = 1.0164

I.23 I264 PING # 6 BOTTOM DATA TRANSDUCER # 1 CONSTANT = 1.0164

I.24 I264 PING # 6 BOTTOM DATA TRANSDUCER # 2 CONSTANT = 1.0164

I.25 I264 PING # 6 BOTTOM DATA TRANSDUCER # 3 CONSTANT = 1.0164

I.26 I264 PING # 6 BOTTOM DATA TRANSDUCER # 4 CONSTANT = 1.0164

I.27 I264 PING # 6 BOTTOM DATA TRANSDUCER # 5 CONSTANT = 1.0164

I.28 I264 PING # 6 BOTTOM DATA TRANSDUCER # 6 CONSTANT = 1.0164

I.29 I264 PING # 7 BOTTOM DATA TRANSDUCER # 1 CONSTANT = 1.0164

I.30 I264 PING # 7 BOTTOM DATA TRANSDUCER # 2 CONSTANT = 1.0164

I.31 I264 PING # 7 BOTTOM DATA TRANSDUCER # 3 CONSTANT = 1.0164

I.32 I264 PING # 7 BOTTOM DATA TRANSDUCER # 4 CONSTANT = 1.0164

I.33 I264 PING # 7 BOTTOM DATA TRANSDUCER # 5 CONSTANT = 1.0164

I.34 I264 PING # 7 BOTTOM DATA TRANSDUCER # 6 CONSTANT = 1.0164

I.35 I264 PING # 4 (RANGE 166 - 246) BOTTOM AUTO-CORRELATION

I.36 I264 PING # 5 (RANGE 166 - 246) BOTTOM AUTO-CORRELATION

I.37 I264 PING # 6 (RANGE 166 - 246) BOTTOM AUTO-CORRELATION

I.38 I264 PING # 7 (RANGE 166 - 246) BOTTOM AUTO-CORRELATION

I.39 BOTTOM AUTO-CORRELATION TRANSDUCER #1 I264 PING #4

I.40 BOTTOM AUTO-CORRELATION TRANSDUCER #1 I264 PING #5

I.41 BOTTOM AUTO-CORRELATION TRANSDUCER #1 I264 PING #6

I.42 BOTTOM AUTO-CORRELATION TRANSDUCER #1 I264 PING #7

I.43 I271 PING # 4 BOTTOM DATA TRANSDUCER # 1

I.44 I271 PING # 4 BOTTOM DATA TRANSDUCER # 2

I.45 I271 PING # 4 BOTTOM DATA TRANSDUCER # 3

I.46 I271 PING # 4 BOTTOM DATA TRANSDUCER # 4

I.47 I271 PING # 4 BOTTOM DATA TRANSDUCER # 5

I.48 I271 PING # 4 BOTTOM DATA TRANSDUCER # 6

I.49 I271 PING # 5 BOTTOM DATA TRANSDUCER # 1

I.50 I271 PING # 5 BOTTOM DATA TRANSDUCER # 2

I.51 I271 PING # 5 BOTTOM DATA TRANSDUCER # 3

I.52 I271 PING # 5 BOTTOM DATA TRANSDUCER # 4

I.53 I271 PING # 5 BOTTOM DATA TRANSDUCER # 5

I.54 I271 PING # 5 BOTTOM DATA TRANSDUCER # 6

I.55 I271 PING # 6 BOTTOM DATA TRANSDUCER # 1

I.56 I271 PING # 6 BOTTOM DATA TRANSDUCER # 2

I.57 I271 PING # 6 BOTTOM DATA TRANSDUCER # 3

I.58 I271 PING # 6 BOTTOM DATA TRANSDUCER # 4

I.59 I271 PING # 6 BOTTOM DATA TRANSDUCER # 5

I.60 I271 PING # 6 BOTTOM DATA TRANSDUCER # 6

I.61 I271 PING # 7 BOTTOM DATA TRANSDUCER # 1

I.62 I271 PING # 7 BOTTOM DATA TRANSDUCER # 2

I.63 I271 PING # 7 BOTTOM DATA TRANSDUCER # 3

I.64 I271 PING # 7 BOTTOM DATA TRANSDUCER # 4

I.65 I271 PING # 7 BOTTOM DATA TRANSDUCER # 5

I.66 I271 PING # 7 BOTTOM DATA TRANSDUCER # 6

I.67 I271 PING # 04 RANGE (166 - 246) TIME CROSS-CORRELATION

I.68 I271 PING # 05 RANGE (166 - 246) TIME CROSS-CORRELATION

I.69 I271 PING # 06 RANGE (166 - 246) TIME CROSS-CORRELATION

I.70 I271 PING # 07 RANGE (166 - 246) TIME CROSS-CORRELATION

I.71 I271 PING # 4 (RANGE 166-246)
T2P1/T1PX, T3P1/T2PX, T4P1/T3PX, T5P1/T4PX, T6P1/T5PX

I.72 I263 PING # 04 VOLUME RAW DATA (1000-39000) TRANSDUCER # 1

I.73 I263 PING # 04 VOLUME RAW DATA (1000-39000) TRANSDUCER # 2

I.74 I263 PING # 04 VOLUME RAW DATA (1000-39000) TRANSDUCER # 3

I.75 I263 PING # 04 VOLUME RAW DATA (1000-39000) TRANSDUCER # 4

I.76 I263 PING # 04 VOLUME RAW DATA (1000-39000) TRANSDUCER # 5

I.77 I263 PING # 04 VOLUME RAW DATA (1000-39000) TRANSDUCER # 6]

I.78 I263 # P4 TRANSDUCER # 1 VOLUME OKt

I.79 I263 # P4 TRANSDUCER # 2 VOLUME OKt

I.80 I263 # P4 TRANSDUCER # 3 VOLUME OKt

I.81 I263 # P4 TRANSDUCER # 4 VOLUME OKt

I.82 I263 # P4 TRANSDUCER # 5 VOLUME OKt

I.83 I263 # P4 TRANSDUCER # 6 VOLUME OKt

I.84 I263 PING # 4 VOLUME RETURN TRANSDUCER #1
P1&2, P2&3, P3&4, P4&5 POINTS

I.85 I263 PING # 4 VOLUME RETURN TRANSDUCER #2
P1&2, P2&3, P3&4, P4&5 POINTS

I.86 I263 PING # 4 VOLUME RETURN TRANSDUCER #3
P1&2, P2&3, P3&4, P4&5 160 POINTS

I.87 I263 PING # 4 VOLUME RETURN TRANSDUCER #4
P1&2, P2&3, P3&4, P4&5 160 POINTS

I.88 I263 PING # 4 VOLUME RETURN TRANSDUCER #5
P1&2, P2&3, P3&4, P4&5 160 POINTS

I.89 I263 PING # 4 VOLUME RETURN TRANSDUCER #6
P1&2, P2&3, P3&4, P4&5 160 POINTS

I.90 I263 PING # 4 VOLUME RETURN TRANSDUCER #1
P1&2, P2&3, P3&4, P4&5 160 POINTS

I.91 I263 PING # 4 VOLUME RETURN TRANSDUCER #2
P1&2, P2&3, P3&4, P4&5 160 POINTS

I.92 I263 PING # 4 VOLUME RETURN TRANSDUCER #3
P1&2, P2&3, P3&4, P4&5 160 POINTS

I.93 I263 PING # 4 VOLUME RETURN TRANSDUCER #4
P17&2, P2&3, P3&4, P4&5 160 POINTS

I.94 I263 PING # 4 VOLUME RETURN TRANSDUCER #5
PI&2, P2&3, P3&4, P4&5 160 POINTS

I.95 I263 PING # 4 TRANSDUCER #6 P1&2, P2&3, P3&4, P4&5
"DENOMINATOR"

In diagrams for which no vertical scale is given, that vertical scale is in arbitrary units.

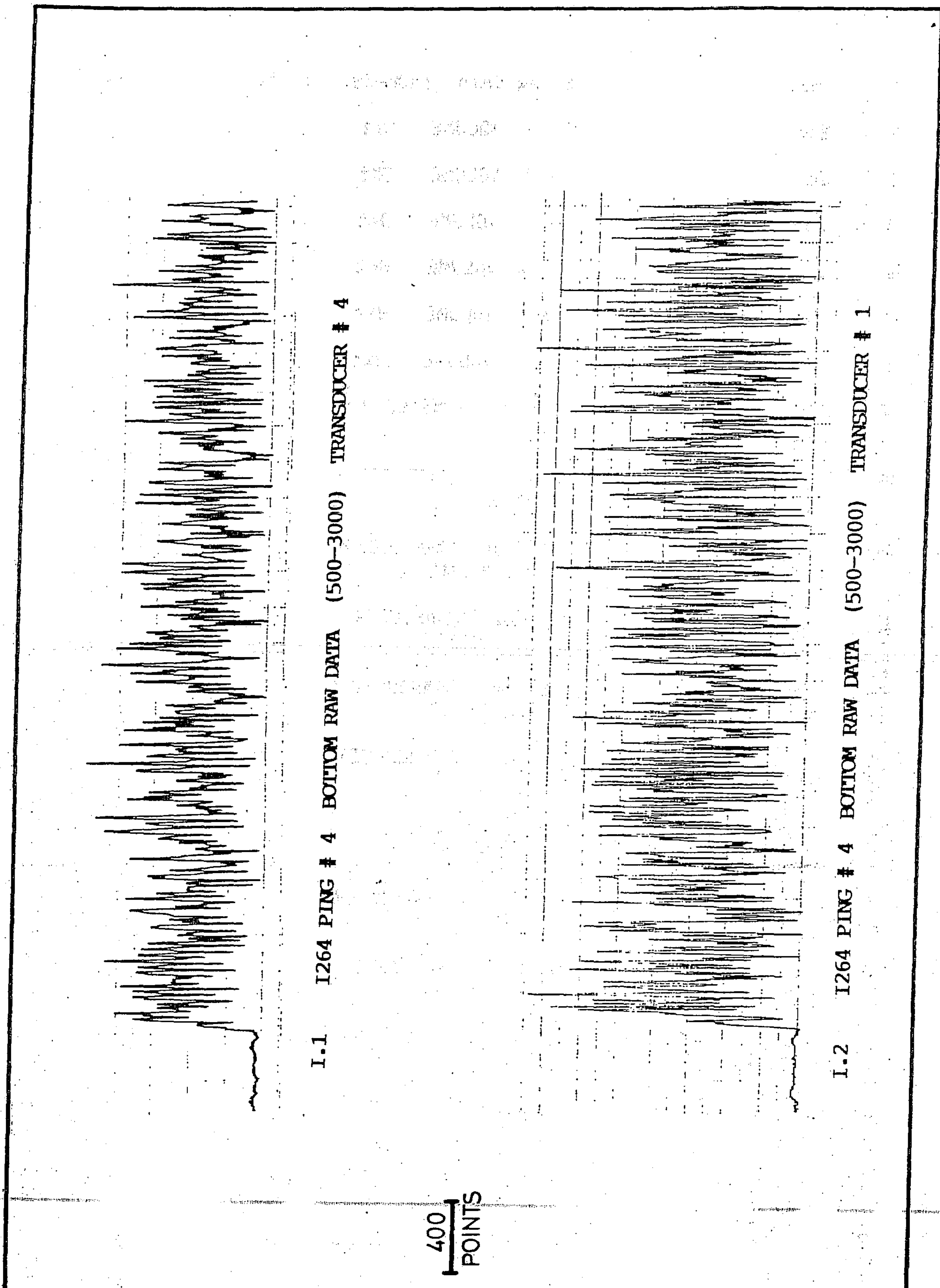
I.1 I264 PING # 4 BOTTOM RAW DATA (500-3000) TRANSDUCER # 4
I.2 I264 PING # 4 BOTTOM RAW DATA (500-3000) TRANSDUCER # 1
400 POINTS

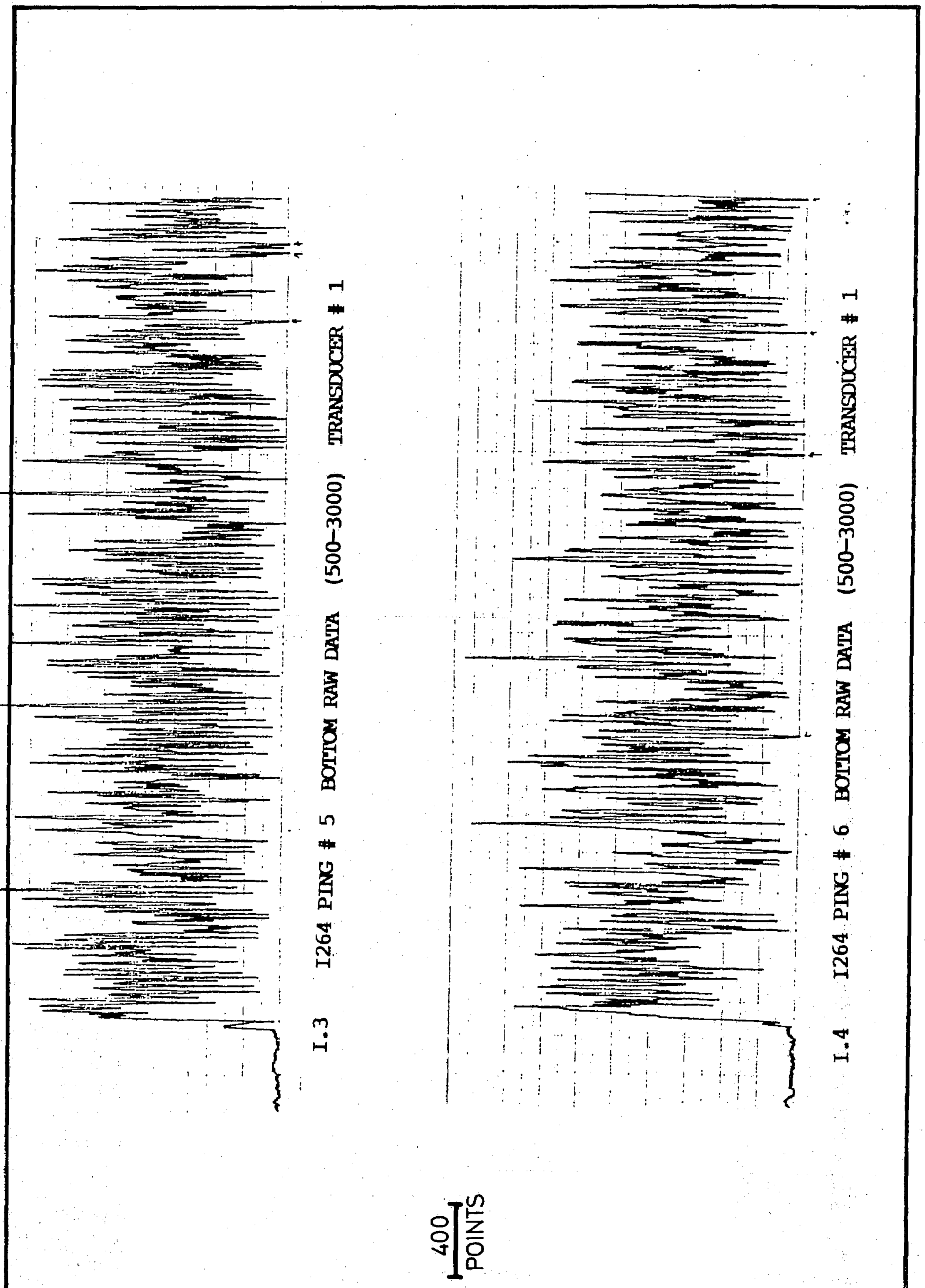
I.3 I264 PING # 5 BOTTOM RAW DATA (500-3000) TRANSDUCER # 1
I.4 I264 PING # 6 BOTTOM RAW DATA (500-3000) TRANSDUCER # 1
400 POINTS

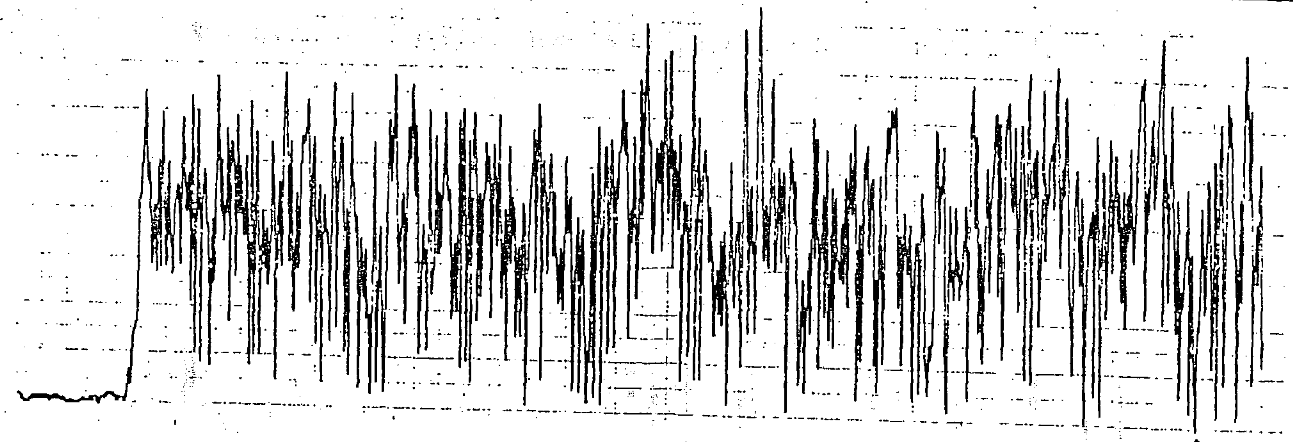

I.5 I264 PING # 7 BOTTOM RAW DATA (500–3000) TRANSDUCER # 1

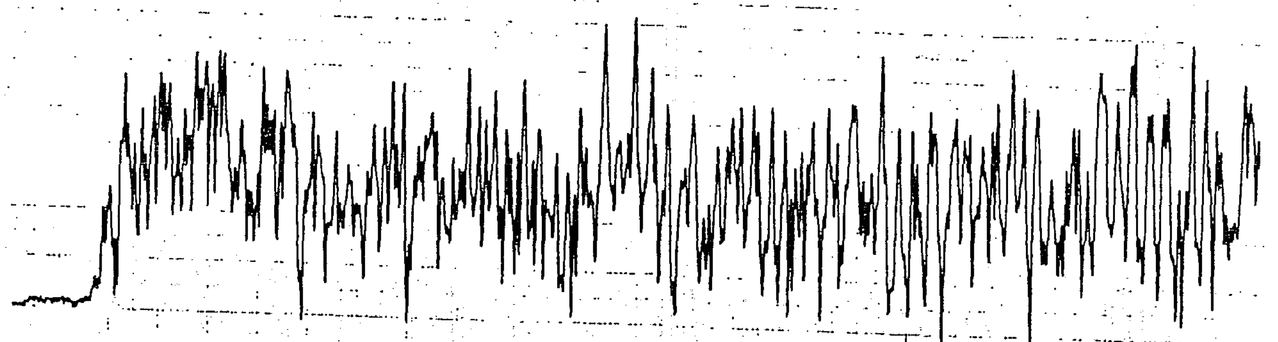

I.6 I264 PING # 4 BOTTOM RAW DATA (500–3000) TRANSDUCER # 4

400 POINTS

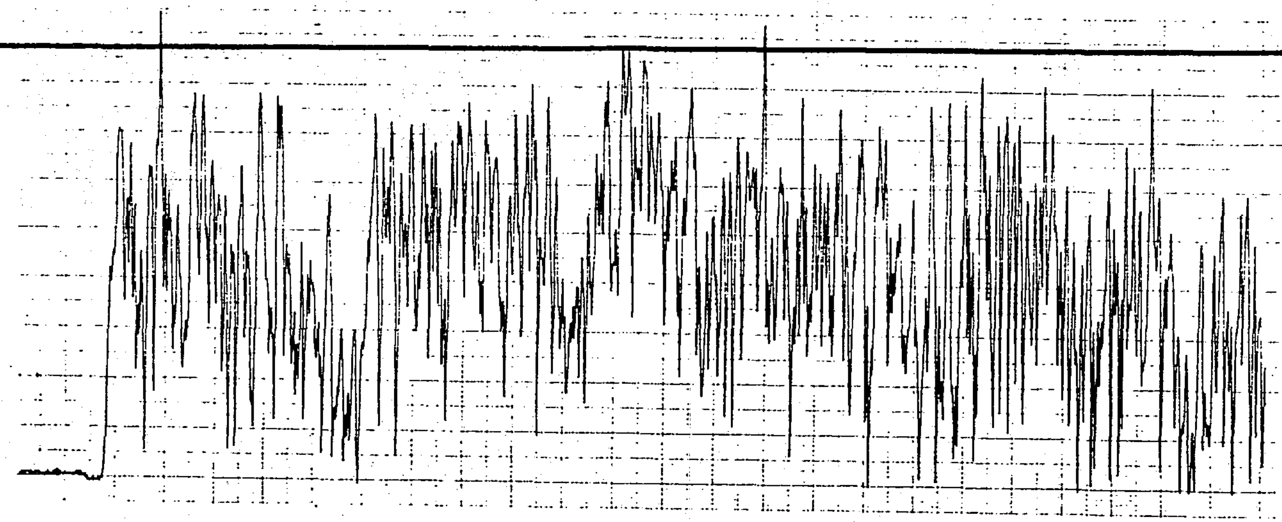

I.7 I264 PING # 4 BOTTOM RAW DATA (500–3000) TRANSDUCER # 1

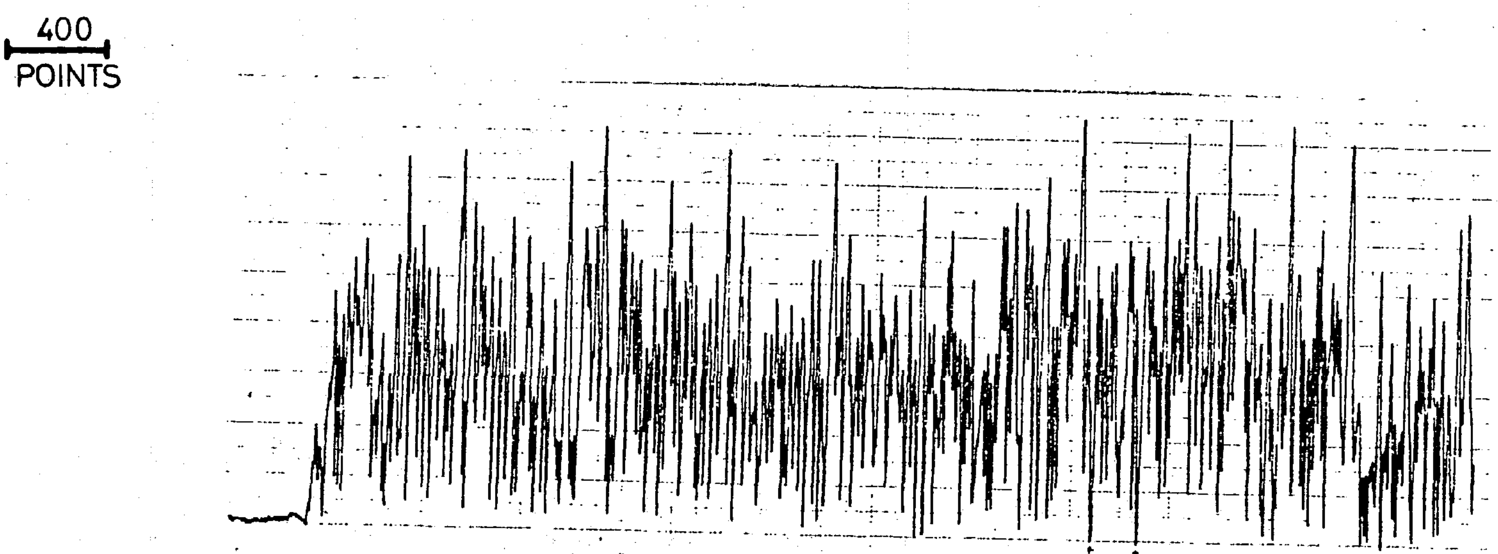

I.8 I264 PING # 5 BOTTOM RAW DATA (500–3000) TRANSDUCER # 1

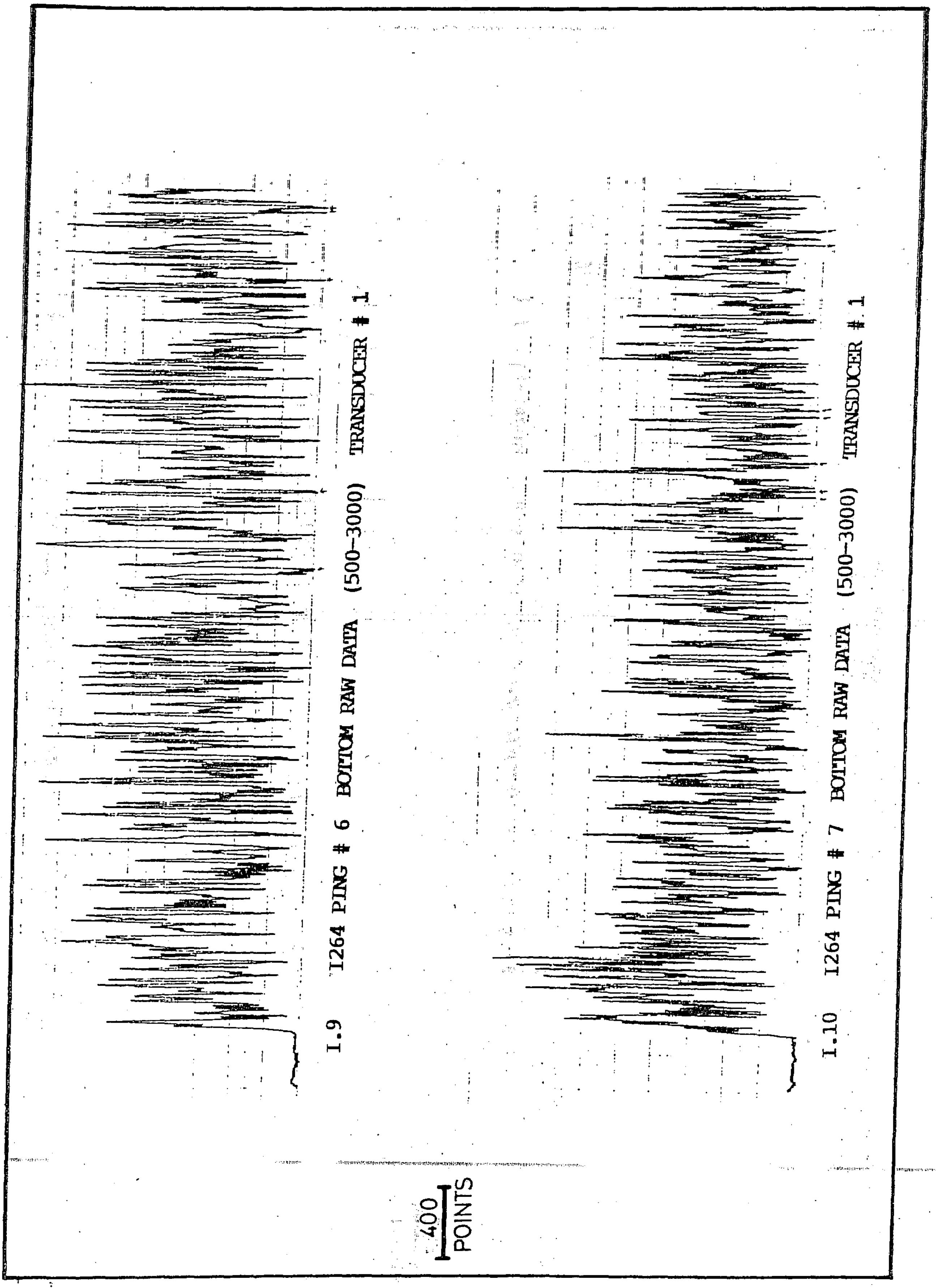

I.9 I264 PING # 6 BOTTOM RAW DATA (500–3000) TRANSDUCER # 1

I.10 I264 PING # 7 BOTTOM RAW DATA (500–3000) TRANSDUCER # 1

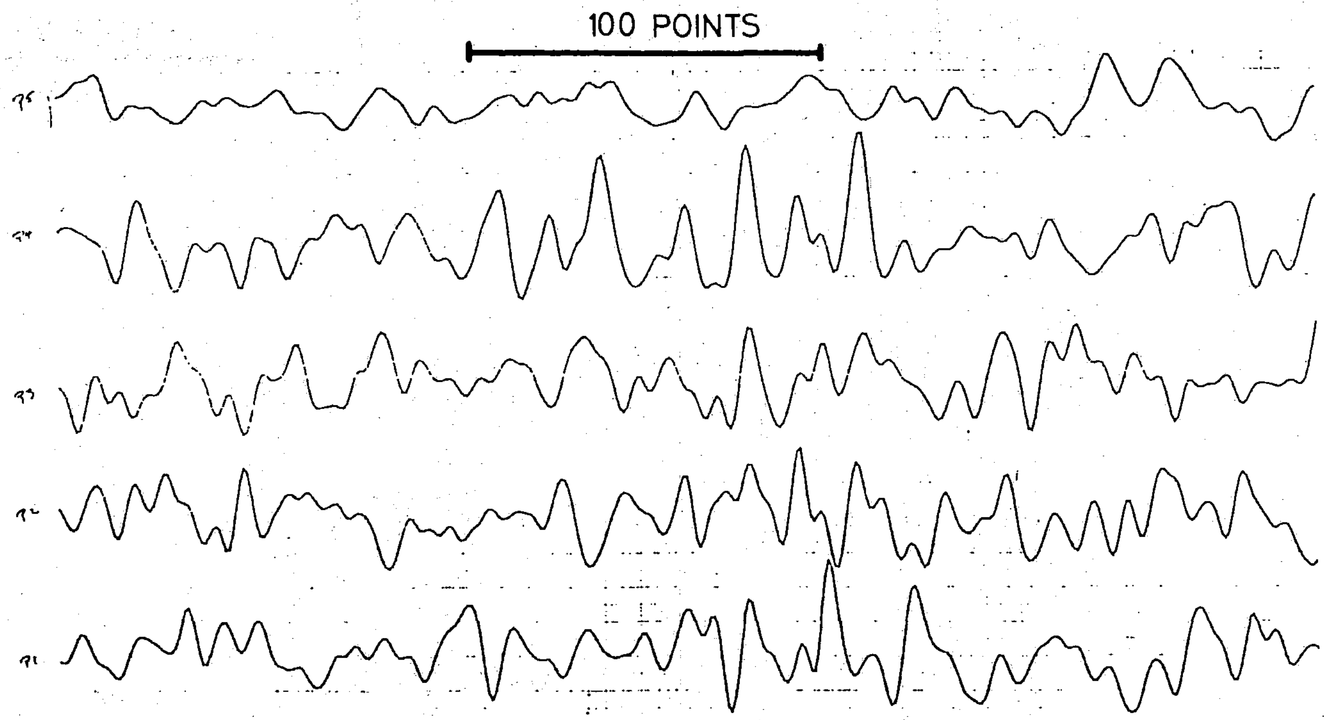

I.11 I264 PING # 4 BOTTOM DATA TRANSDUCER # 1 CONSTANT = 1.0164

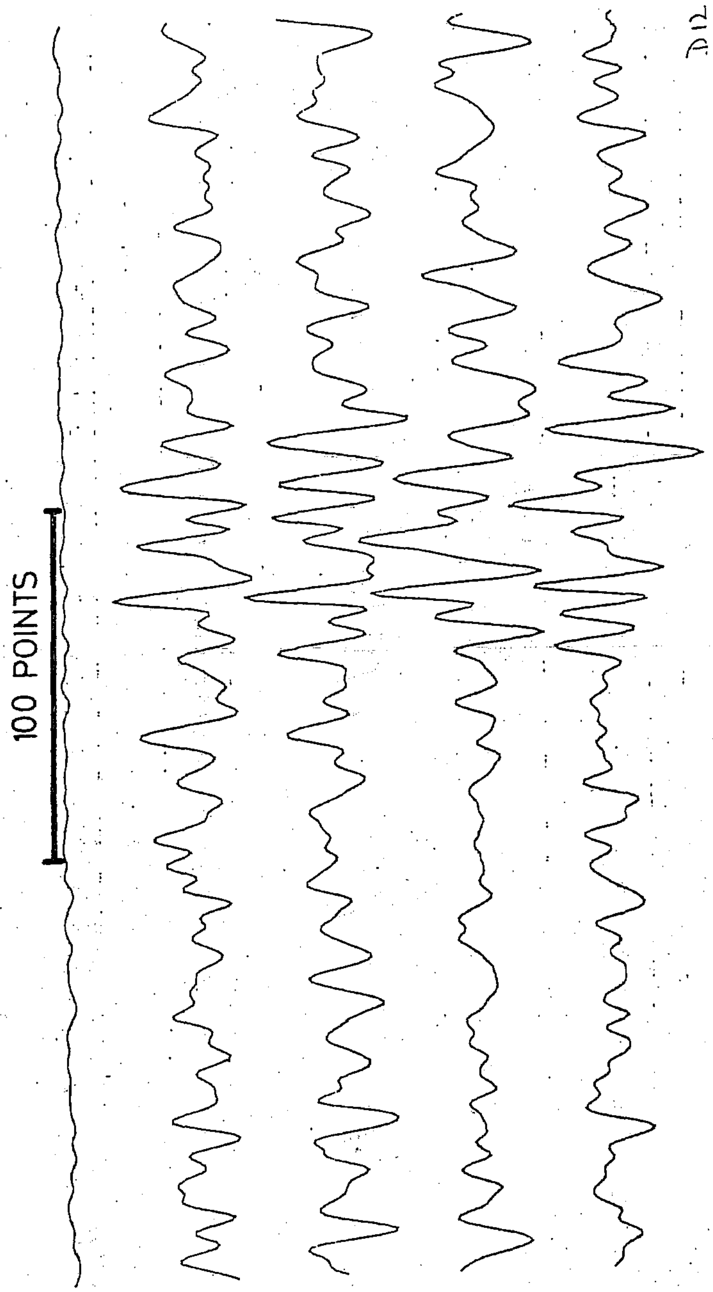

I.12 I264 PING # 4 BOTTOM DATA TRANSDUCER # 2 CONSTANT = 1.0164

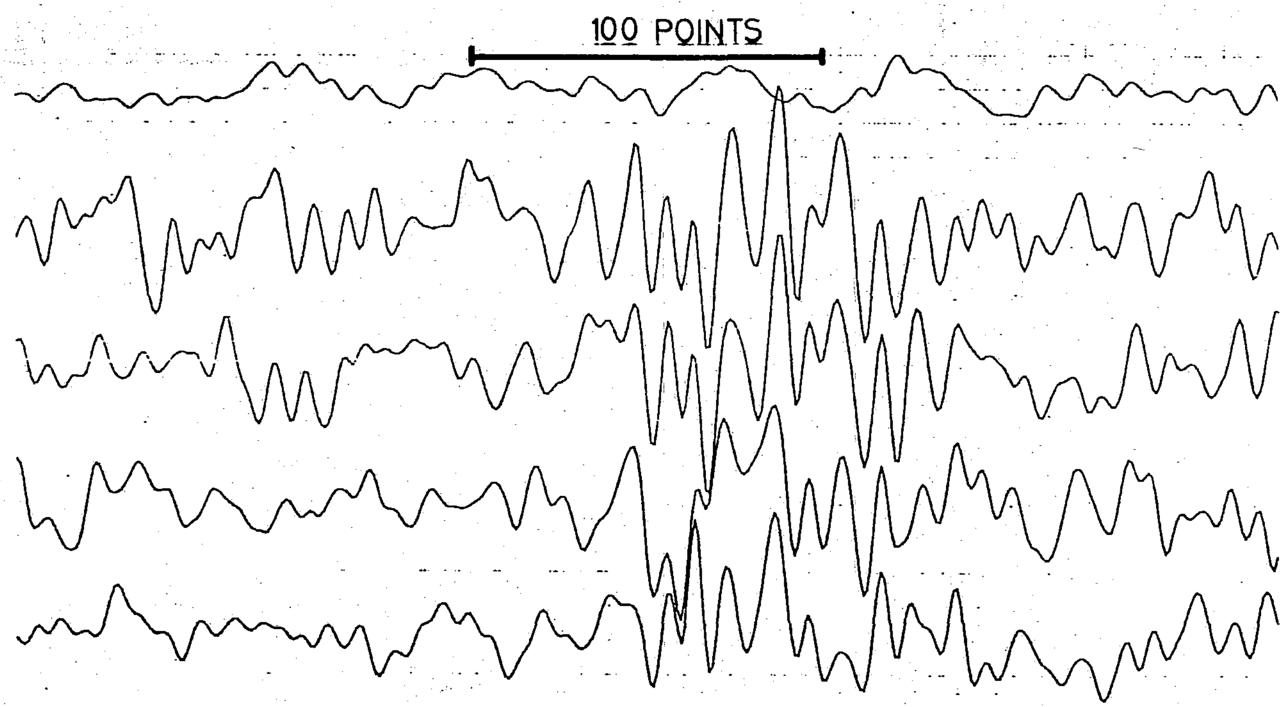

I.13 I264 PING # 4 BOTTOM DATA TRANSDUCER # 3 CONSTANT = 1.0164

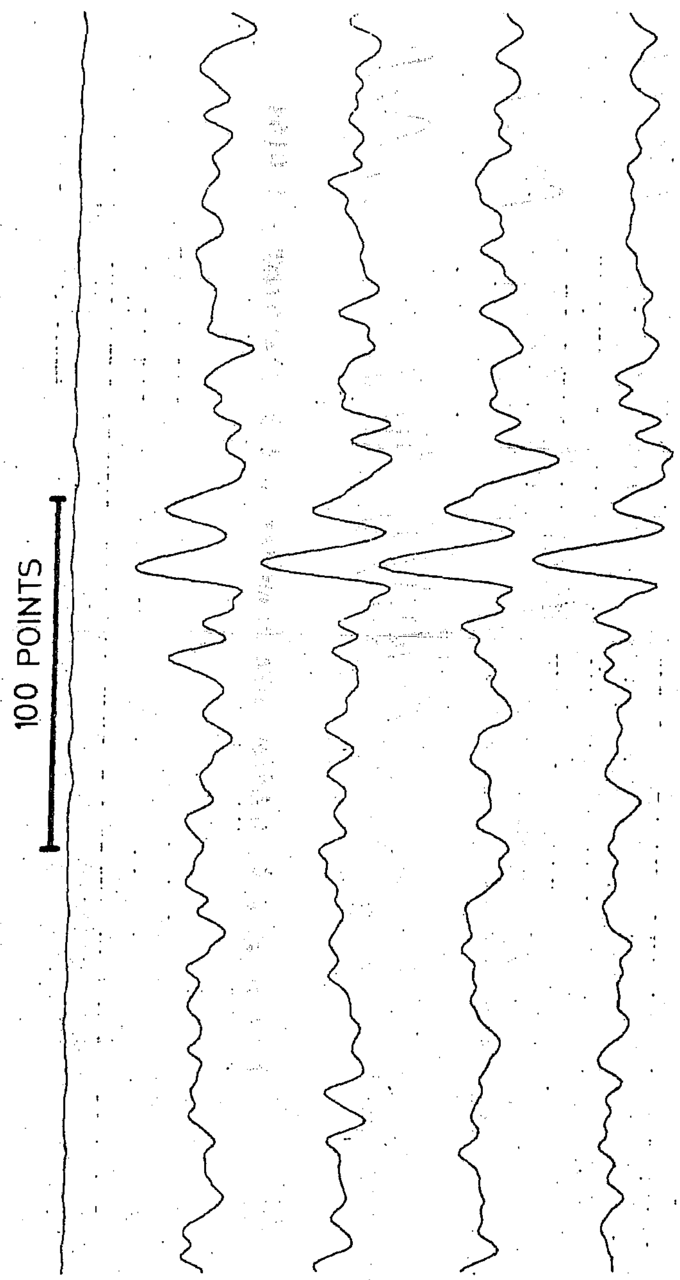

I.14 I264 PING # 4 BOTTOM DATA TRANSDUCER # 4 CONSTANT = 1.0164

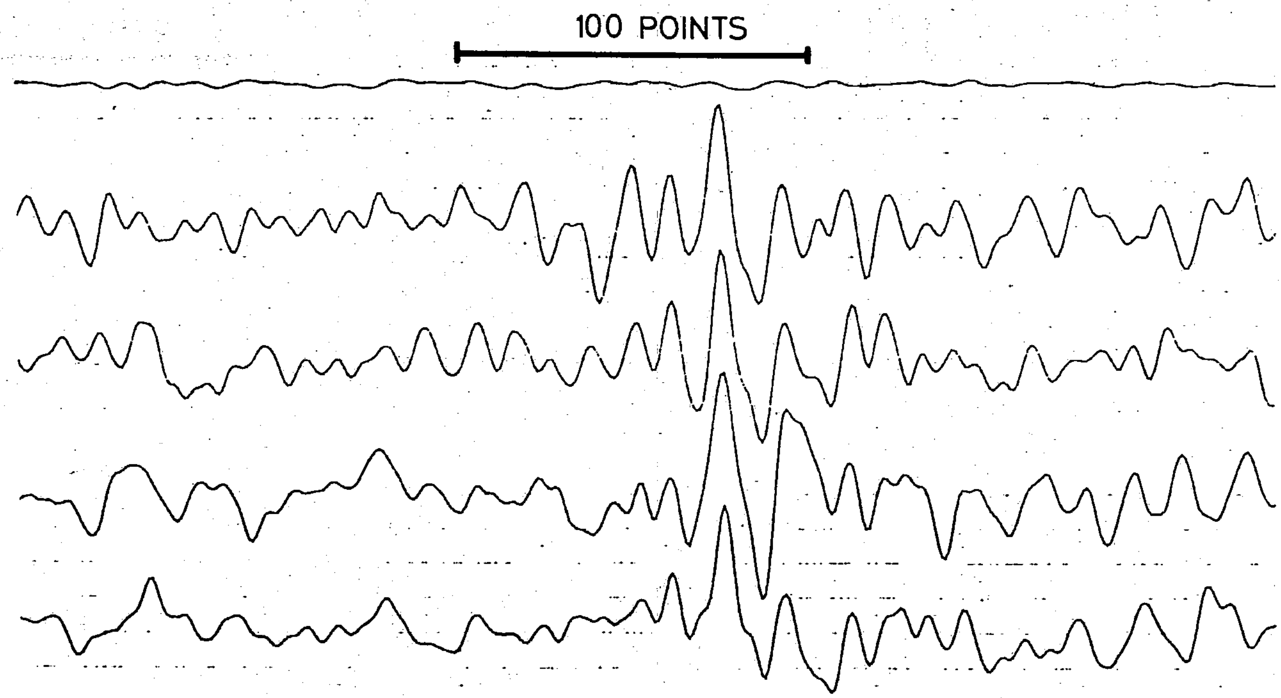

I.15 I264 PING # 4 BOTTOM DATA TRANSDUCER # 5 CONSTANT = 1.0164

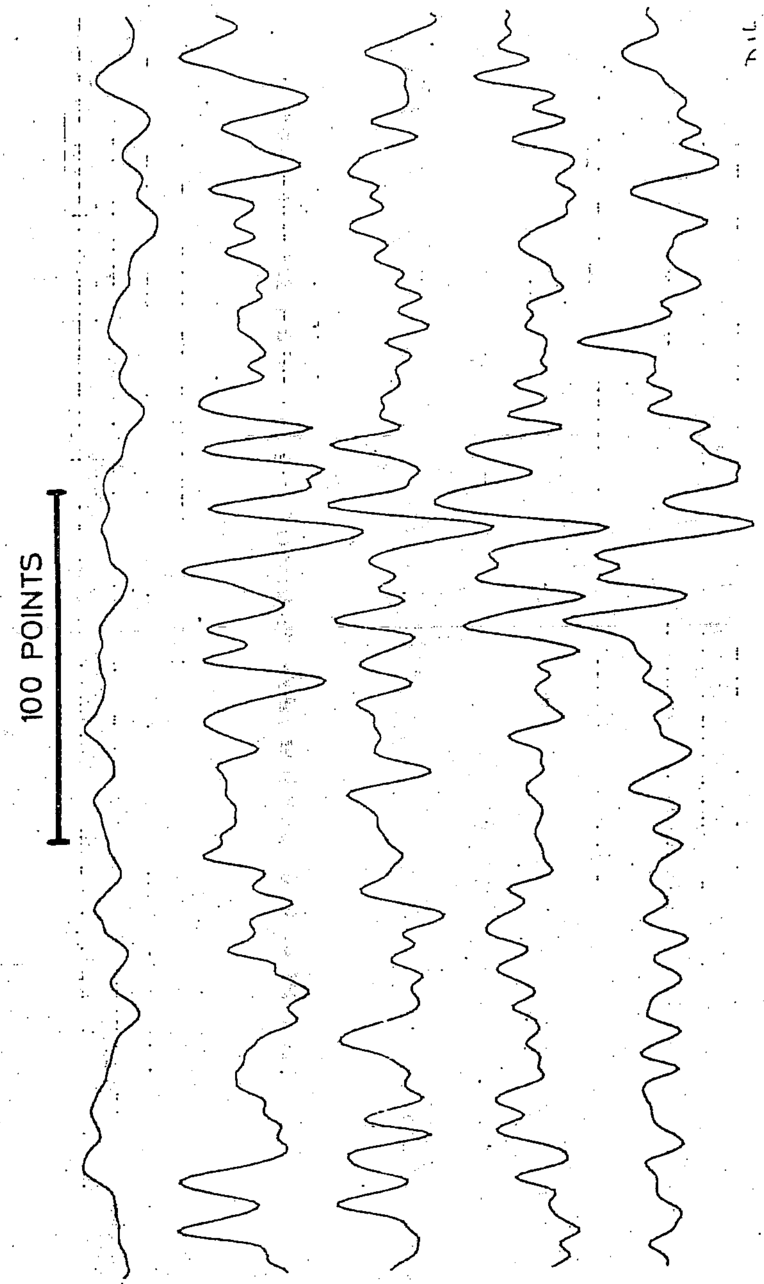

I.16 I264 PING # 4 BOTTOM DATA TRANSDUCER # 6 CONSTANT = 1.0164

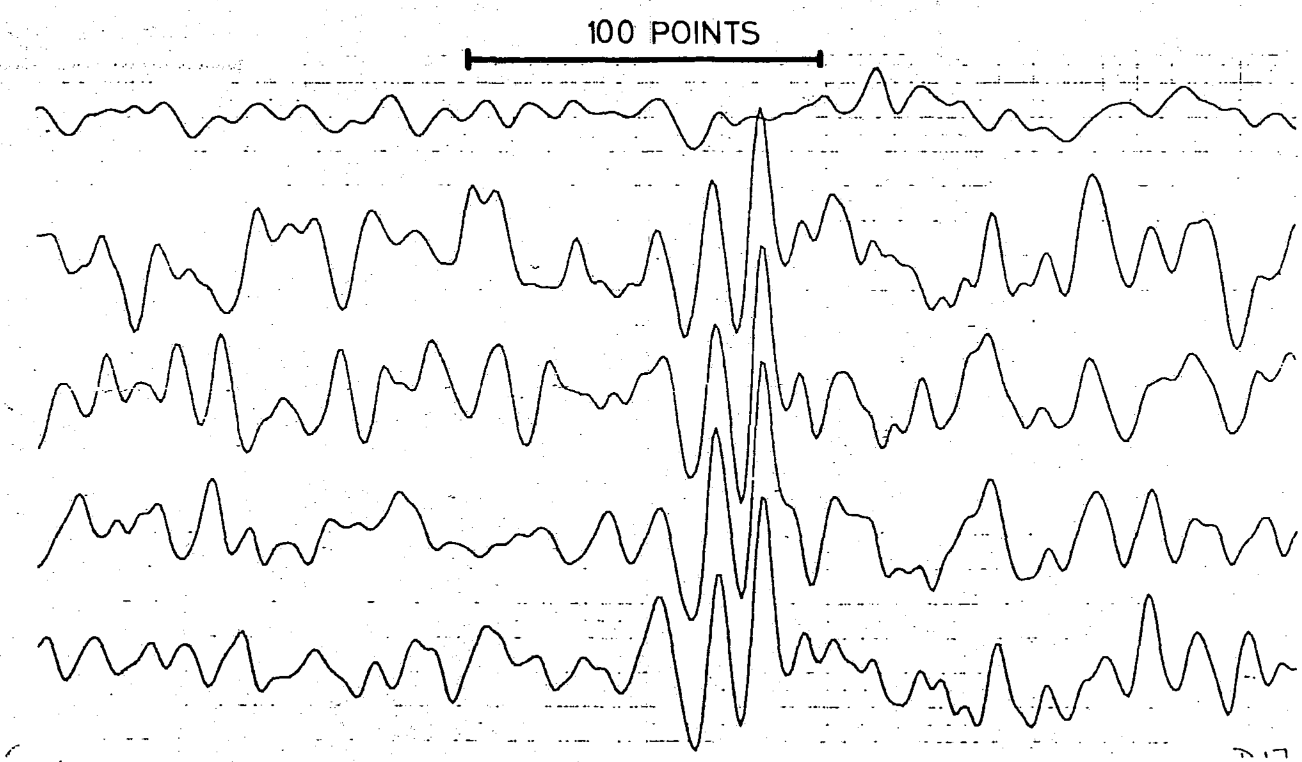

I.17 I264 PING # 5 BOTTOM DATA TRANSDUCER # 1 CONSTANT = 1.0164

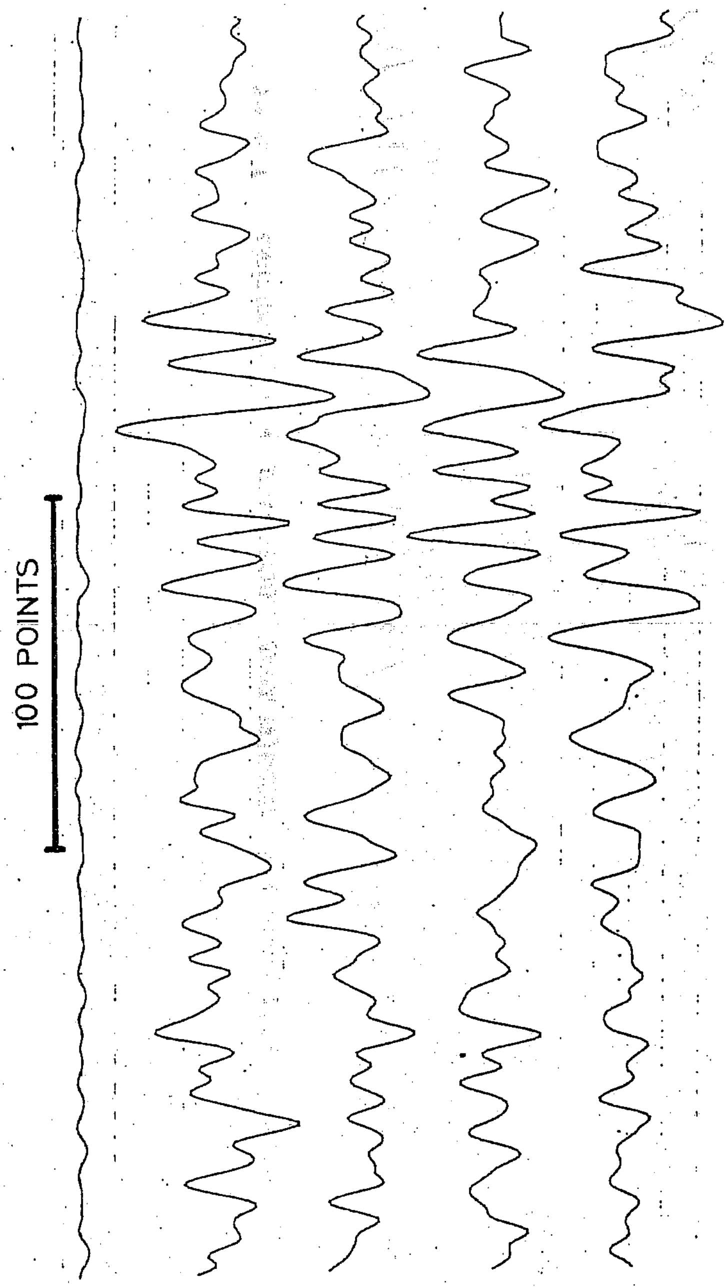

I.18 I264 PING # 5 BOTTOM DATA TRANSDUCER # 2 CONSTANT = 1.0164

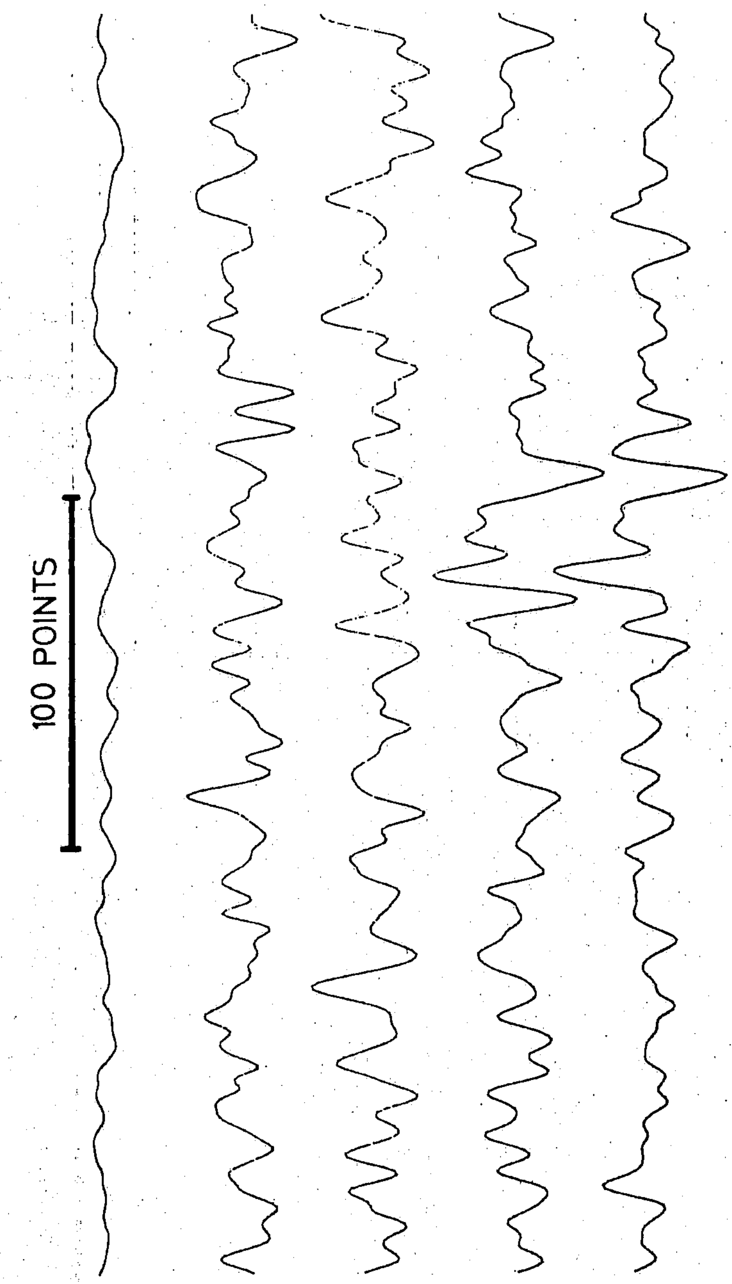

I.19 I264 PING # 5 BOTTOM DATA TRANSDUCER # 3 CONSTANT = 1.0164

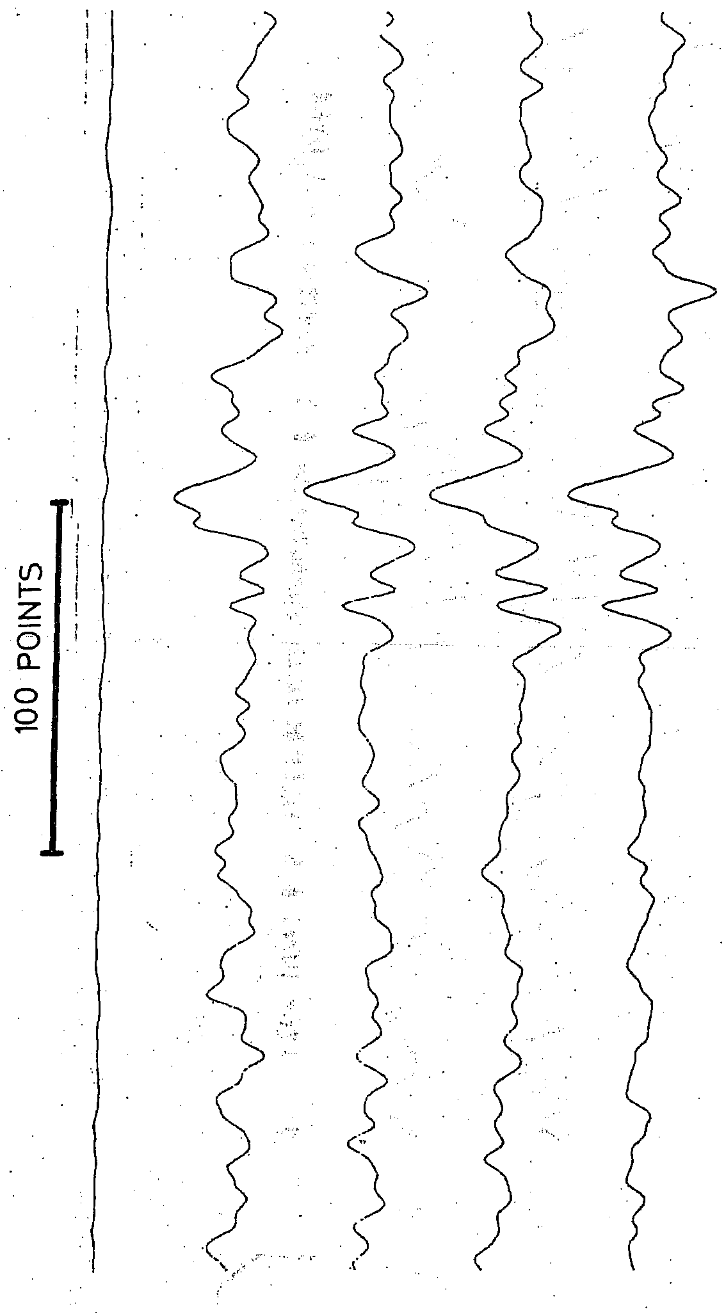

I.20 I264 PING # 5 BOTTOM DATA TRANSDUCER # 4 CONSTANT = 1.0164

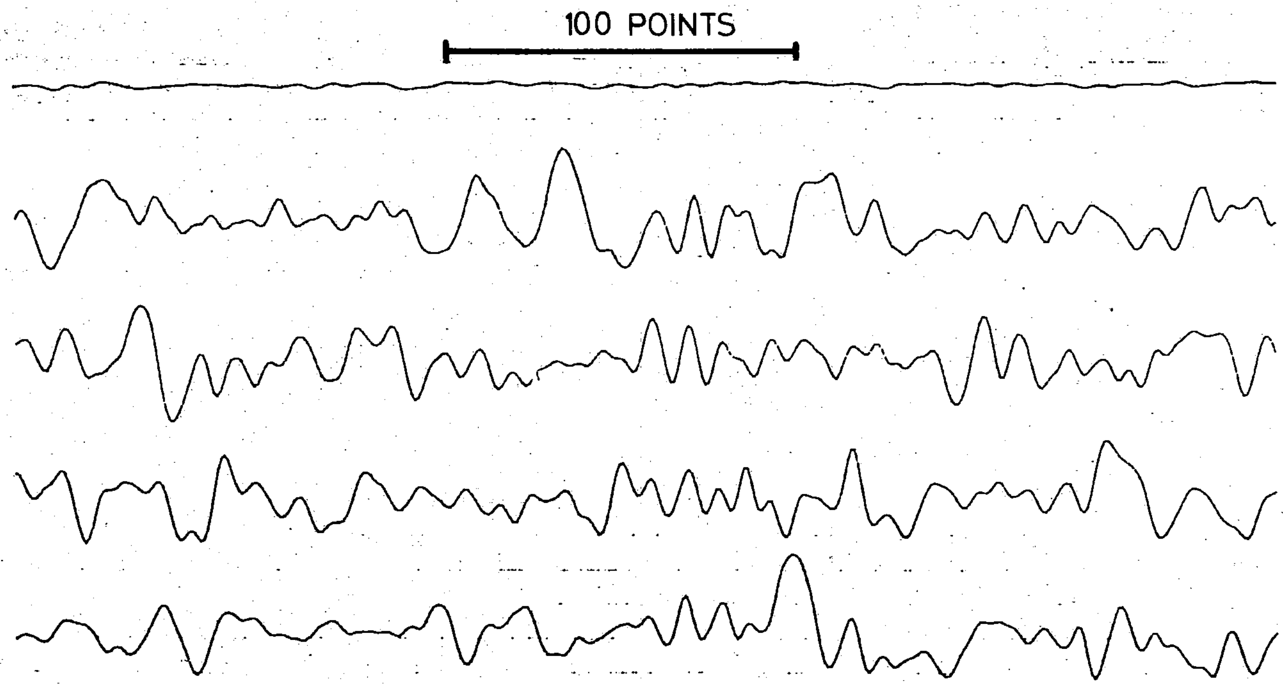

I.21 I264 PING # 5 BOTTOM DATA TRANSDUCER # 5 CONSTANT = 1.0164

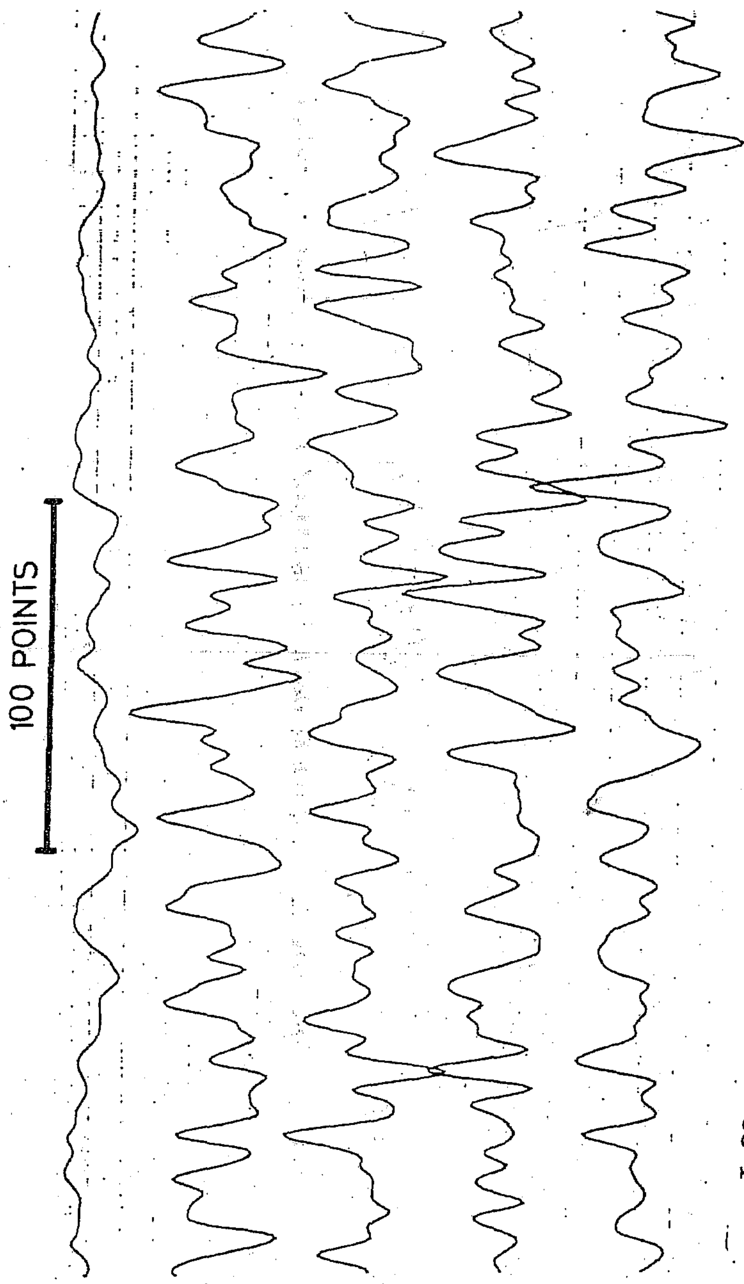

I.22 I264 PING # 5 BOTTOM DATA TRANSDUCER # 6 CONSTANT = 1.0164

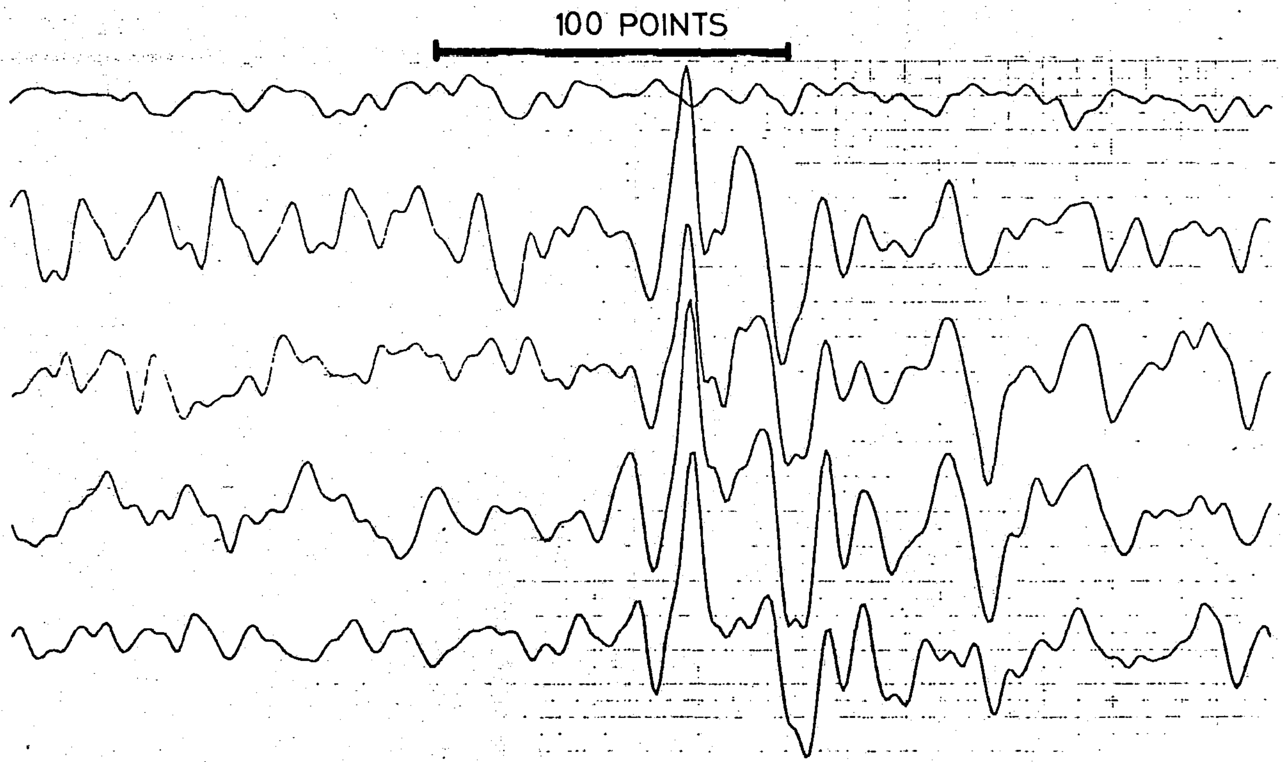

I.23 I264 PING # 6 BOTTOM DATA TRANSDUCER # 1 CONSTANT = 1.0164

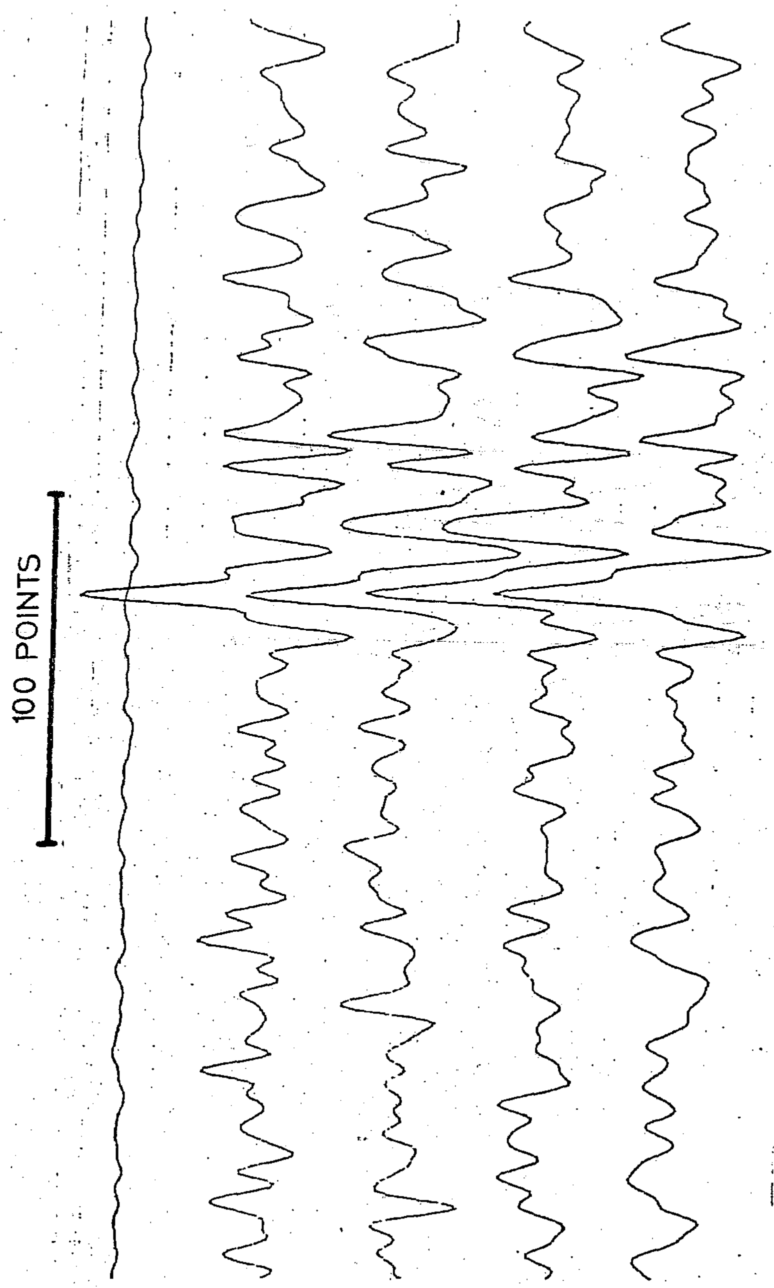

I.24 I264 PING # 6 BOTTOM DATA TRANSDUCER # 2 CONSTANT = 1.0164

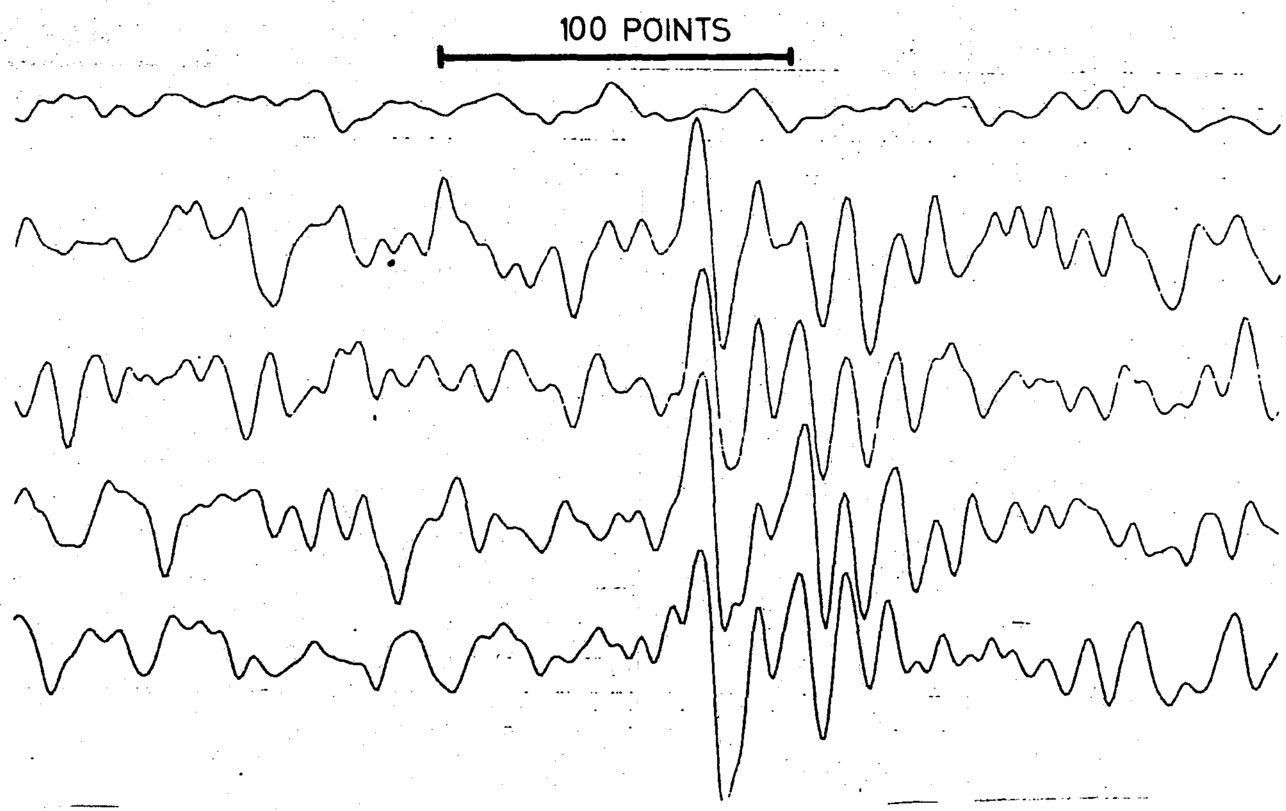

I.25 I264 PING # 6 BOTTOM DATA TRANSDUCER # 3 CONSTANT = 1.0164

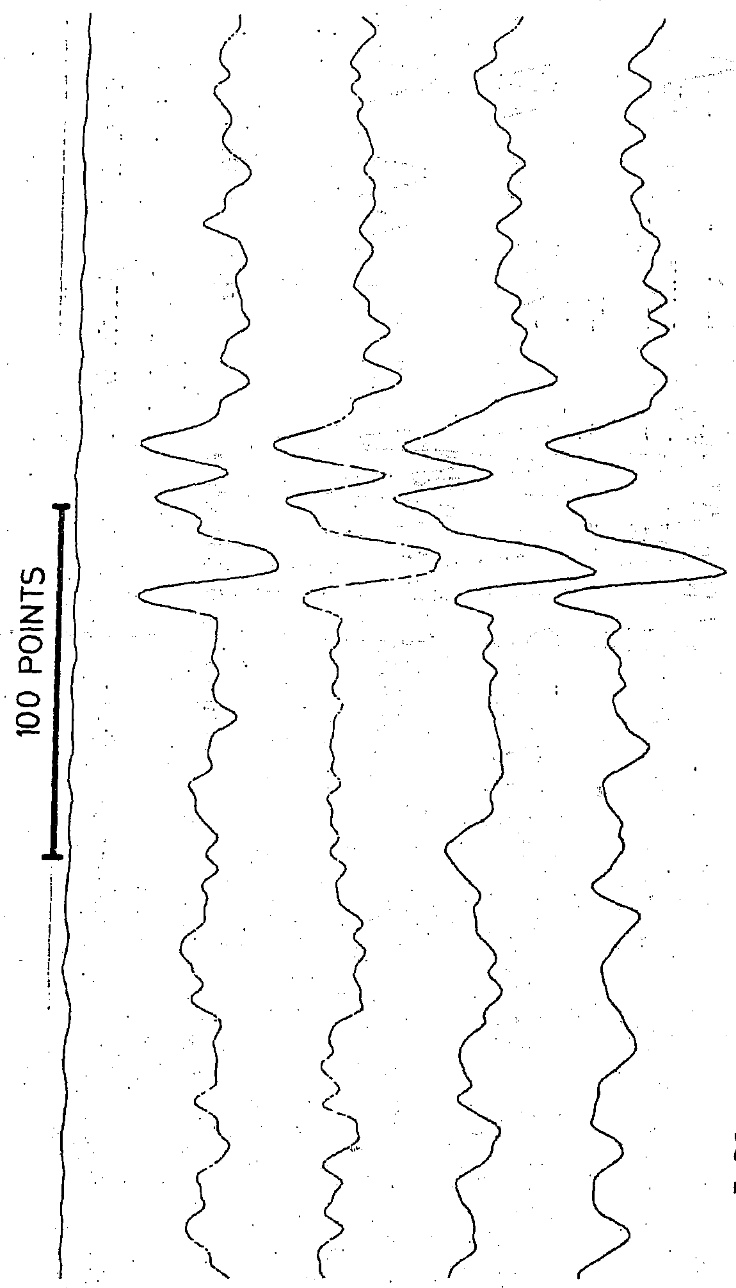

1.26 I264 PING # 6 BOTTOM DATA TRANSDUCER # 4 CONSTANT = 1.0164

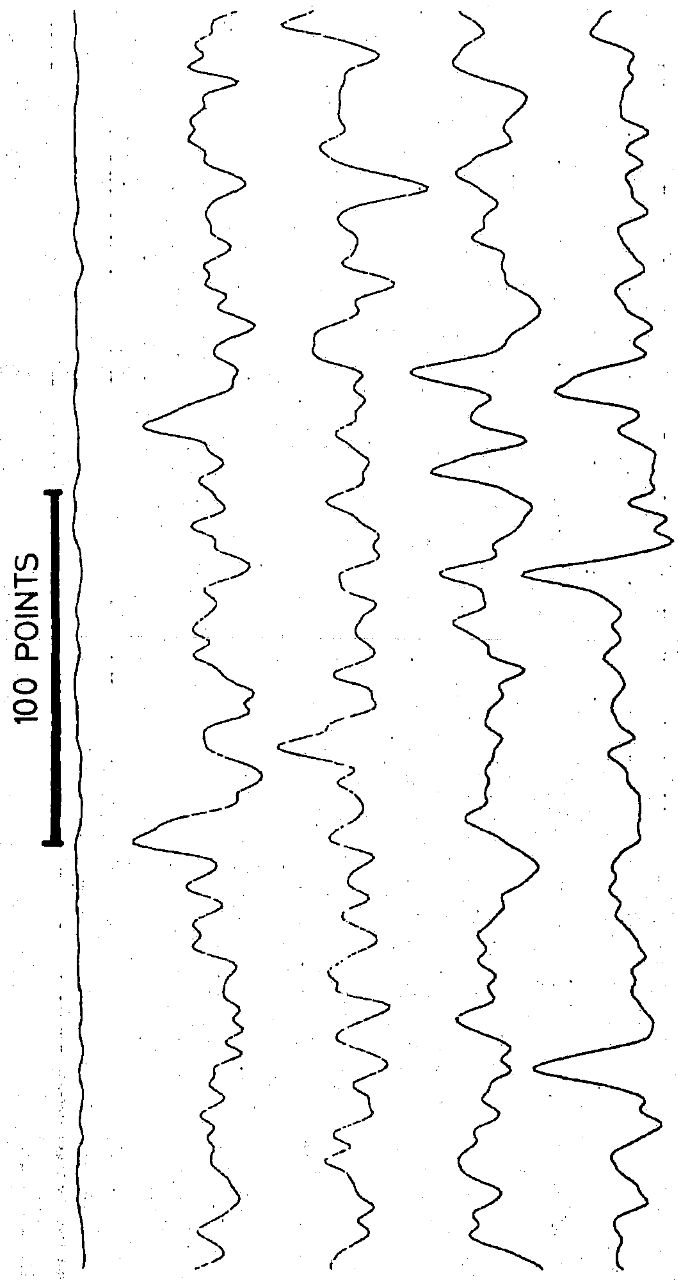

I.27 I264 PING # 6 BOTTOM DATA TRANSDUCER # 5 CONSTANT = 1.0164

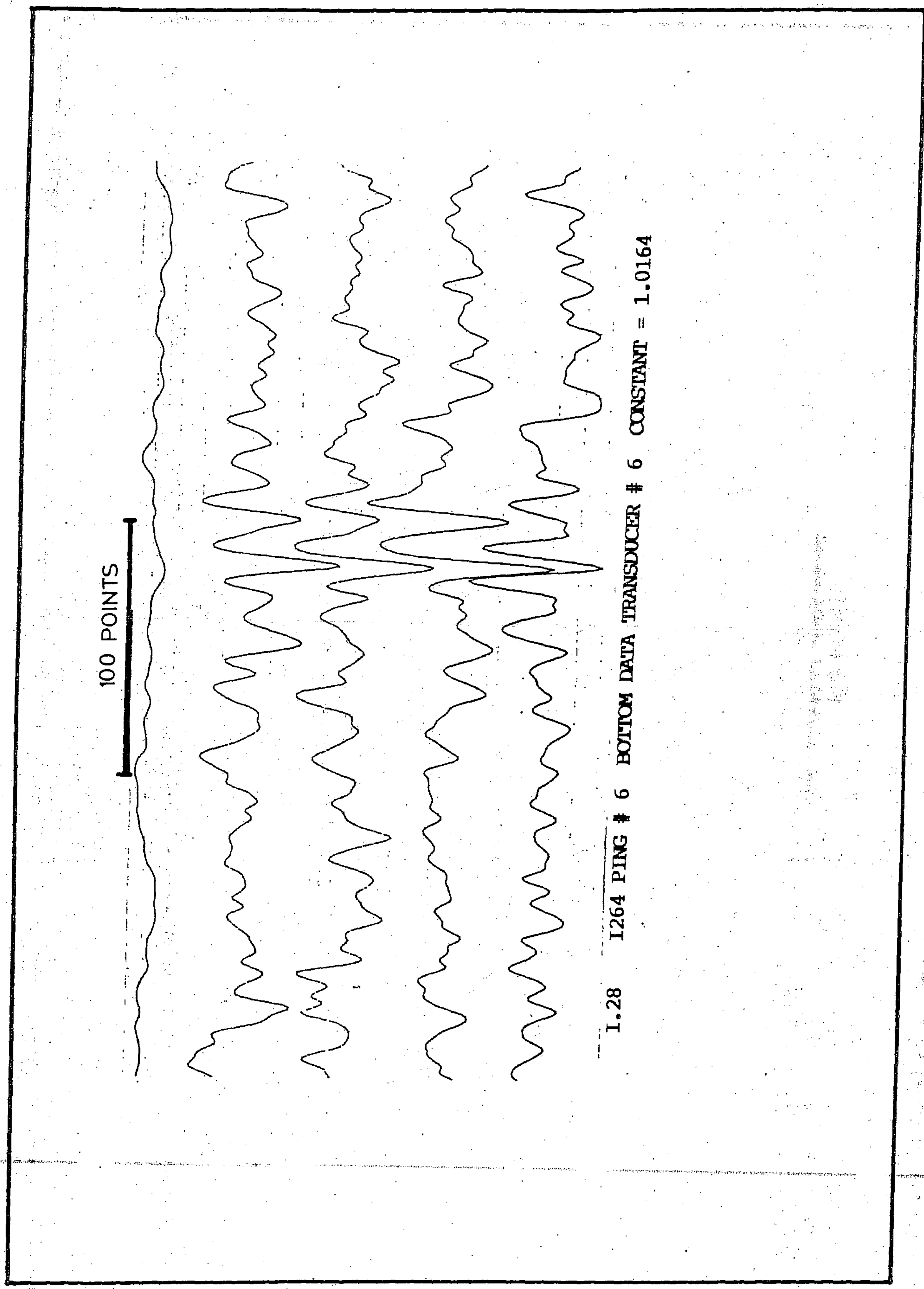
100 POINTS
1.28
I264 PING # 6 BOTTOM DATA TRANSDUCER # 6 CONSTANT = 1.0164

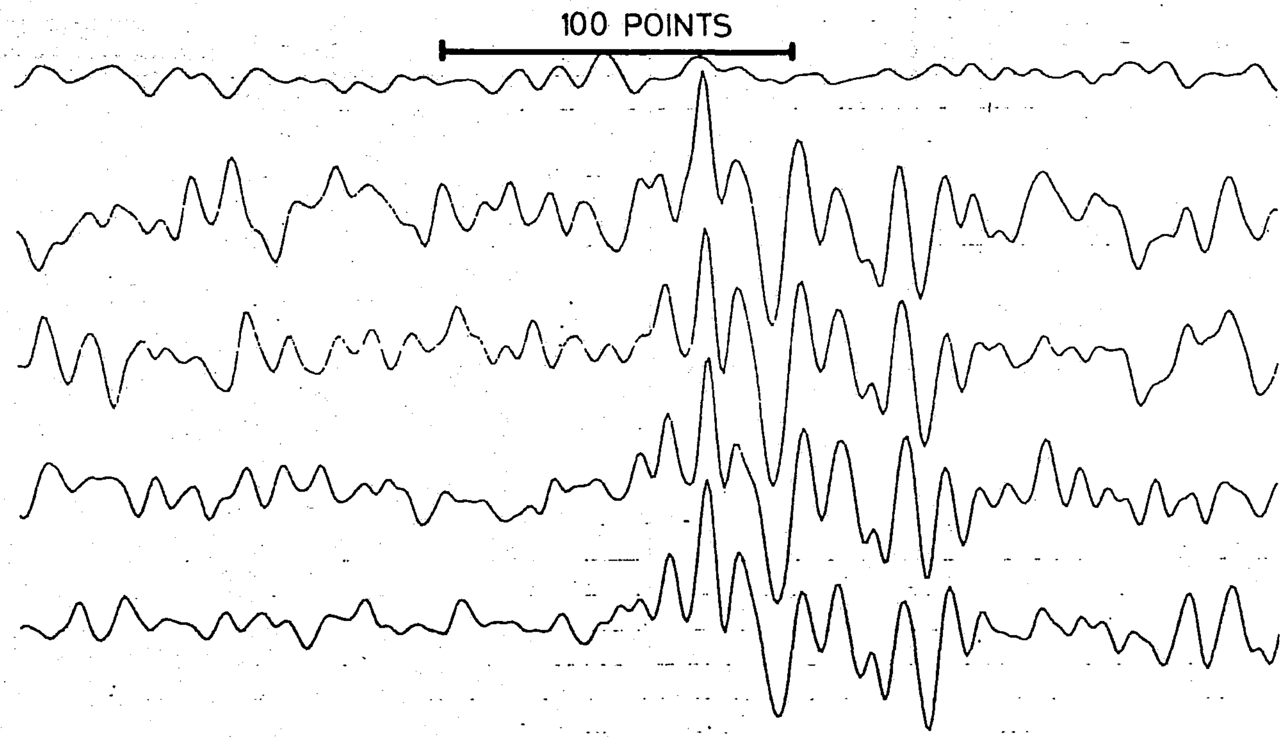

I.29 I264 PING # 7 BOTTOM DATA TRANSDUCER # 1 CONSTANT = 1.0164

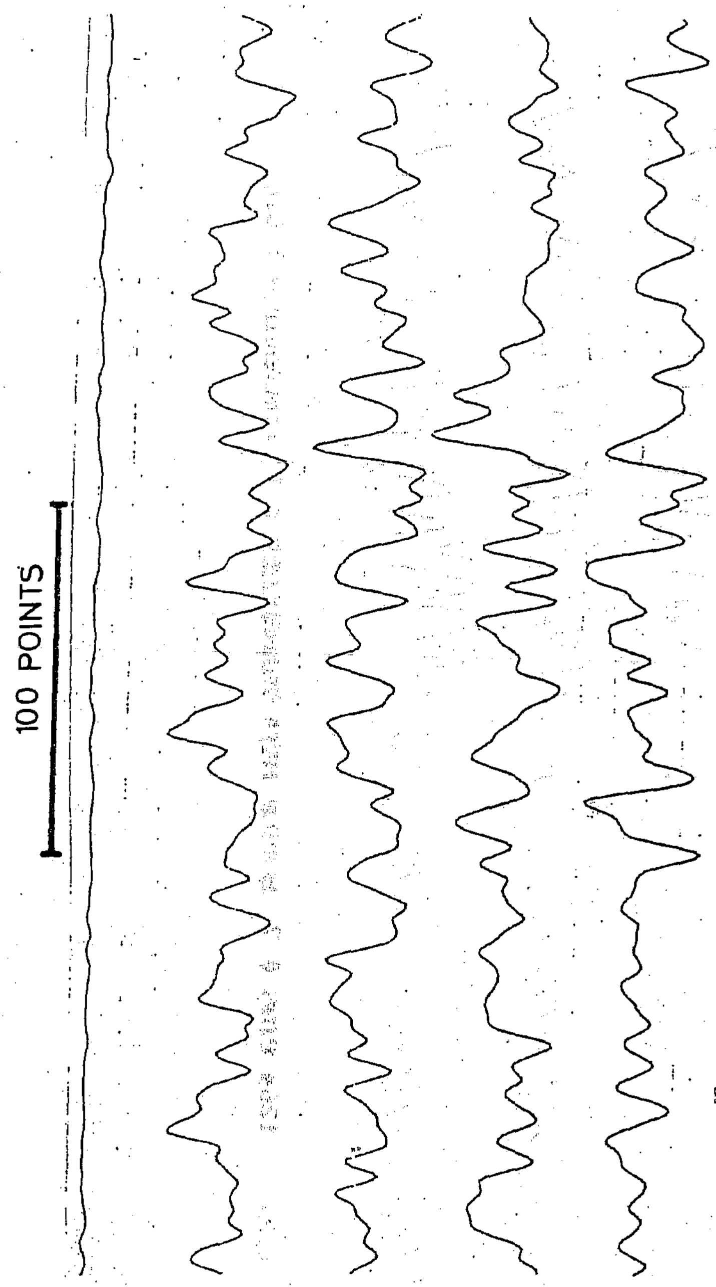

I.30 I264 PING # 7 BOTTOM DATA TRANSDUCER # 2 CONSTANT = 1.0164

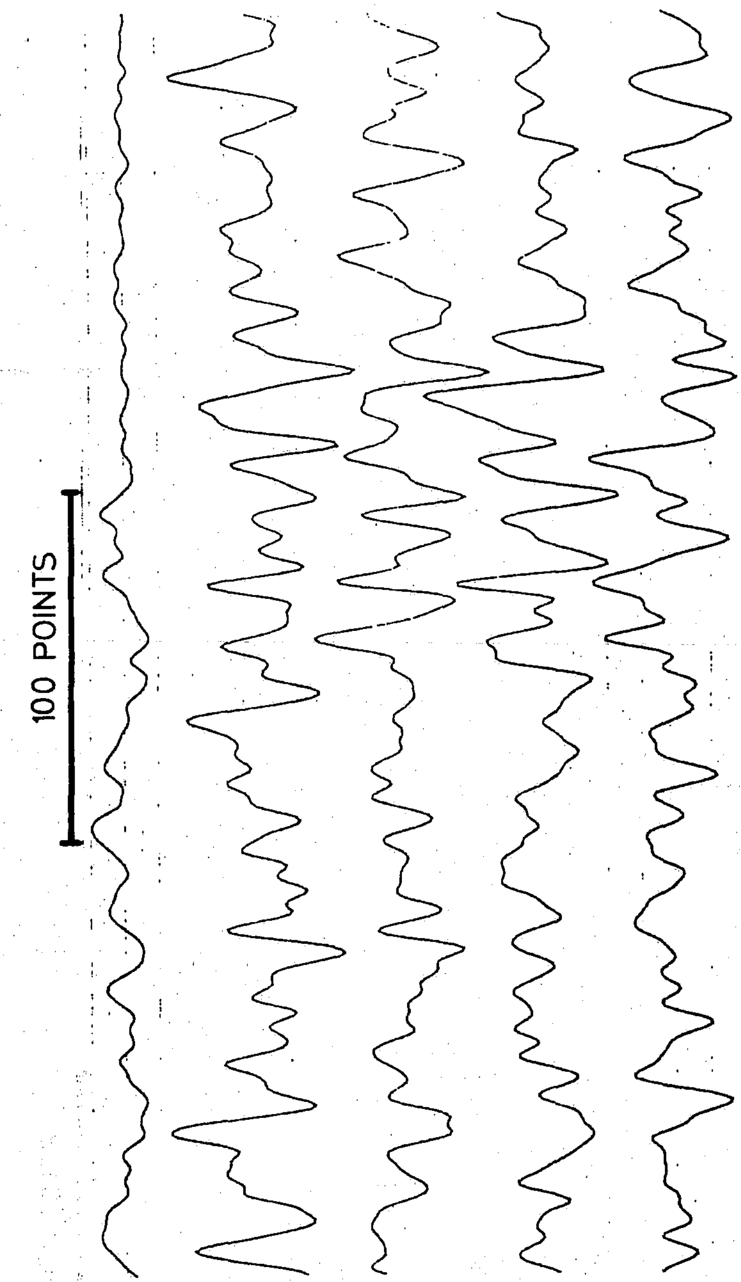

I.31 I264 PING # 7 BOTTOM DATA TRANSDUCER # 3 CONSTANT = 1.0164

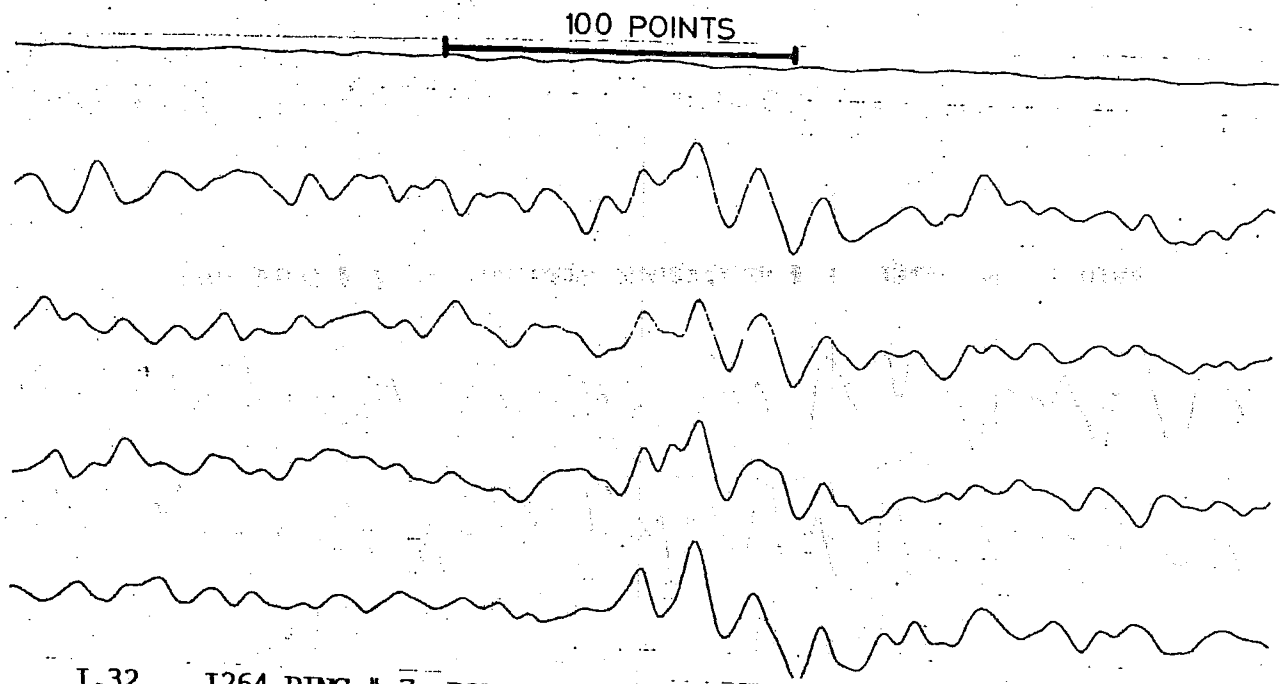

I.32 I264 PING # 7 BOTTOM DATA TRANSDUCER # 4 CONSTANT = 1.0164

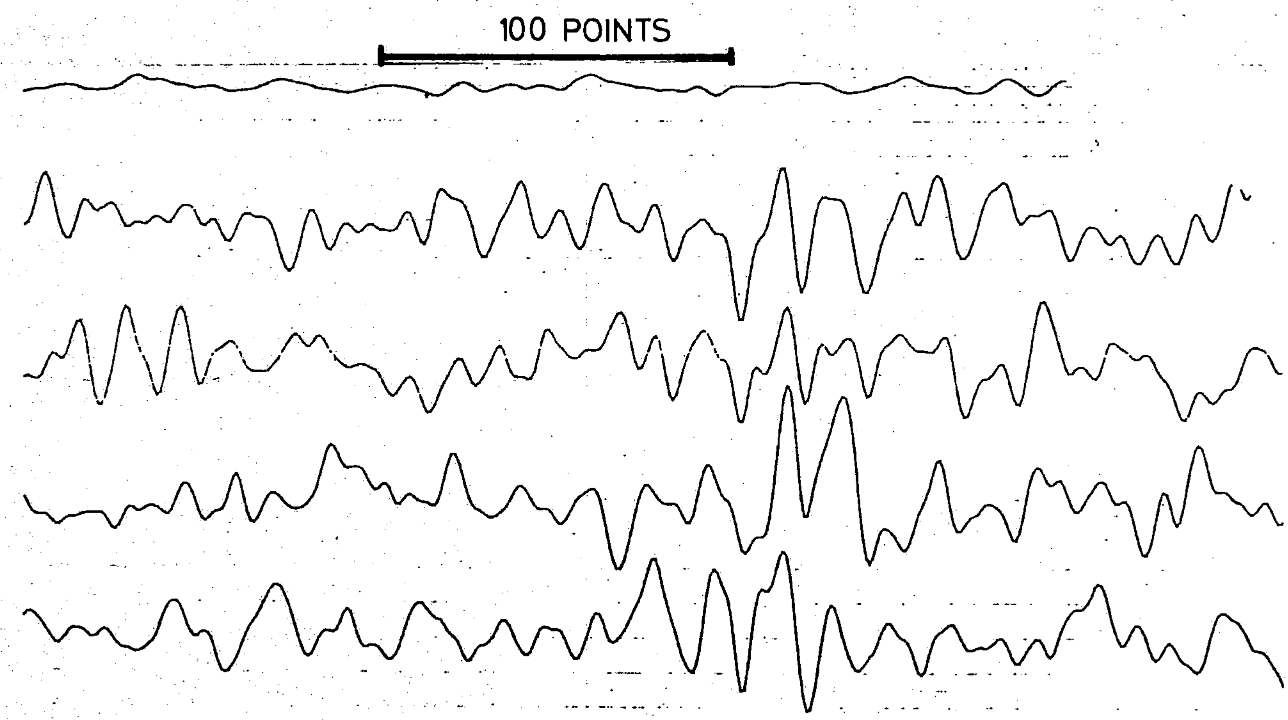

I.33 I264 PING # 7 BOTTOM DATA TRANSDUCER # 5 CONSTANT = 1.0164

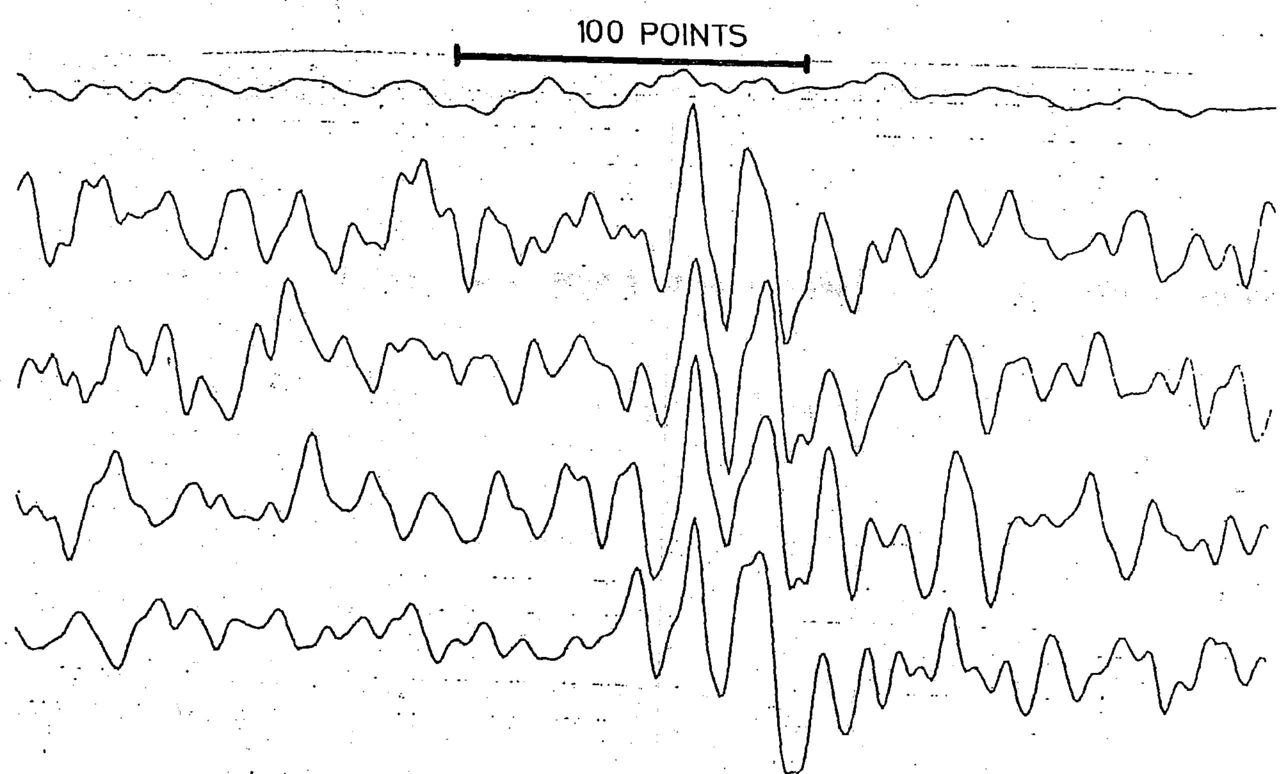

I.34 I264 PING # 7 BOTTOM DATA TRANSDUCER # 6 CONSTANT = 1.0164

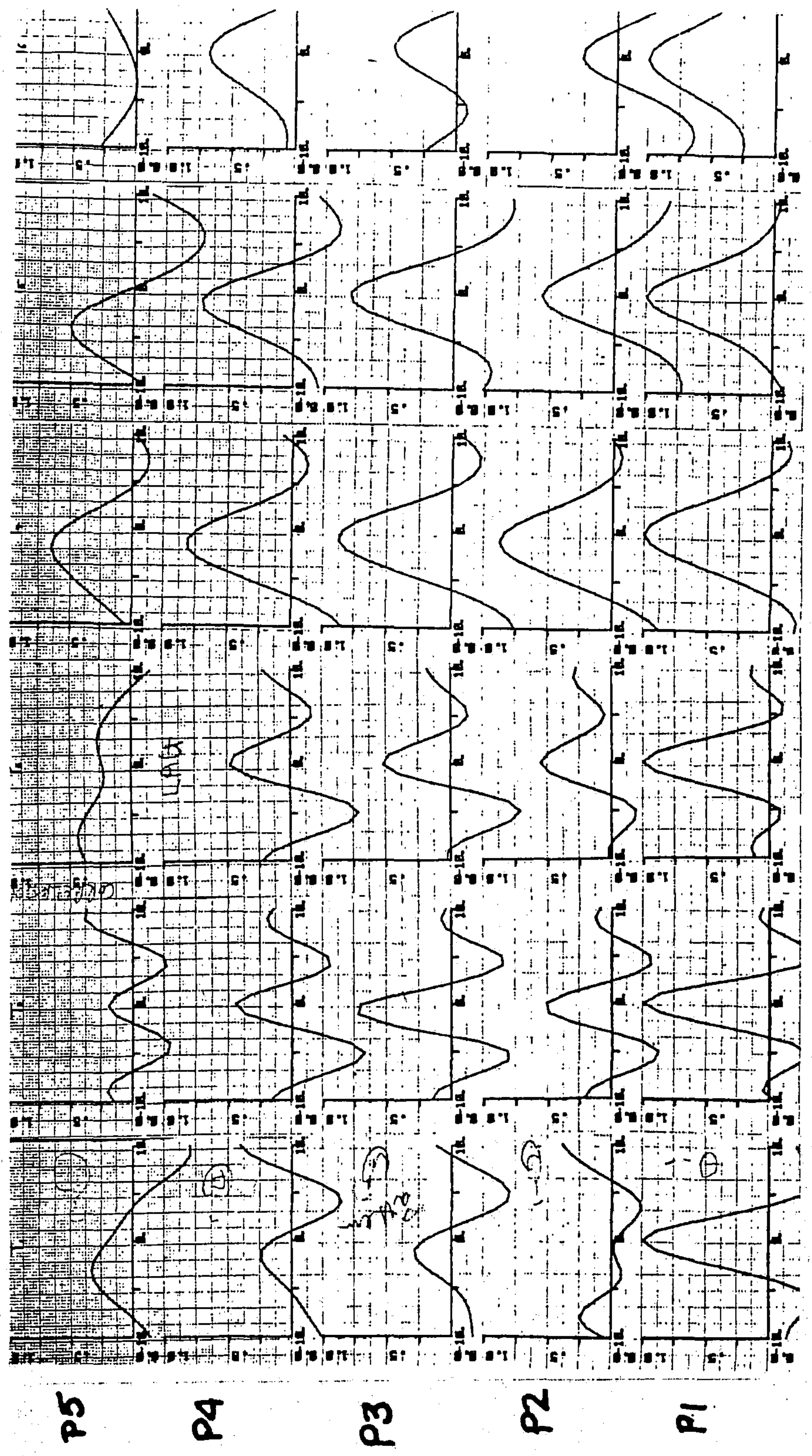

I.35 I264 PING # 4 (RANGE 166 - 246) BOTTOM AUTO-CORRELATION

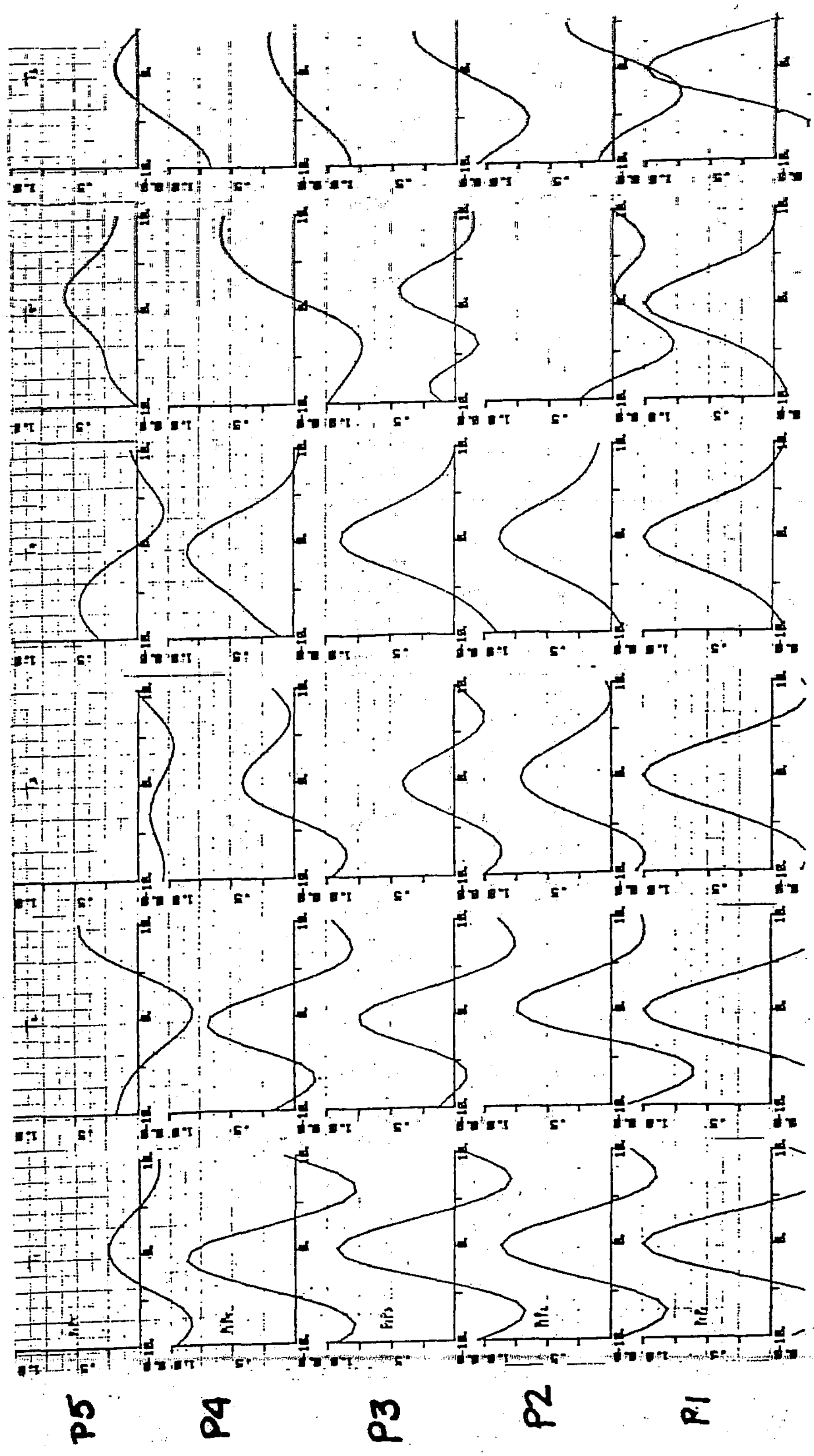

I.36 I264 PING # 5 (RANGE 166 - 246) BOTTOM AUTO-CORRELATION

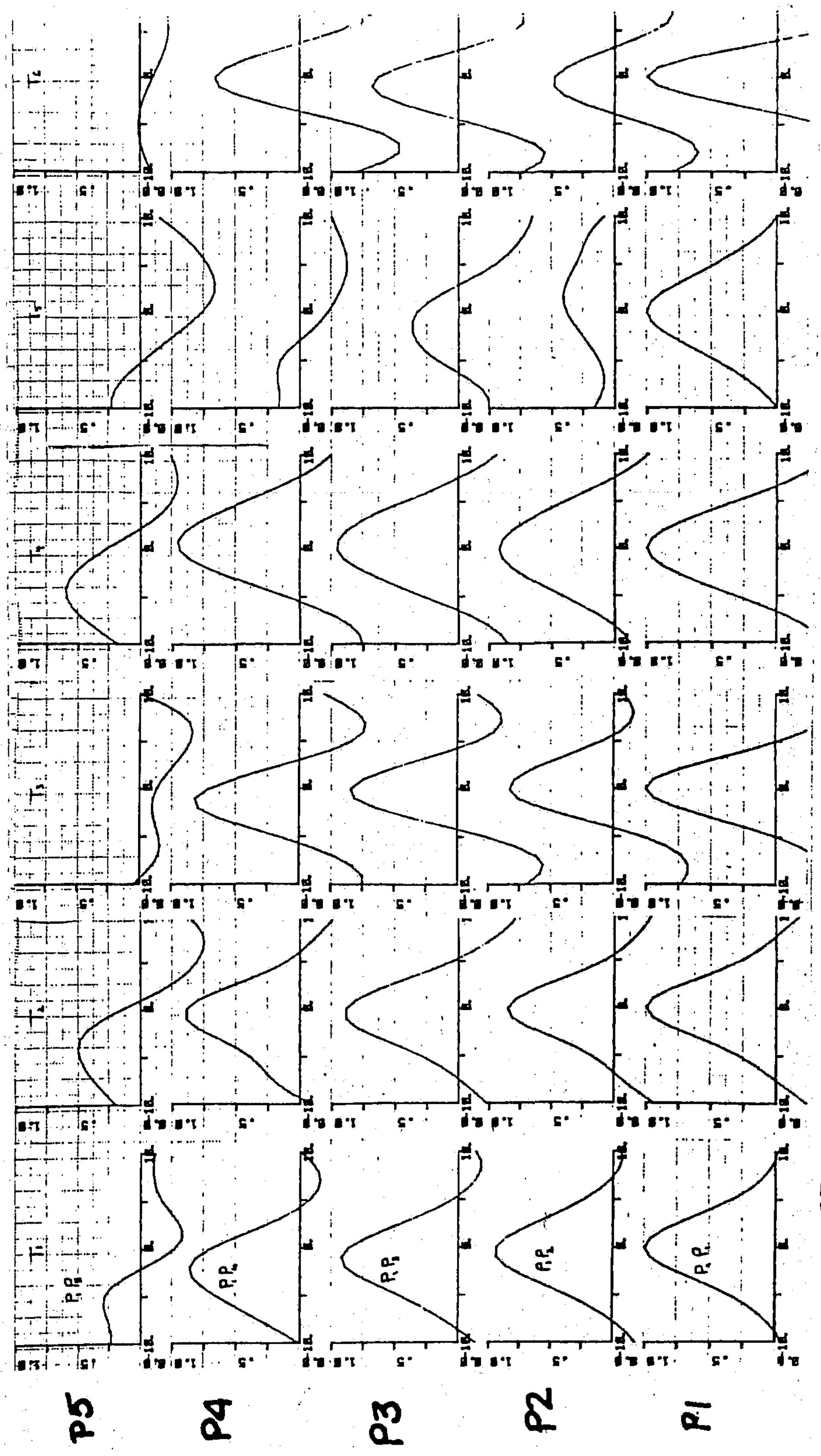

I.37 I264 PING # 6 (RANGE 166 - 246) BOTTOM AUTO-CORRELATION

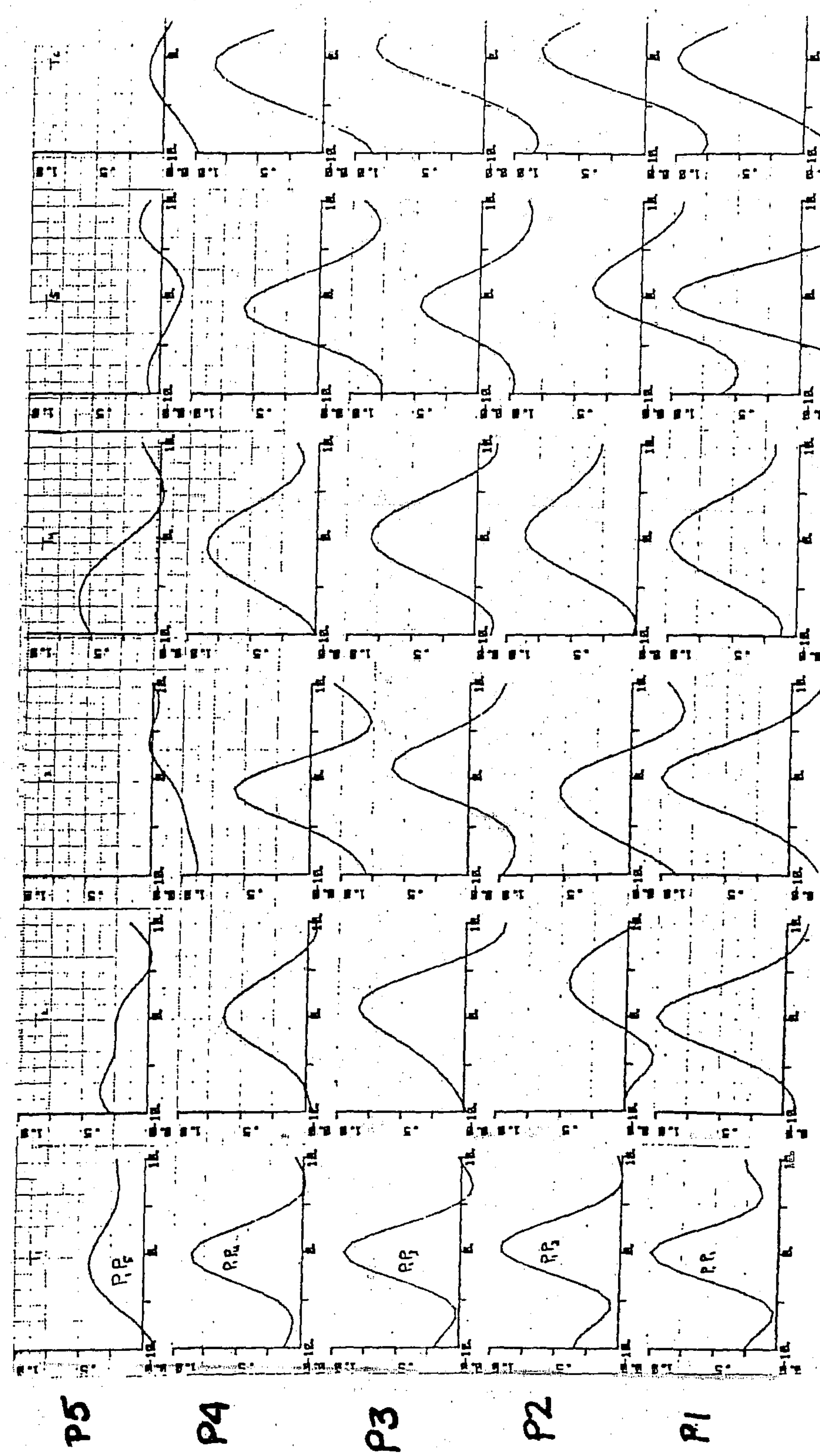

I.38 I264 PING # 7 (RANGE 166 - 246) BOTTOM AUTO-CORRELATION

BOTTOM AUTO-CORRELATION TRANSDUCER #1 (RANGE 166 - 246)(CONSTANT = 1.0164)

I264 PING #4		I39	I264 PING #5		I40
ROW	TMAX	AUTO-CORRELATION	ROW	TMAX	AUTO-CORRELATION
1	.0002	1.0000	1	.0000	1.0000
2	10.0023	.3891	2	-.0017	.8723
3	-1.0026	.2863	3	-.0010	.9211
4	10.0038	.4107	4	-.9955	.8624
5	-3.0000	.3294	5	.0005	.2425
I264 PING #4			**I264 PING #5**		
1	-.0009	1.0000	1	.0001	1.0000
2	-.0134	.5149	2	.0076	.7437
3	-.9756	.7191	3	-.0061	.7414
4	-.0042	.4480	4	-.9960	.6756
5	9.0049	.3792	5	10.0000	.4660
I264 PING #4			**I264 PING #5**		
1	.0002	1.0000	1	.0001	1.0000
2	.0014	.5510	2	.0005	.7176
3	.0068	.5187	3	-.0015	.4080
4	.0081	.4731	4	.0001	.4164
5	-7.0003	.4300	5	10.00019	.0159
I264 PING #4			**I264 PING #5**		
1	.0000	1.0000	1	.0000	1.0000
2	-.9997	.8820	2	.0009	.8872
3	-.9983	.8786	3	.0020	.8875
4	-1.0030	.8116	4	-.9993	.8470
5	-2.0000	.6477	5	-6.0001	.4573
I264 PING #4			**I264 PING #5**		
1	.0000	1.0000	1	.0001	1.0000
2	.0000	.5718	2	.0596	.2563
3	-.0045	.7994	3	1.9977	.4375
4	-1.0032	.7158	4	8.0001	.5652
5	-4.0005	.5009	5	1.9996	.5671
I264 PING #4			**I264 PING #5**		
1	-.0000	1.0000	1	.0002	1.0000
2	.0015	.2682	2	4.9997	.3804
3	.9992	.4856	3	3.9999	.3357
4	-.0002	.6820	4	3.0001	.2059
5	9.0000	.3702	5	.9998	.1748

BOTTOM AUTO-CORRELATION TRANSDUCER #1 (RANGE 166 - 246)(CONSTANT = 1.0164)

I264 PING #6 <u>I41</u>

ROW	TMAX	AUTO-CORRELATION
1	.0000	1.0000
2	-.9969	.9415
3	-1.0014	.9246
4	-2.0009	.8628
5	-5.9998	.2968

I264 PING #6

ROW	TMAX	AUTO-CORRELATION
1	-.0001	1.0000
2	-.0019	.8500
3	-.0038	.8871
4	-.0046	.8885
5	-4.0001	.5031

I264 PING #6

ROW	TMAX	AUTO-CORRELATION
1	.0000	1.0000
2	.0020	.8269
3	-.0044	.8399
4	-1.0051	.8126
5	-1.0062	.0497

I264 PING #6

ROW	TMAX	AUTO-CORRELATION
1	.0000	1.0000
2	.0000	.9187
3	.0015	.9562
4	.9985	.9510
5	-4.0005	.5974

I264 PING #6

ROW	TMAX	AUTO-CORRELATION
1	.0000	1.0000
2	1.9998	.4085
3	-1.0007	.3633
4	-6.0003	.1759
5	-6.0268	.2276

I264 PING #6

ROW	TMAX	AUTO-CORRELATION
1	.0000	1.0000
2	-.9960	.4828
3	-.9984	.6809
4	-.0029	.6629
5	-5.0000	.0133

I264 PING #7 <u>I42</u>

ROW	TMAX	AUTO-CORRELATION
1	.0000	1.0000
2	-.0070	.9227
3	-.0011	.9183
4	-.0027	.8644
5	-1.0000	.4204

I264 PING #7

ROW	TMAX	AUTO-CORRELATION
1	.0000	1.0000
2	3.9996	.4387
3	1.0005	.8366
4	.0006	.6438
5	-7.9997	.3619

I264 PING #7

ROW	TMAX	AUTO-CORRELATION
1	.0000	1.0000
2	-1.0010	.5418
3	1.0026	.6070
4	-1.0030	.5805
5	4.0000	.0258

I264 PING #7

ROW	TMAX	AUTO-CORRELATION
1	.0000	1.0000
2	.9991	.8706
3	.0011	.8226
4	-.9996	.8581
5	6.0002	.5977

I264 PING #7

ROW	TMAX	AUTO-CORRELATION
1	.0000	1.0000
2	.9995	.3748
3	-.9988	.4651
4	-1.0012	.5838
5	7.9997	.4711

I264 PING #7

ROW	TMAX	AUTO-CORRELATION
1	.0000	1.0000
2	.9988	.8043
3	1.0009	.8462
4	-.9981	.8506
5	-1.0001	.1108

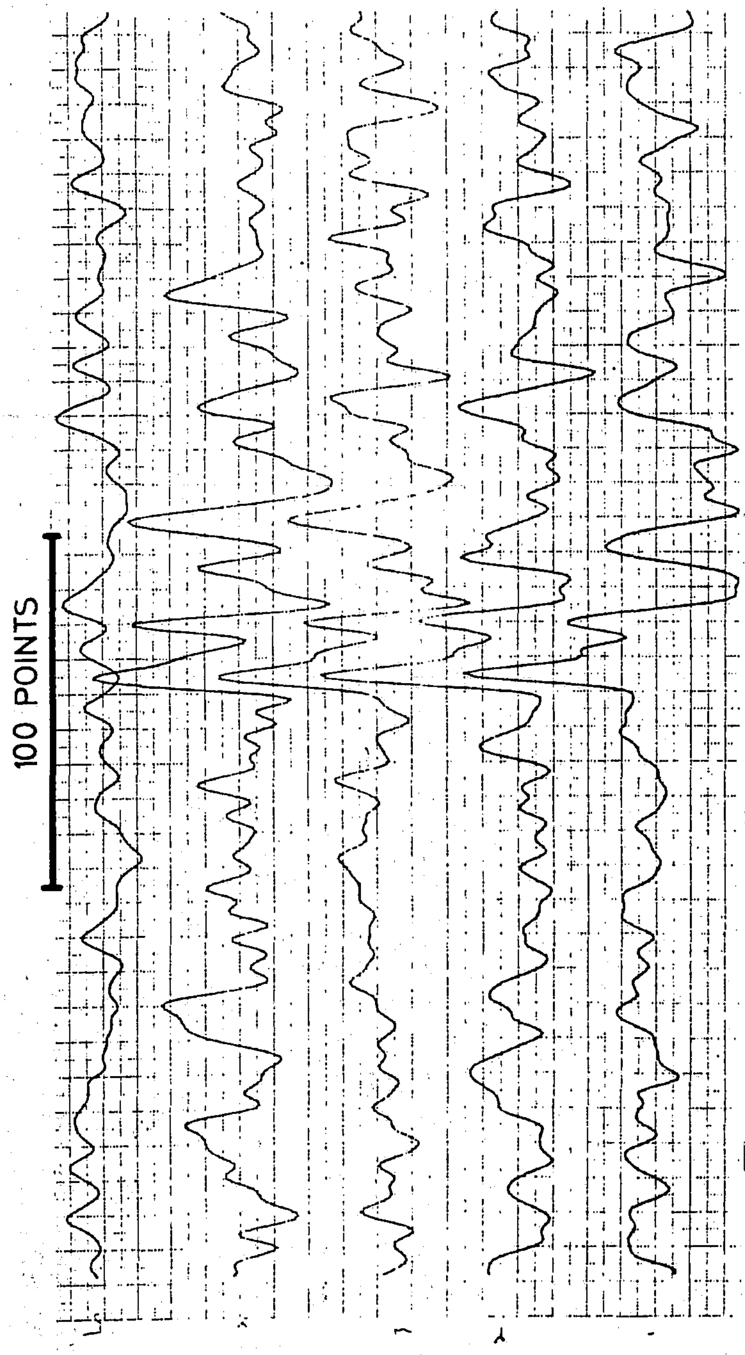

I.43 I271 PING # 4 BOTTOM DATA TRANSDUCER # 1

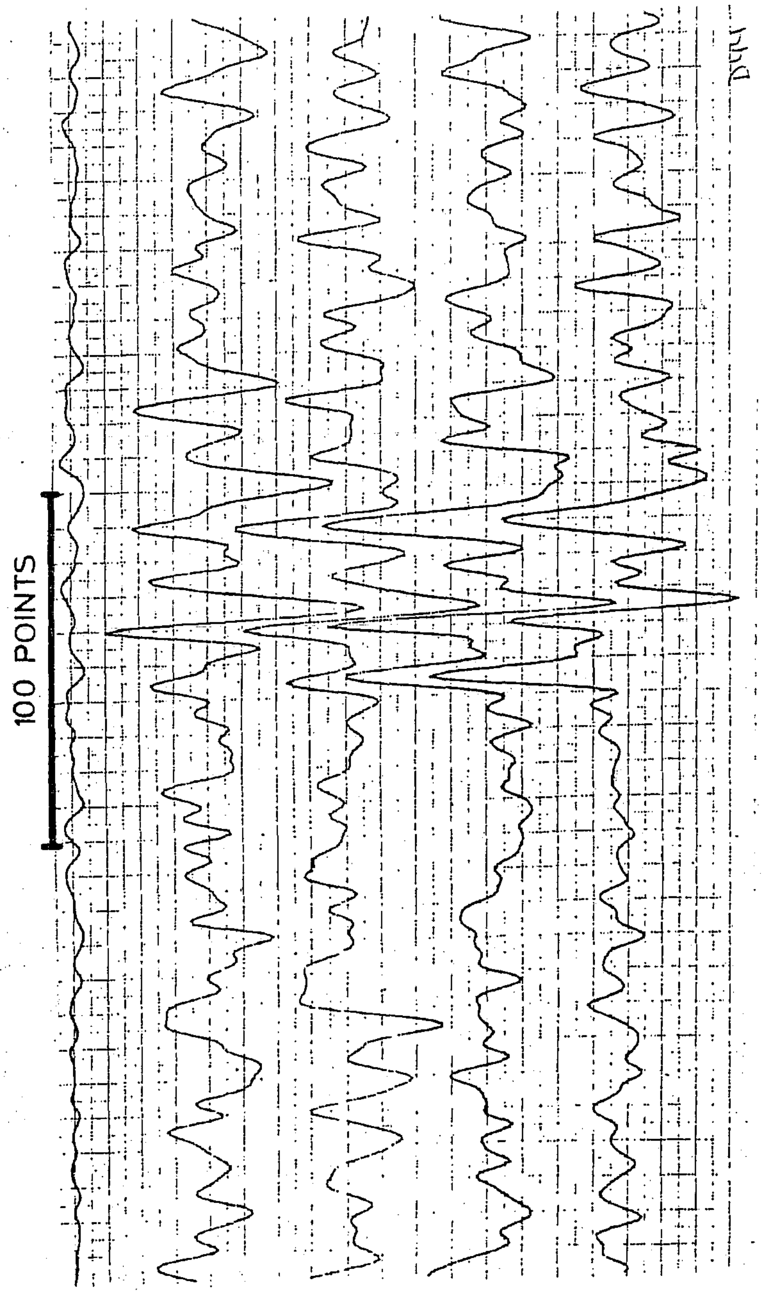

I.44 I271 PING # 4 BOTTOM DATA TRANSDUCER # 2

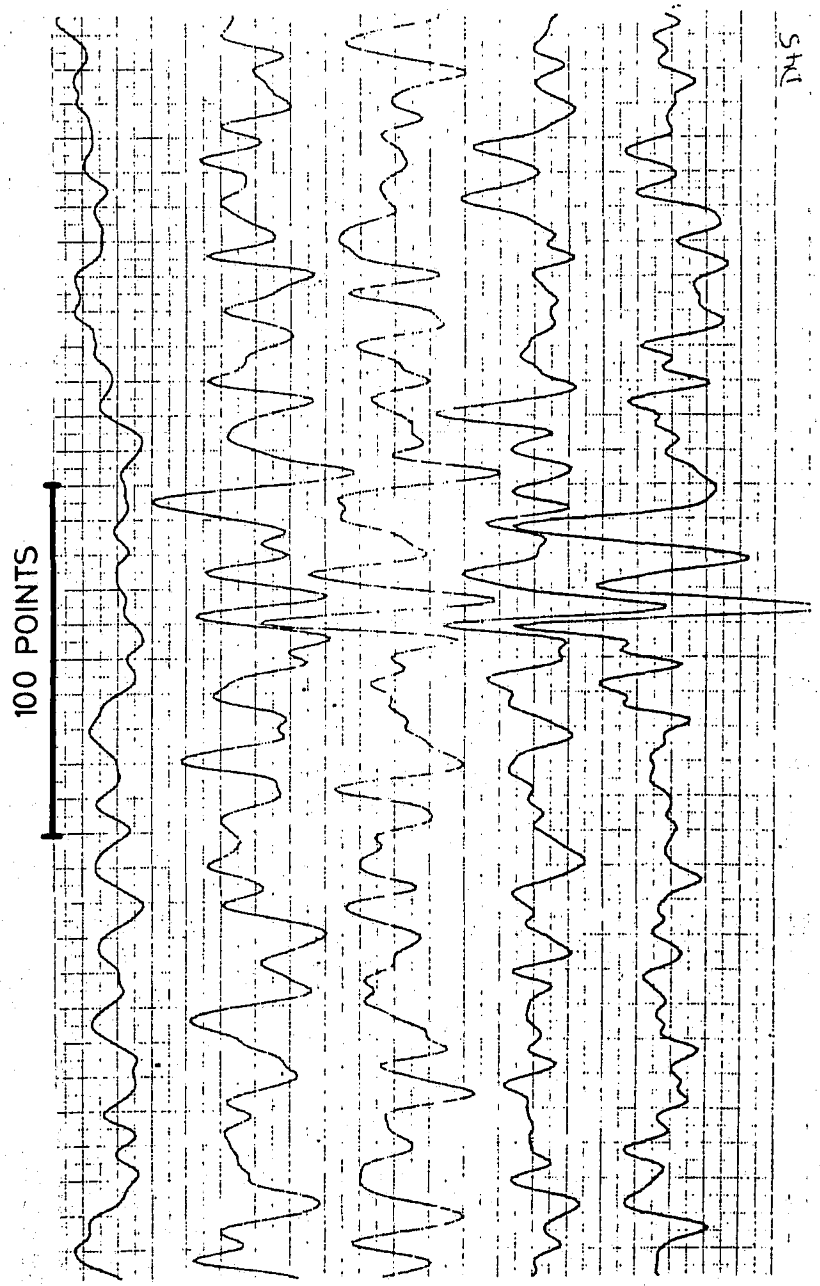

I.45 I271 PING # 4 BOTTOM DATA TRANSDUCER # 3

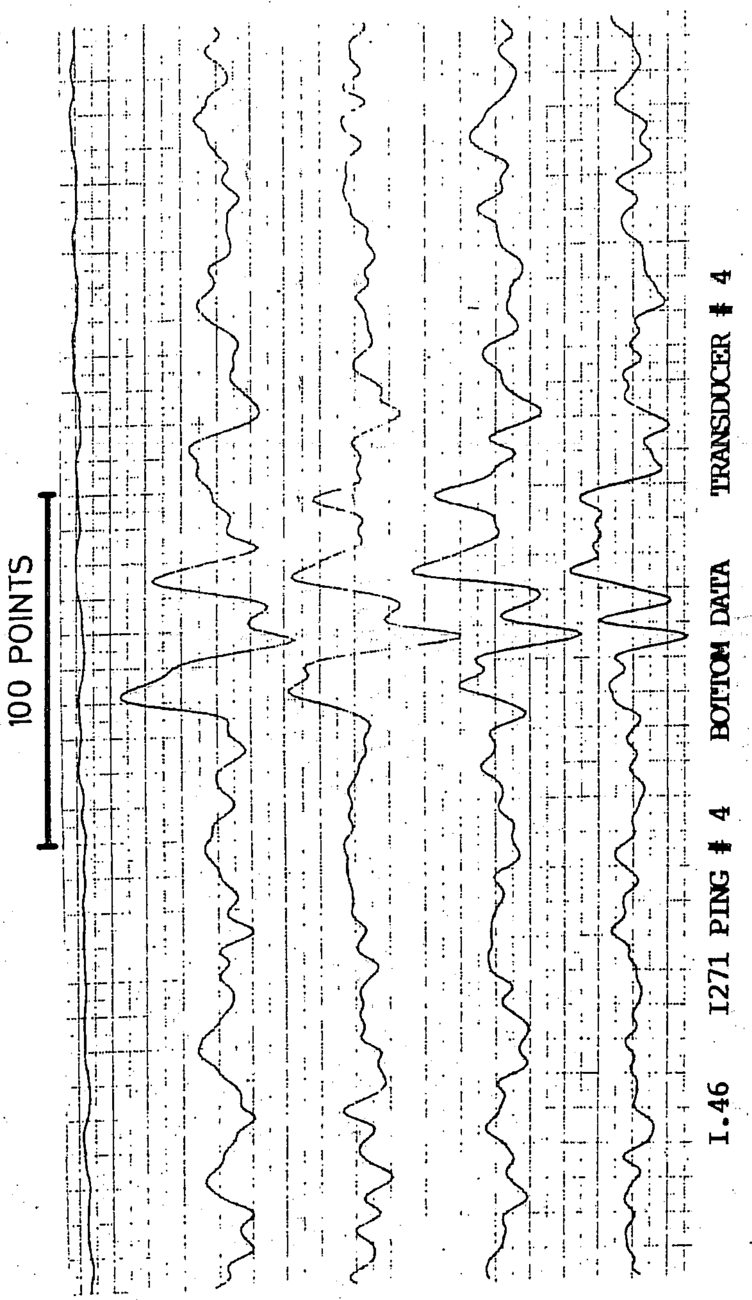
100 POINTS
I.46 I271 PING # 4 BOTTOM DATA TRANSDUCER # 4

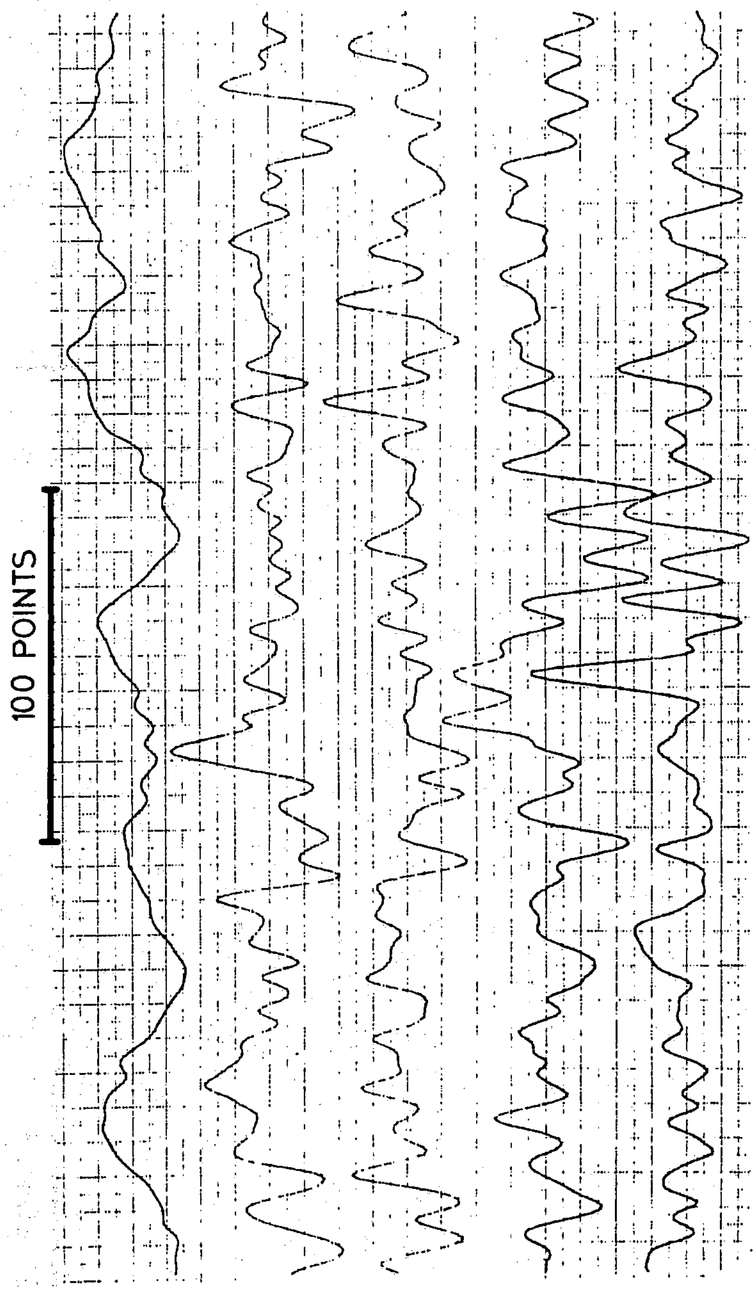

I.48 I271 PING # 4 BOTTOM DATA TRANSDUCER # 6

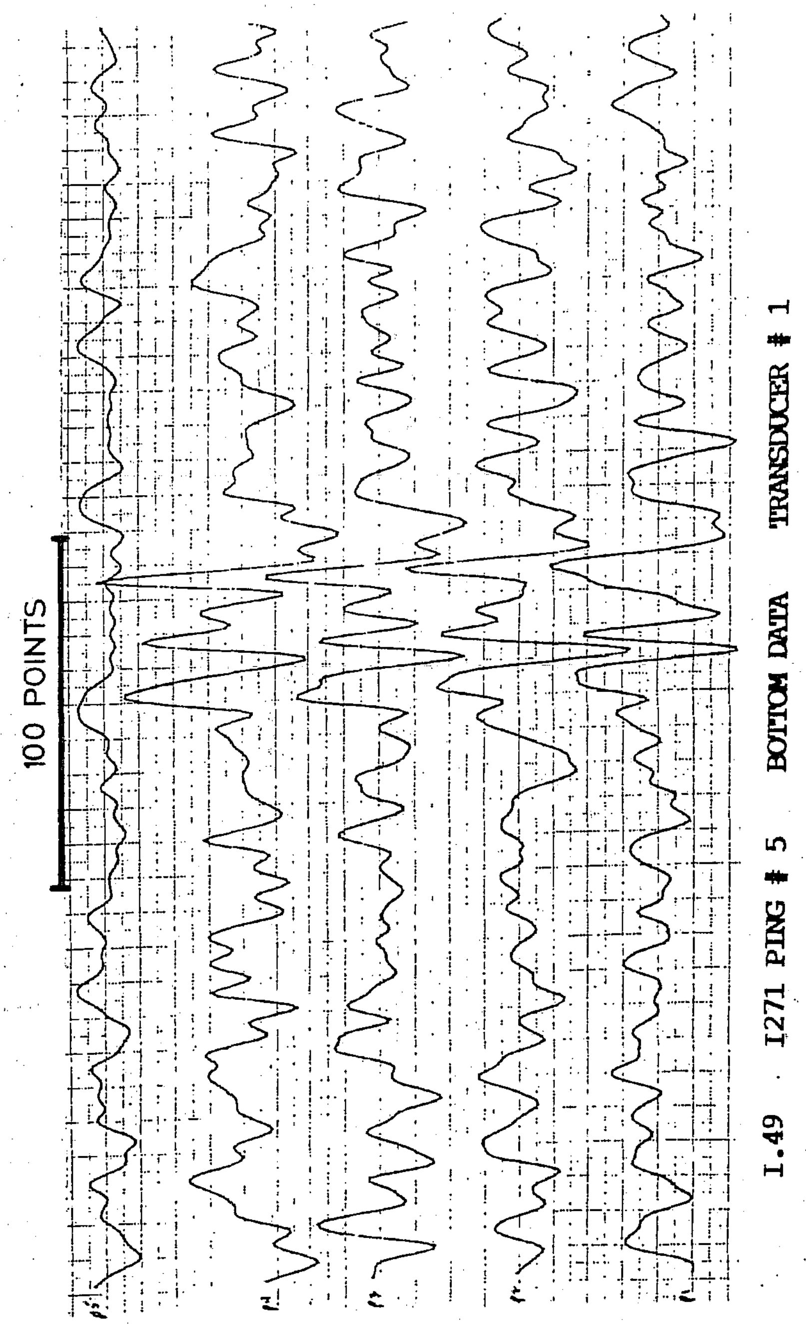
100 POINTS
I.49 I271 PING # 5 BOTTOM DATA TRANSDUCER # 1

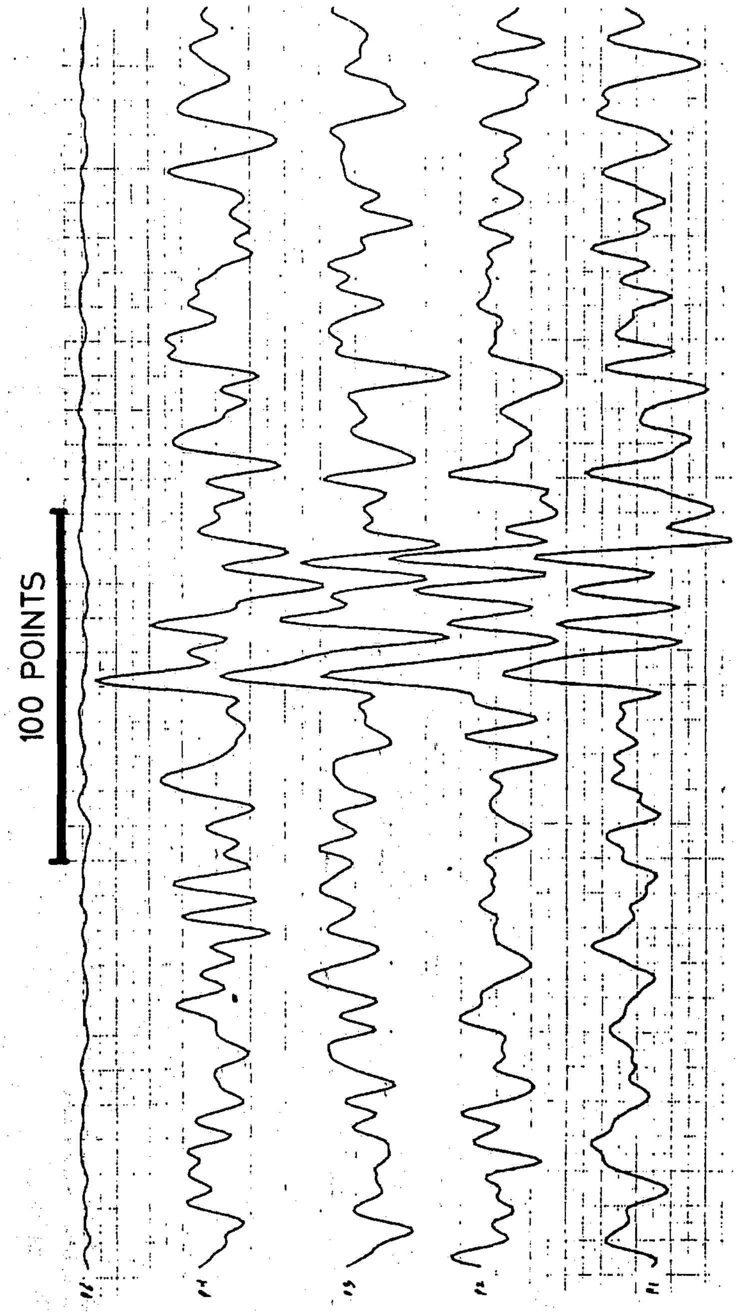

I.50 I271 PING # 5 BOTTOM DATA TRANSDUCER # 2

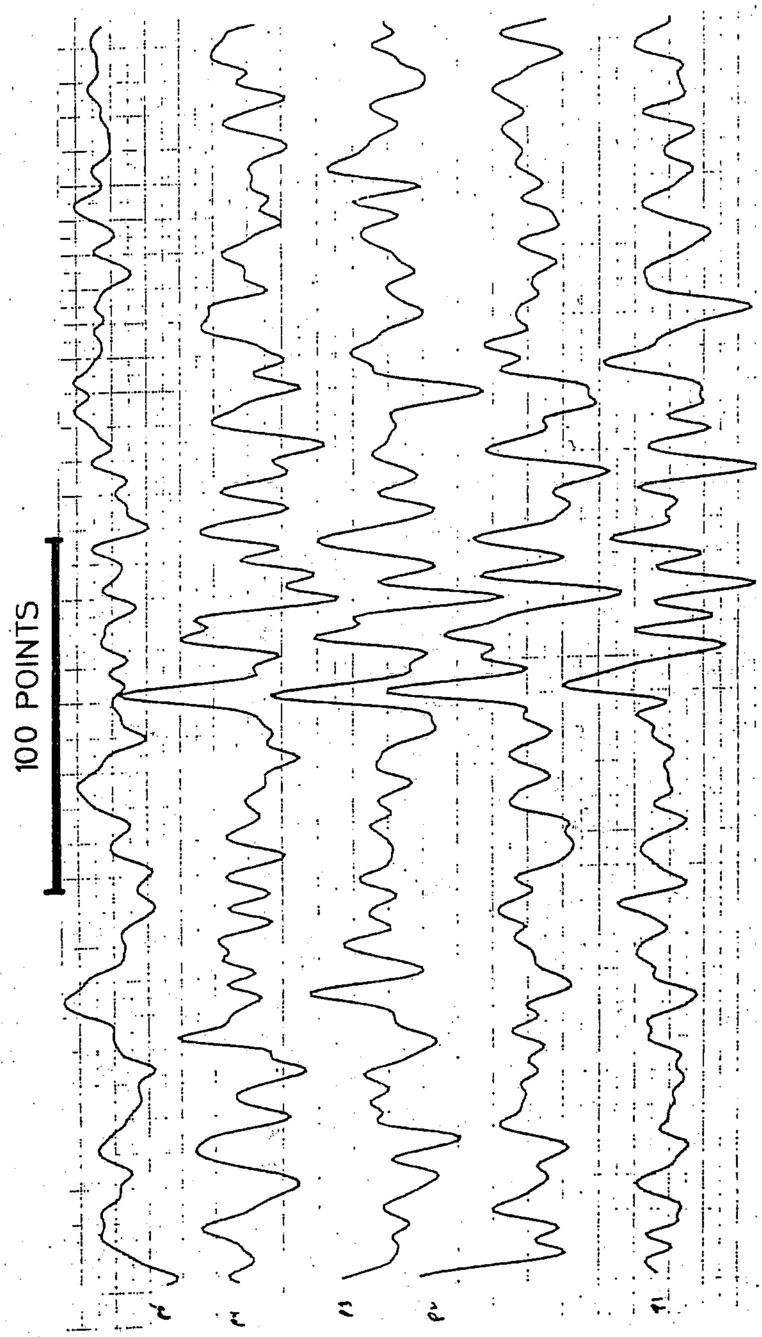

I.51 I271 PING # 5 BOTTOM DATA TRANSDUCER # 3

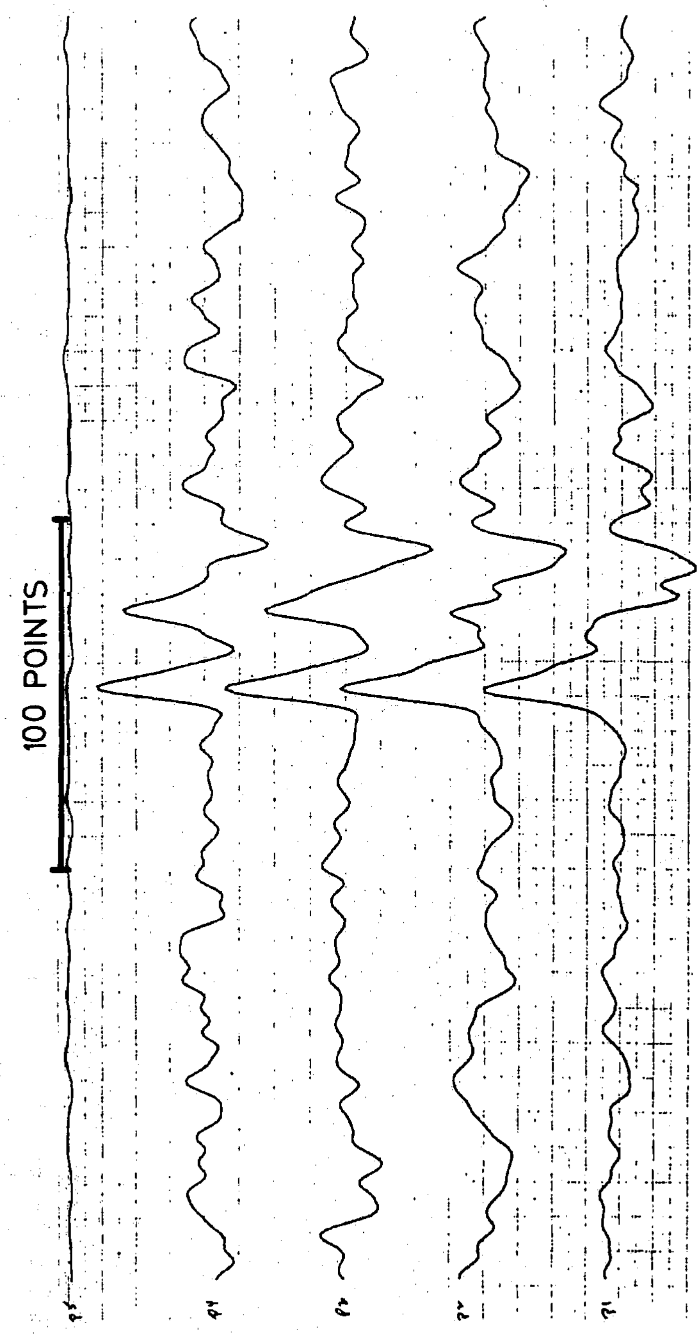

I.52 I271 PING # 5 BOTTOM DATA TRANSDUCER # 4

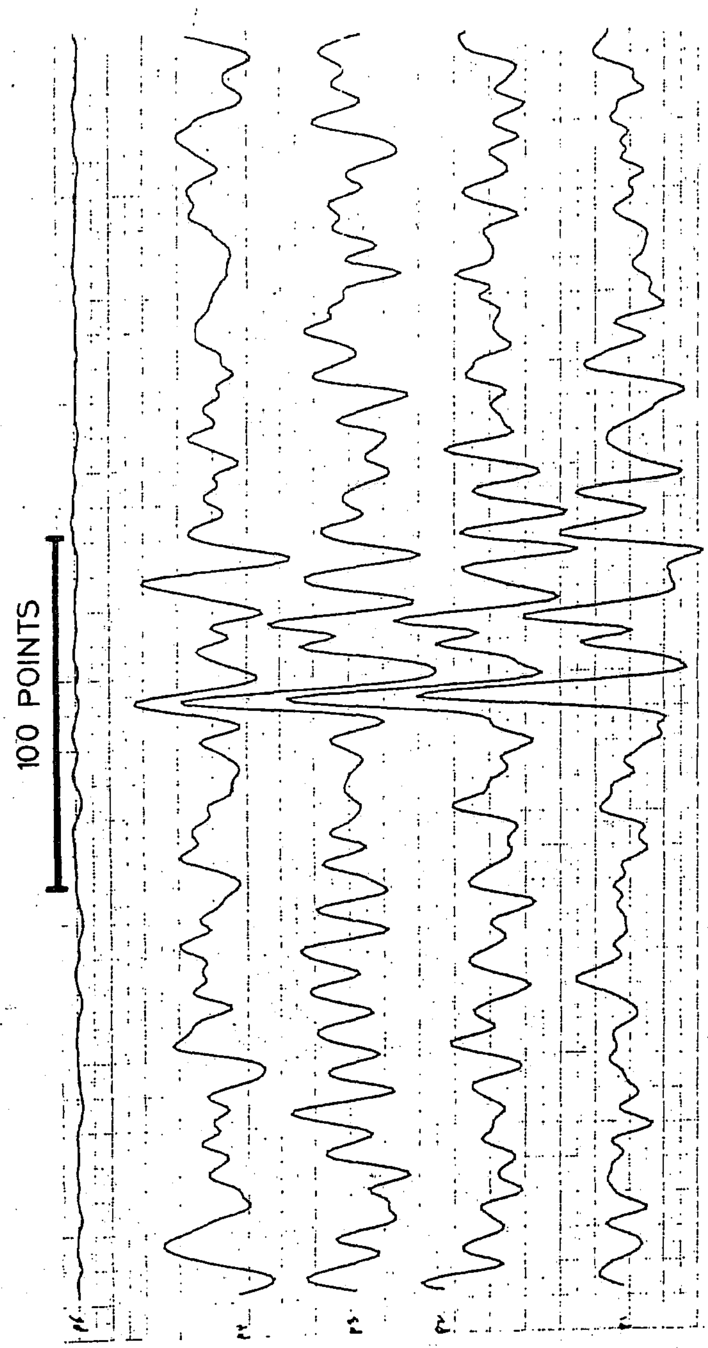

I.53 I271 PING # 5 BOTTOM DATA TRANSDUCER # 5

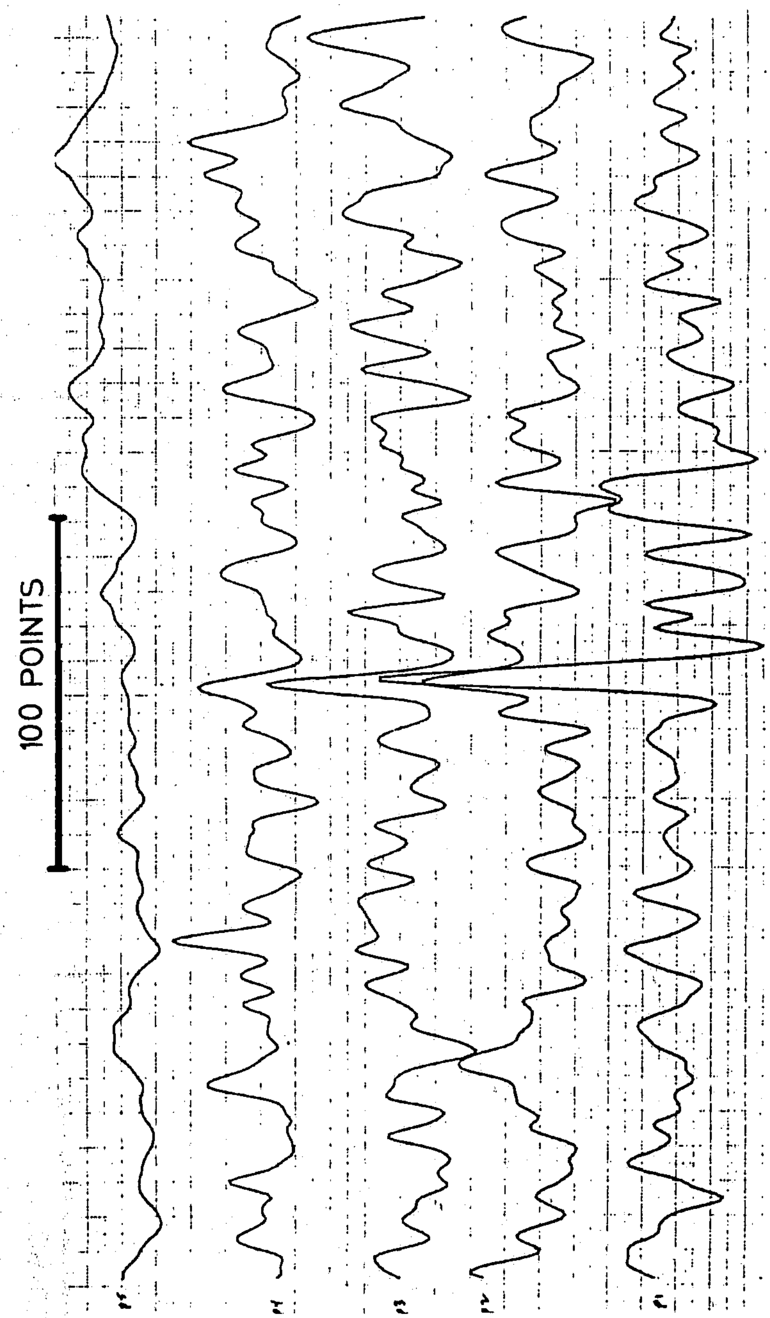

I.54 I271 PING # 5 BOTTOM DATA TRANSDUCER # 6

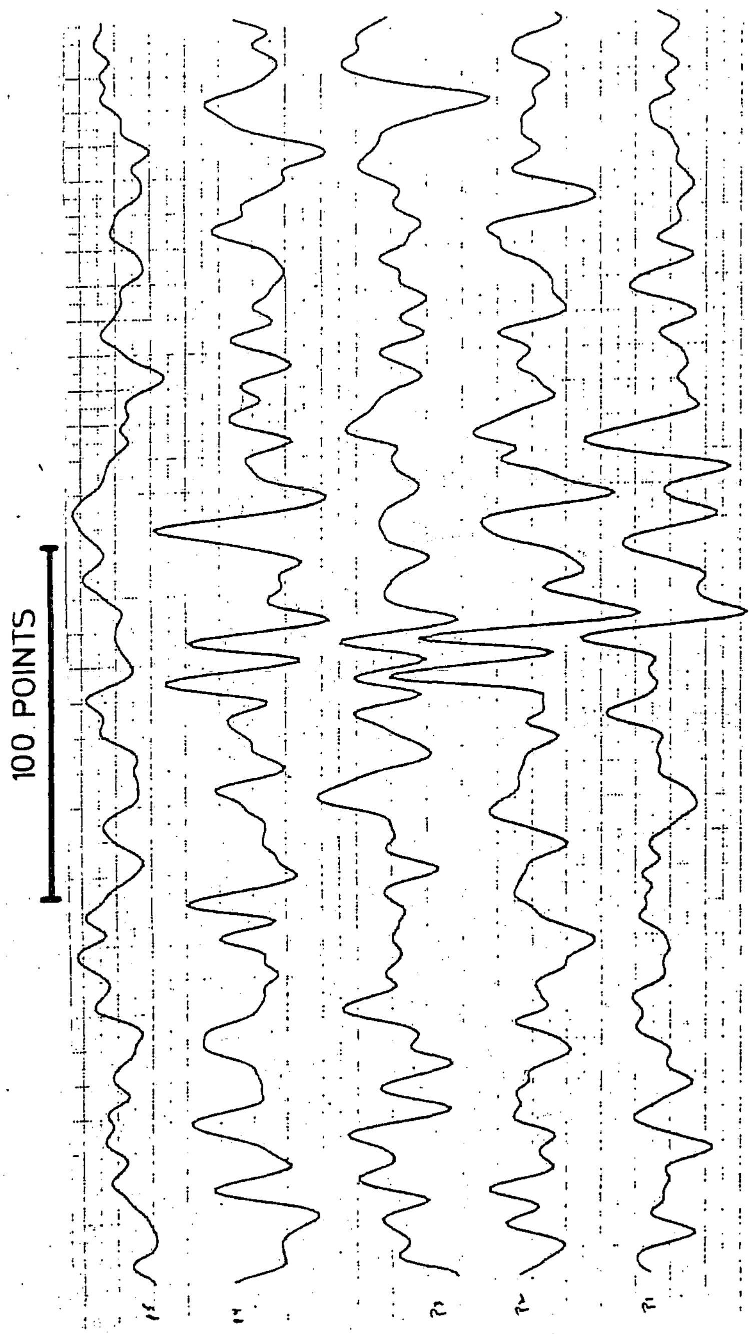

I.55 I271 PING # 6 BOTTOM DATA TRANSDUCER # 1

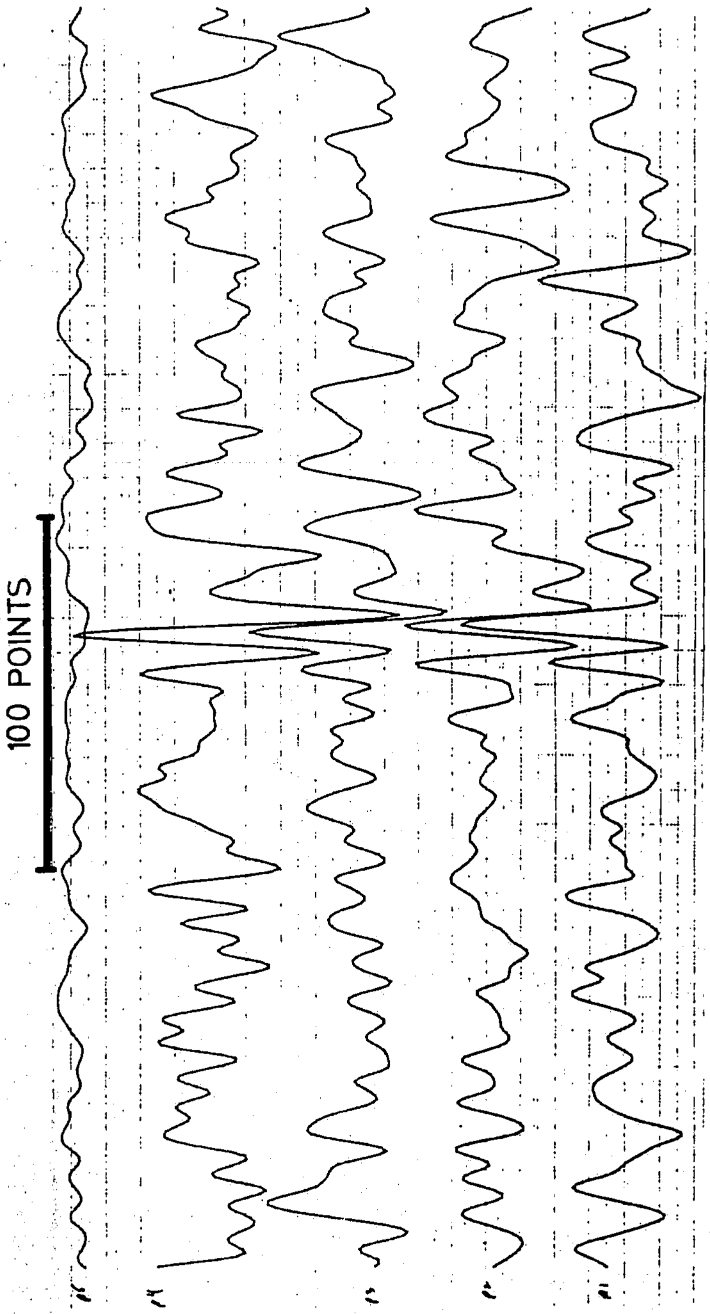

I.56 I271 PING # 6 BOTTOM DATA TRANSDUCER # 2

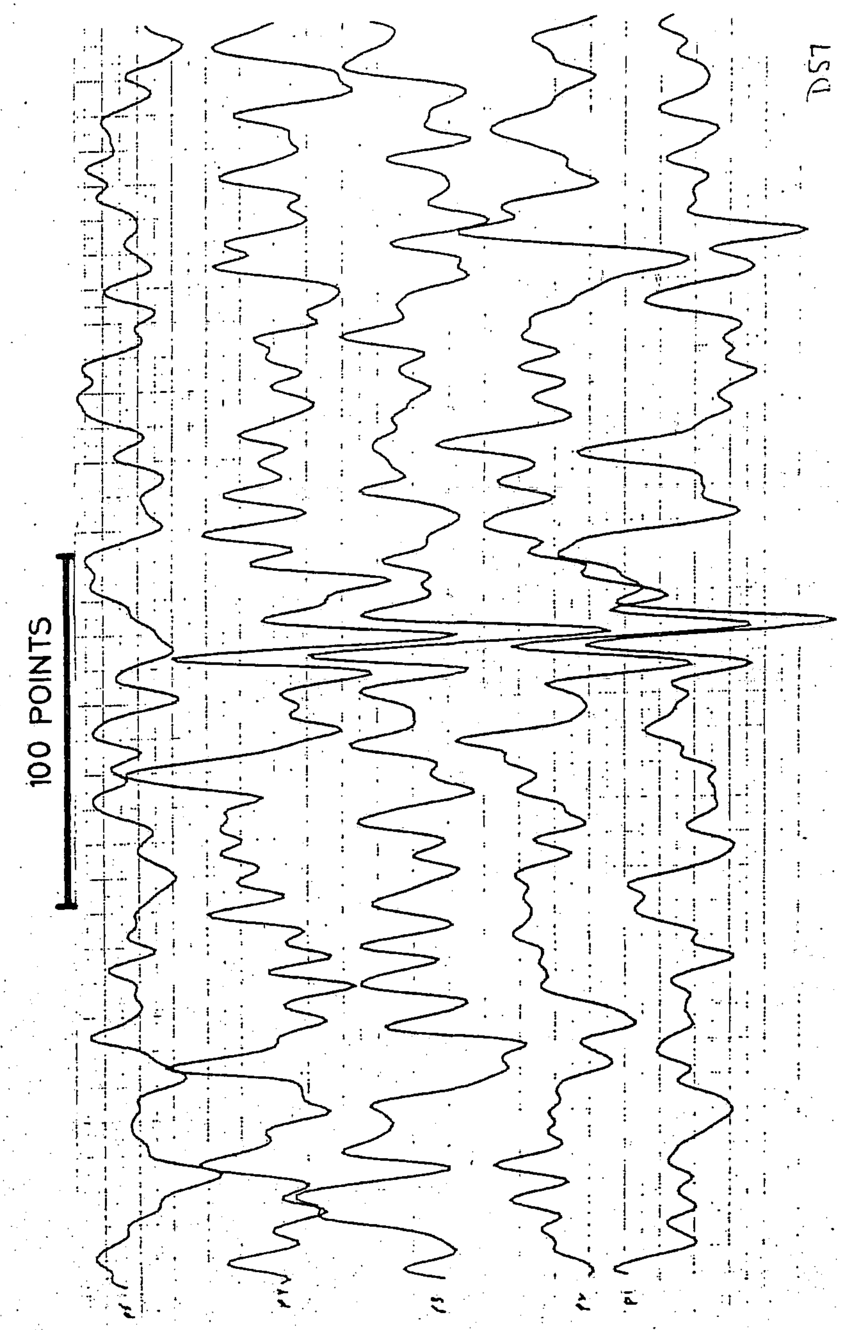

I.57 I271 PING # 6 BOTTOM DATA TRANSDUCER # 3

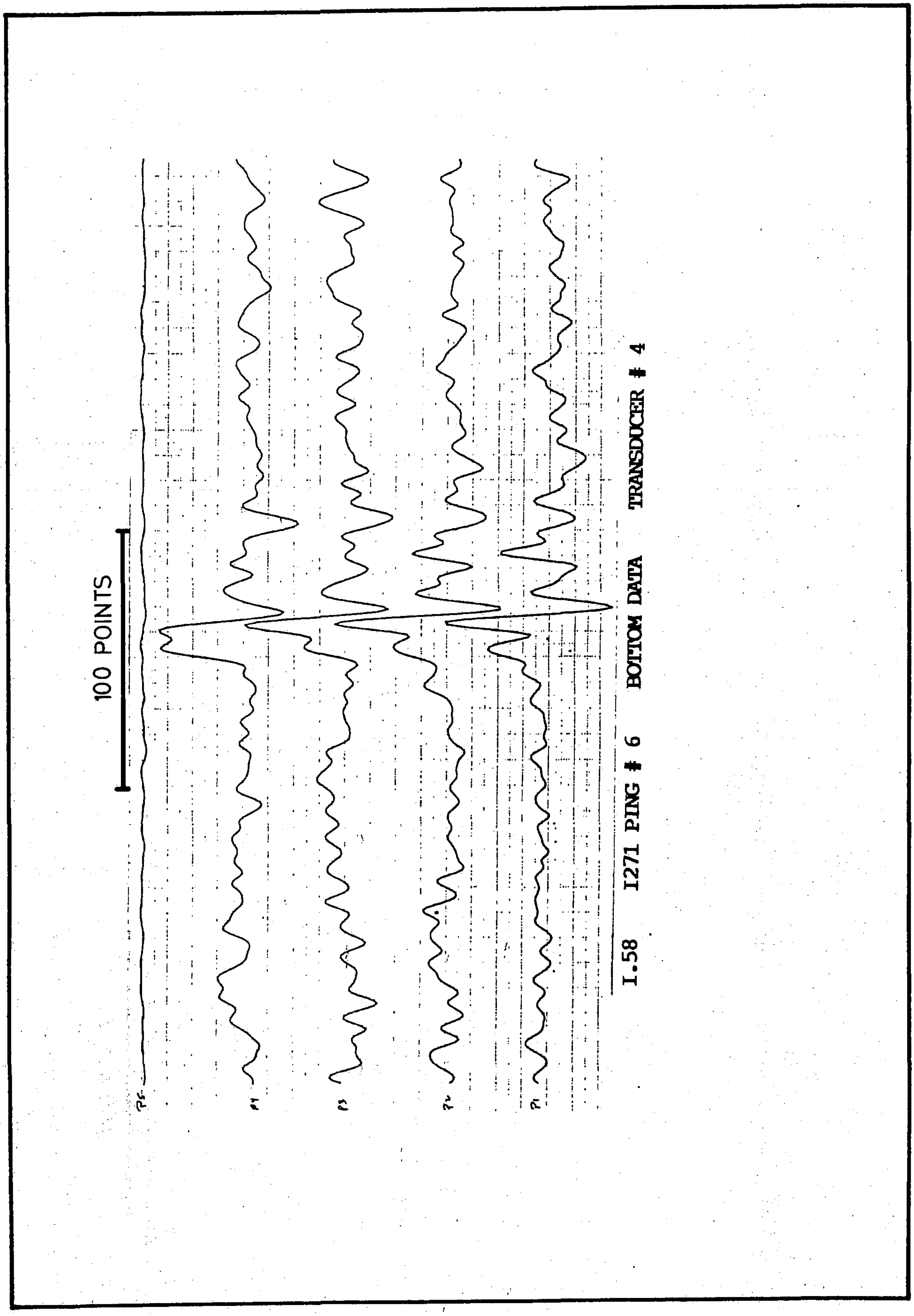
100 POINTS
I.58 I271 PING # 6 BOTTOM DATA TRANSDUCER # 4

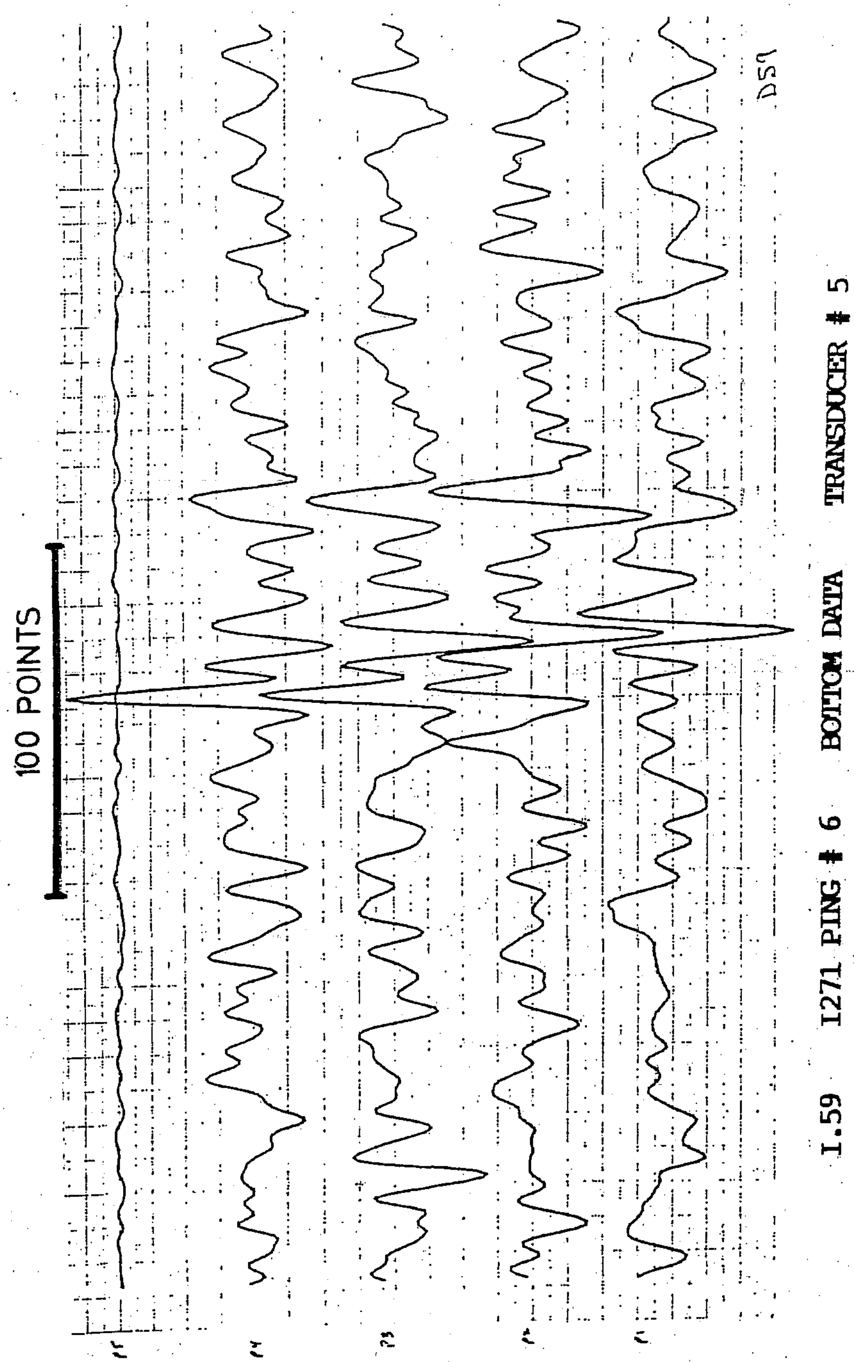
100 POINTS
I.59 I271 PING # 6 BOTTOM DATA TRANSDUCER # 5

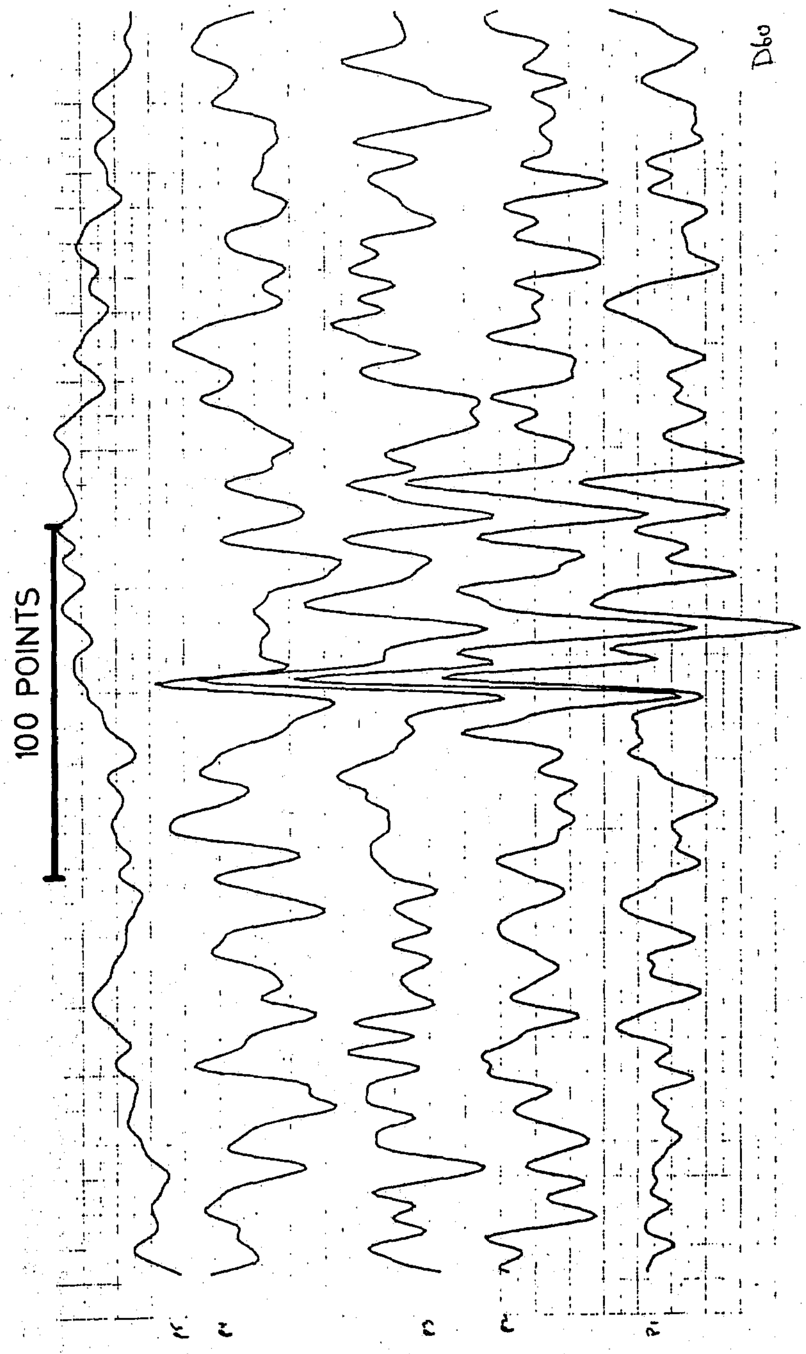

I.60 I271 PING # 6 BOTTOM DATA TRANSDUCER # 6

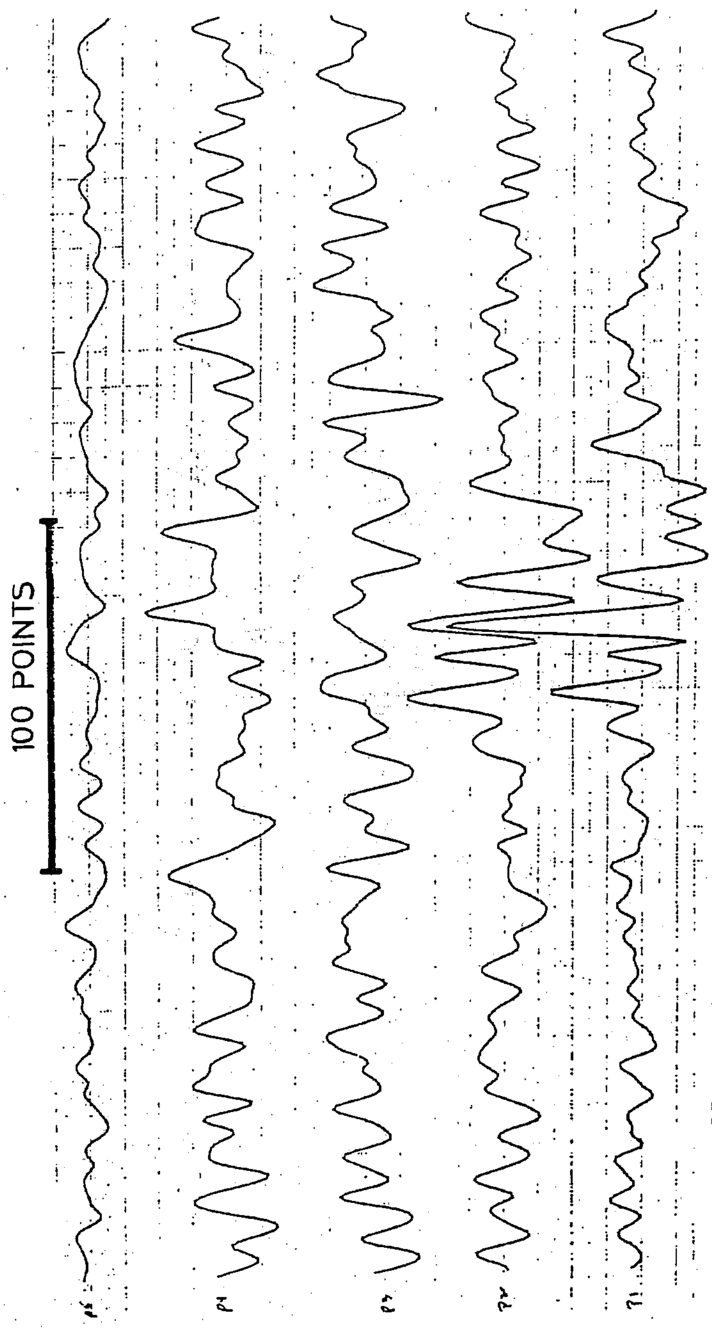

I.61 I271 PING # 7 BOTTOM DATA TRANSDUCER # 1

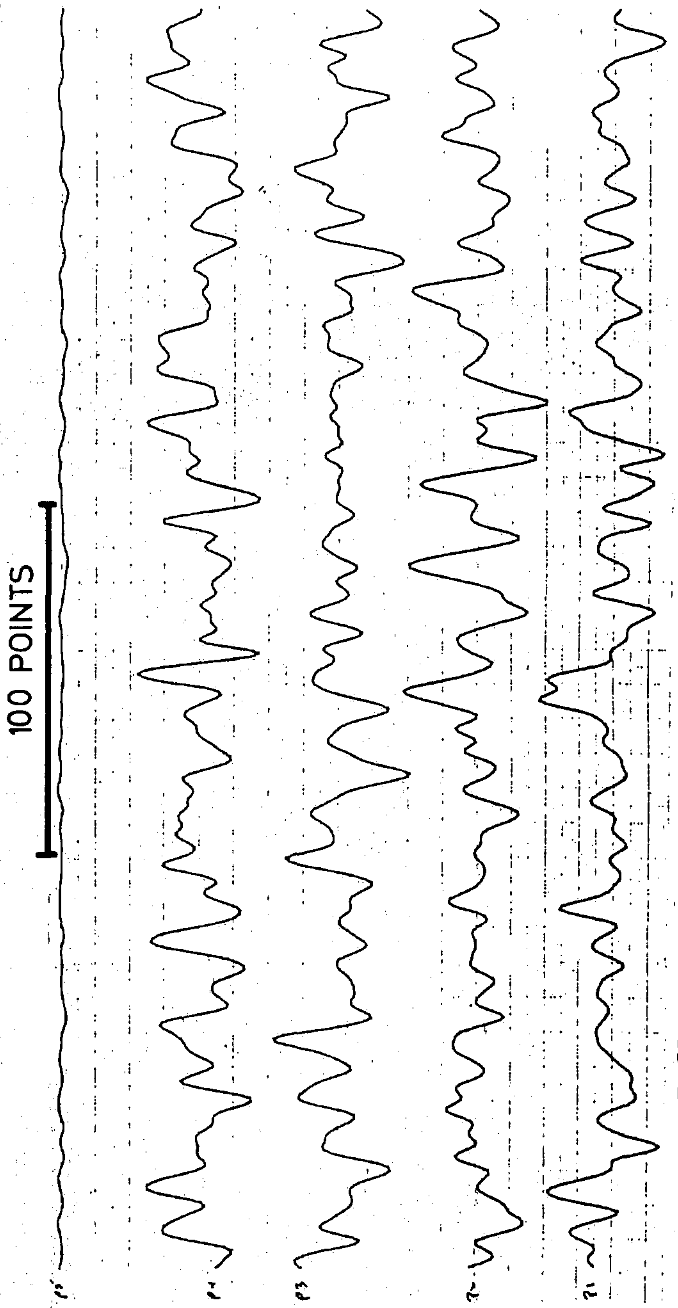

I.62 I271 PING # 7 BOTTOM DATA TRANSDUCER # 2

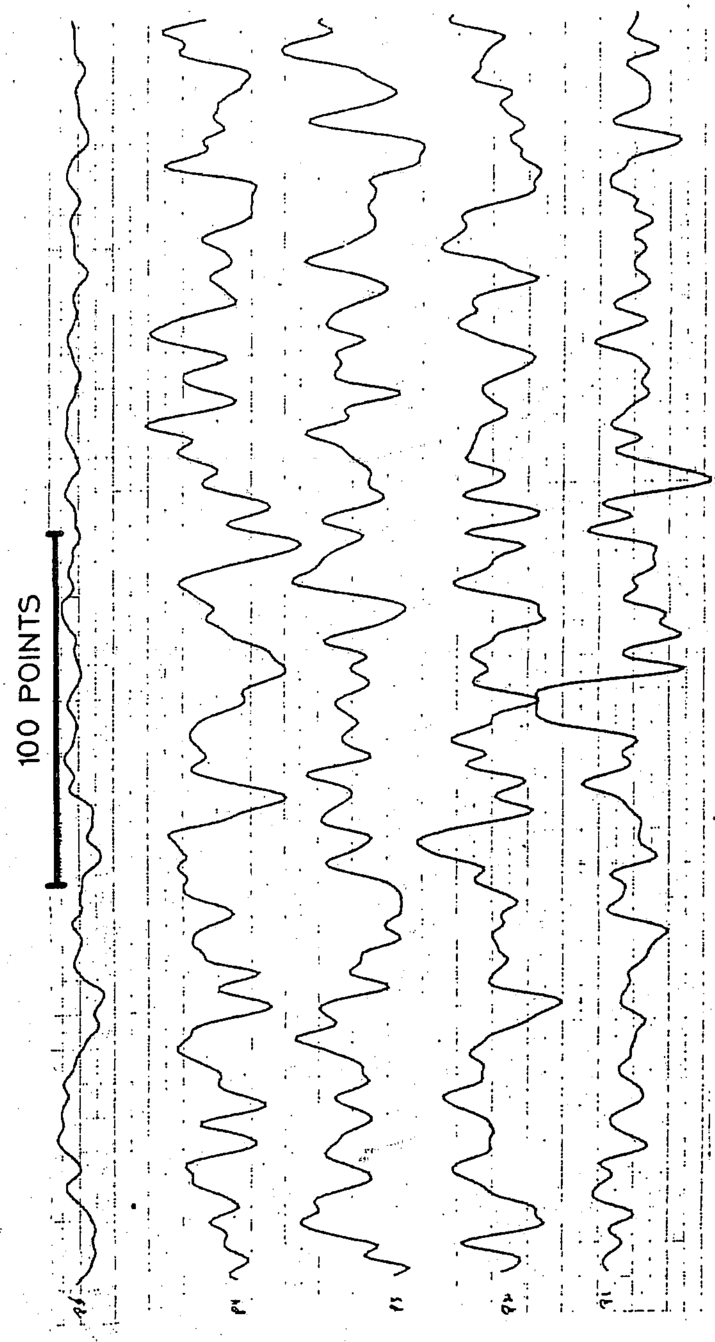

I.63 I271 PING # 7 BOTTOM DATA TRANSDUCER # 3

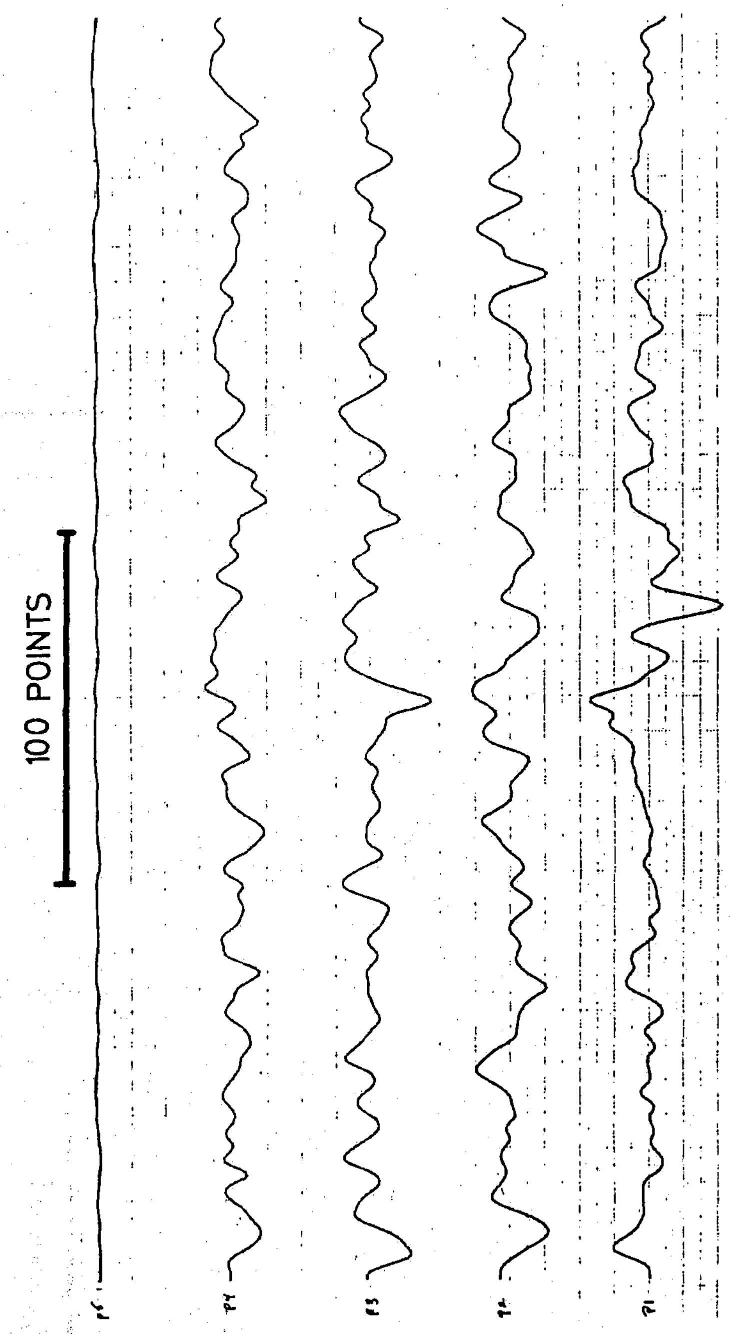

I.64 I271 PING # 7 BOTTOM DATA TRANSDUCER # 4

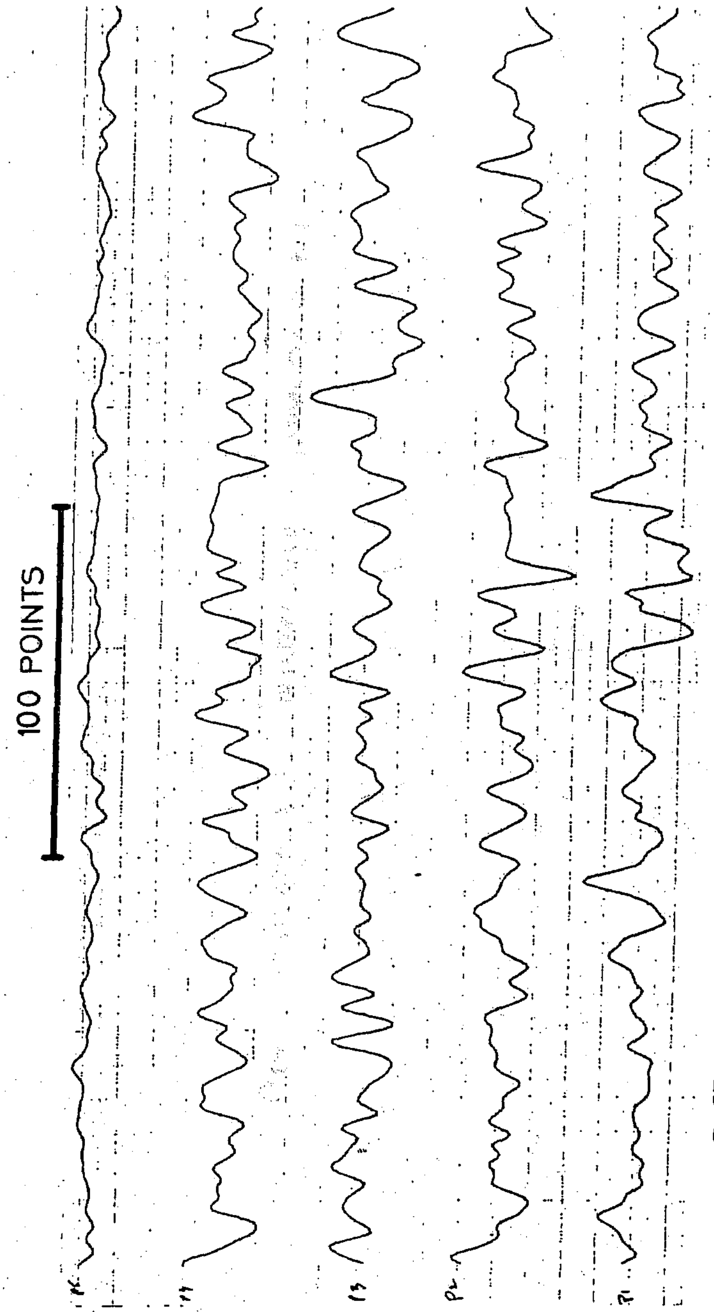

I.65 I271 PING # 7 BOTTOM DATA TRANSDUCER # 5

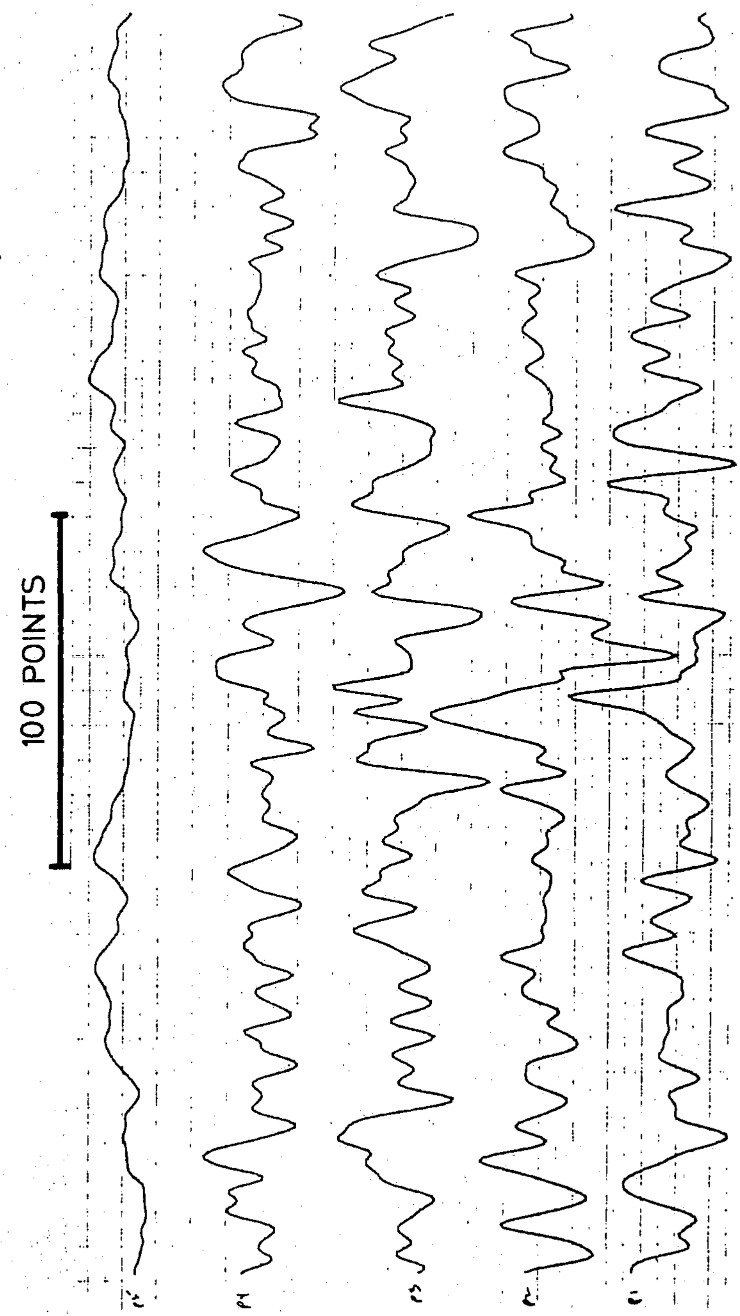

I.66 I271 PING # 7 BOTTOM DATA TRANSDUCER # 6

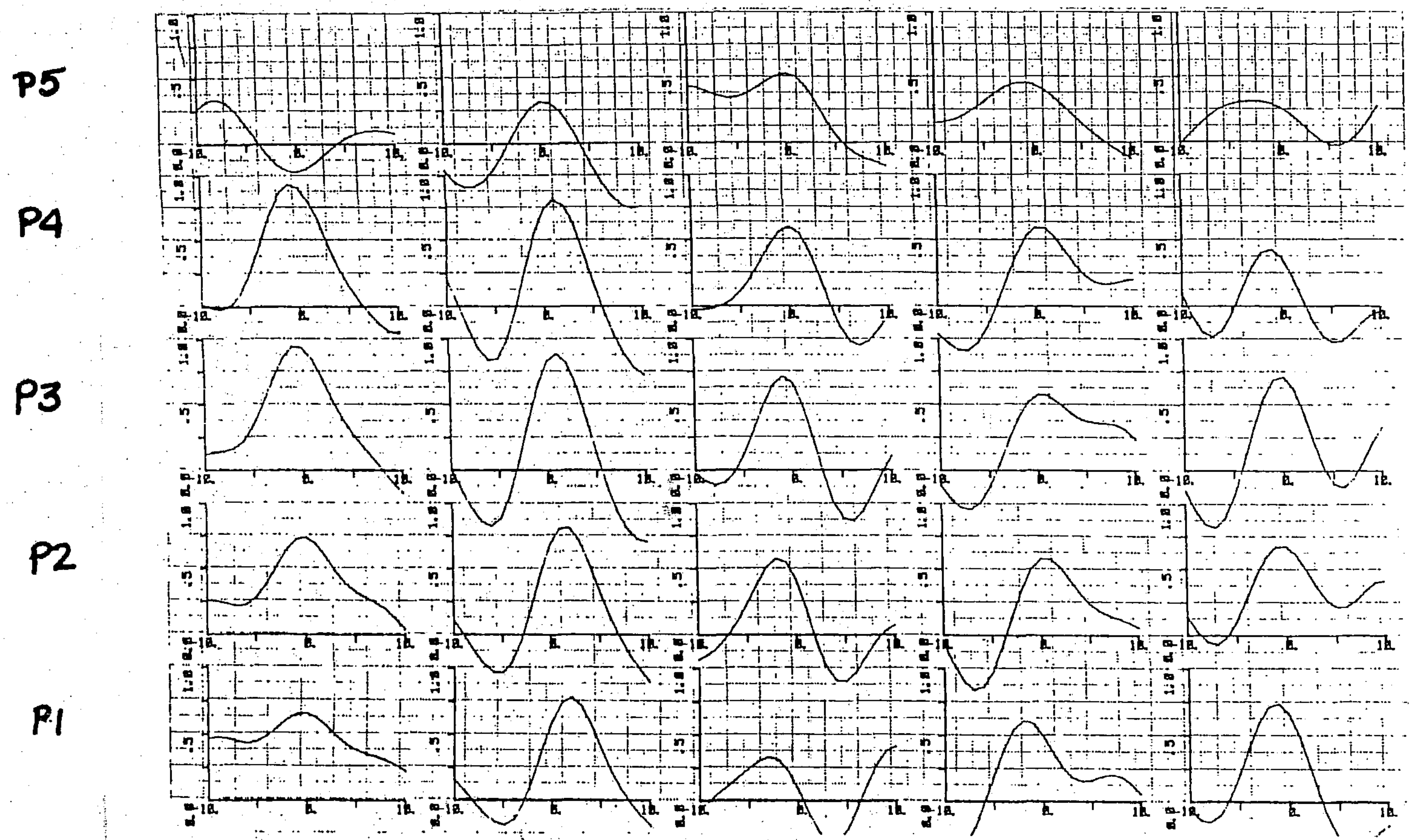

T2P1/T1PX, T3P1/T2PX, T4P1/T3PX, T5P1/T4PX, T6P1/T5PX

I.67 I271 PING # 04 RANGE (166 - 246) TIME CROSS-CORRELATION

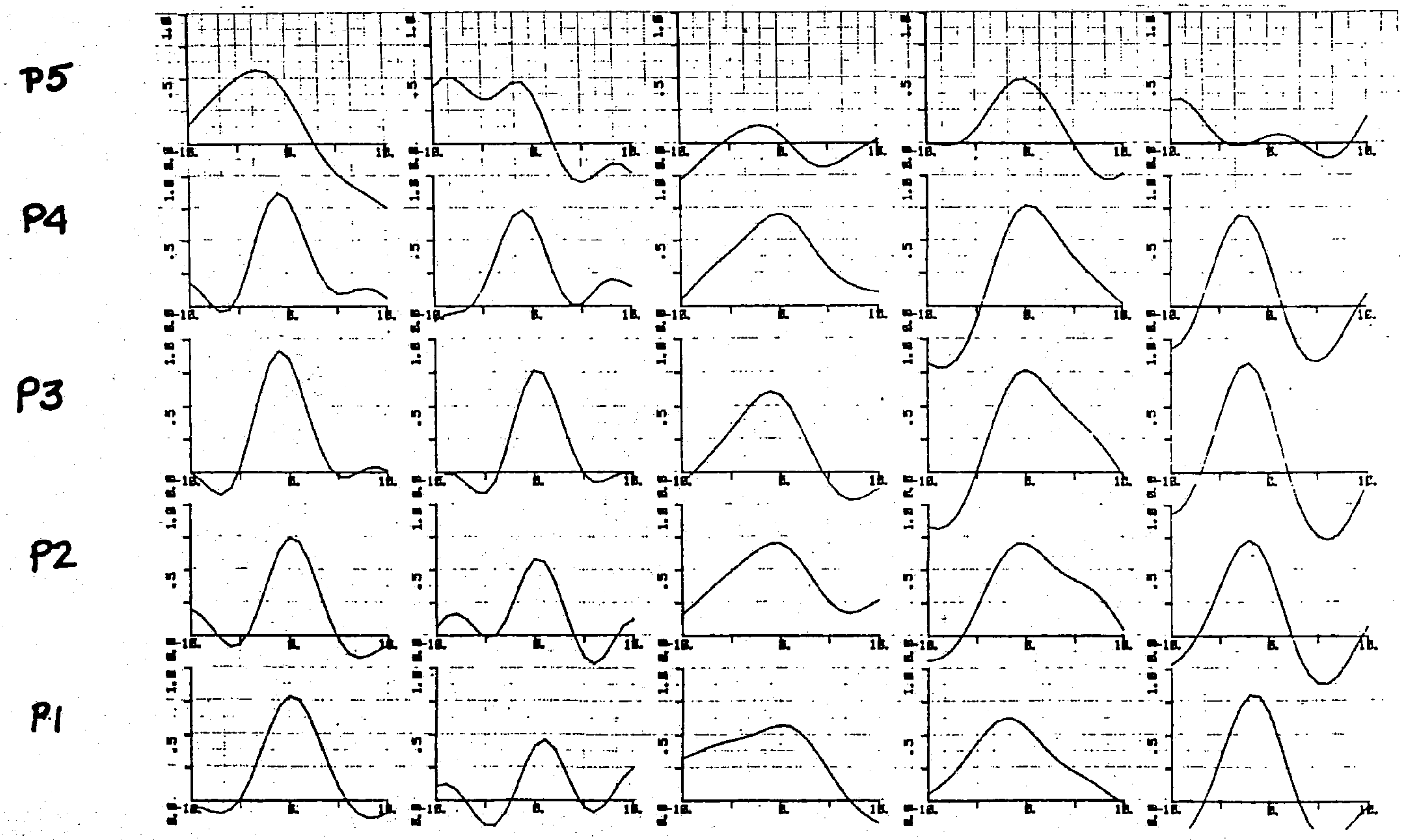

T2P1/T1PX, T3P1/T2PX, T4P1/T3PX, T5P1/T4PX, T6P1/T5PX

I.68 I271 PING # 05 RANGE (166 - 246) TIME CROSS-CORRELATION

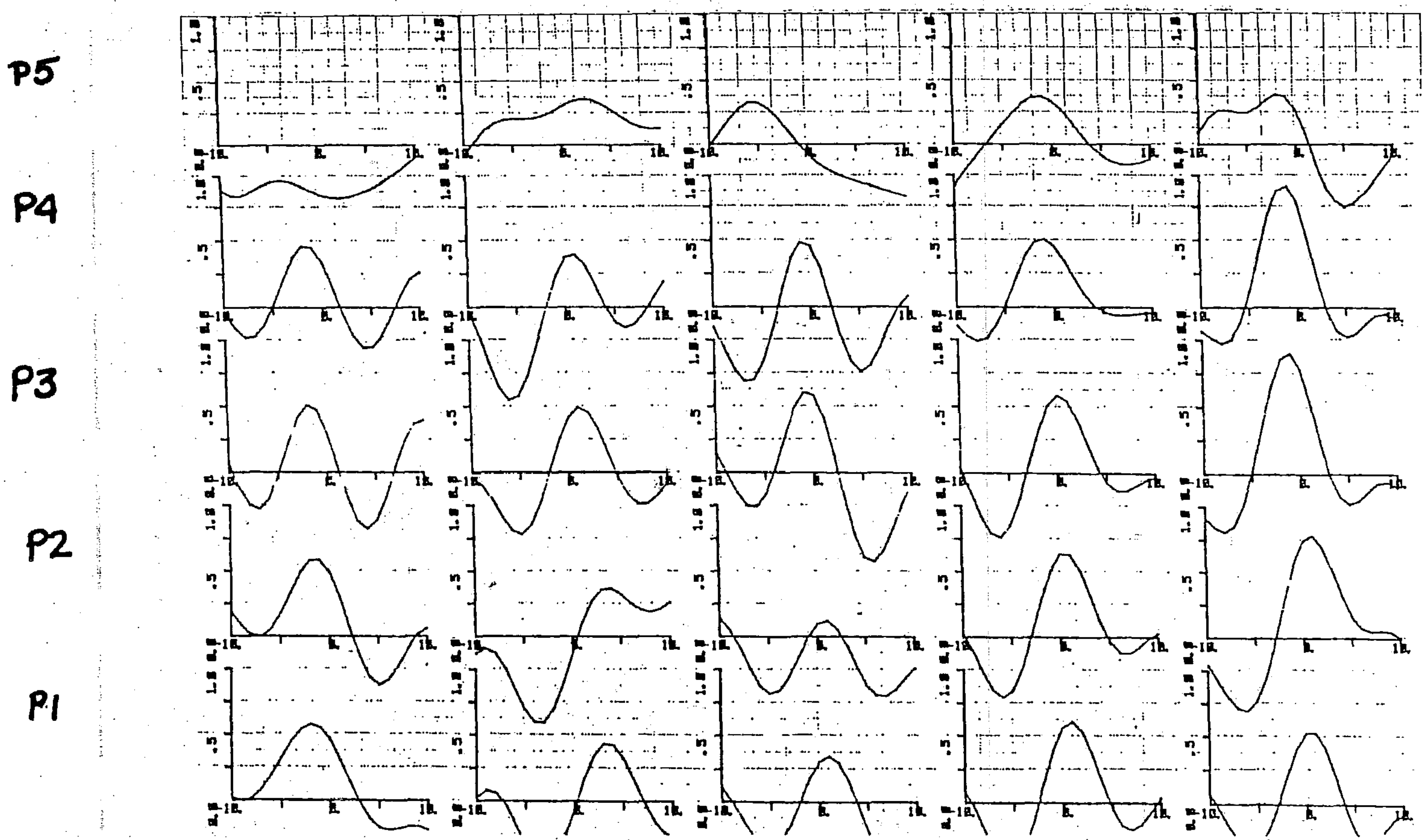

T2P1/T1PX, T3P1/T2PX, T4P1/T3PX, T5P1/T4PX, T6P1/T5PX

I.69 I271 PING # 06 RANGE (166 - 246) TIME CROSS-CORRELATION

COL	ROW	TMAX	CROSS-CORRELATION
1	1	-.0006	.6599
1	2	-.0011	.7428
1	3	-.9962	.9467
1	4	-.9977	.9343
1	5	-3.0003	.3405
2	1	1.9990	.7803
2	2	1.9949	.8140
2	3	.9990	.8902
2	4	1.0015	.8123
2	5	.0012	.3177
3	1	9.9128	.4191
3	2	-1.9980	.5785
3	3	-.9989	.7102
3	4	-.0006	.5909
3	5	.0002	.5255
4	1	-1.9982	.6125
4	2	.0032	.5824
4	3	.0011	.5742
4	4	.0022	.5854
4	5	1.0001	.4540
5	1	-1.0028	.7404
5	2	-.0023	.6753
5	3	-.0047	.7078
5	4	-1.0016	.4253
5	5	-3.0000	.3022

COL	ROW	TMAX	CROSS-CORRELATION
1	1	.0023	.7867
1	2	.0034	.7501
1	3	-.9966	.9144
1	4	-.9967	.8716
1	5	-3.0000	.5681
2	1	.9988	.4605
2	2	.0054	.5791
2	3	.0078	.7652
2	4	-1.0014	.7351
2	5	-8.0014	.5070
3	1	.0001	.5768
3	2	-.0009	.6991
3	3	-.9998	.6125
3	4	-.0002	.7065
3	5	-1.9999	.1362
4	1	-1.9998	.6305
4	2	-.9983	.7019
4	3	.0001	.7698
4	4	.0019	.7738
4	5	-.0010	.4886
5	1	-1.9957	.8021
5	2	-1.9996	.7302
5	3	-2.0026	.8273
5	4	-2.9959	.6933
5	5	-9.0012	.3421

I271 PING # 06 (RANGE 166 - 246)
T2P1/T1PX, T3P1/T2PX, T4P1/T3PX, T5P1/T4PX, T6P1/T5PX

COL	ROW	TMAX	CROSS-CORRELATION
1	1	-1.9996	.5832
1	2	-1.0049	.5925
1	3	-1.9956	.5136
1	4	-1.9958	.4580
1	5	9.9968	.1017
2	1	3.0041	.4365
2	2	3.9991	.3690
2	3	1.0023	.4927
2	4	.9966	.3963
2	5	2.0002	.3565
3	1	.9996	.3474
3	2	.9975	.1437
3	3	-.9930	.6050
3	4	-.9925	.4814
3	5	-5.0010	.3245
4	1	.9977	.6154
4	2	.0078	.6378
4	3	.0020	.5876
4	4	-1.0010	.5094
4	5	-1.0006	.3697
5	1	.9928	.5327
5	2	.9973	.7896
5	3	-1.0062	.9028
5	4	-1.0063	.9162
[illegible]	[illegible]	[illegible]	[illegible]

I271 PING # 07 (RANGE 166 - 246)
T2P1/T1PX, T3P1/T2PX, T4P1/T3PX, T5P1/T4PX, T6P1/T5PX

COL	ROW	TMAX	CROSS-CORRELATION
1	1	-8.0010	.4369
1	2	-7.0004	.3829
1	3	-5.9998	.3842
1	4	9.9907	-.1369
1	5	9.9758	.2422
2	1	-1.0000	.5476
2	2	2.0011	.4355
2	3	9.9343	.3665
2	4	-7.0029	.5510
2	5	9.9933	.1553
3	1	-6.9994	.5560
3	2	9.9845	.2083
3	3	-1.9994	.2646
3	4	1.9999	-.0208
3	5	6.0001	-.1094
4	1	9.8458	.5554
4	2	2.0000	.5632
4	3	10.0001	.0402
4	4	9.9919	.1435
4	5	-5.0000	.3909
5	1	-3.9997	.3913
5	2	-4.0478	.2837
5	3	8.0002	.5322
[illegible]	[illegible]	[illegible]	[illegible]

I.71 I271 PING # 4 (RANGE 166-246) T2P1/T1PX, T3P1/T2PX, T4P1/T3PX, T5P1/T4PX, T6P1/T5PX

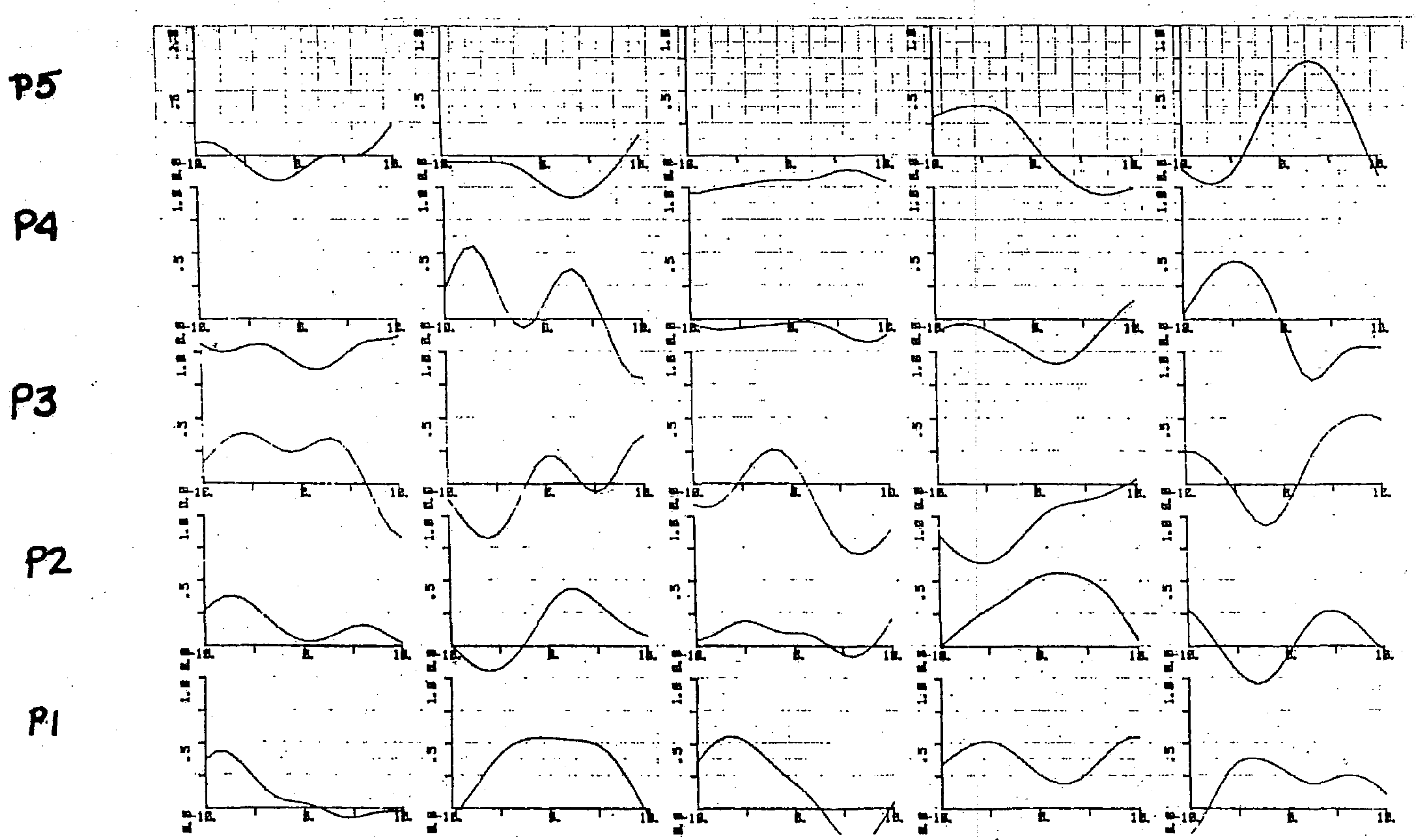

T2P1/T1PX, T3P1/T2PX, T4P1/T3PX, T5P1/T4PX, T6P1/T5PX

I.70 I271 PING # 07 RANGE (166 - 246) TIME CROSS-CORRELATION

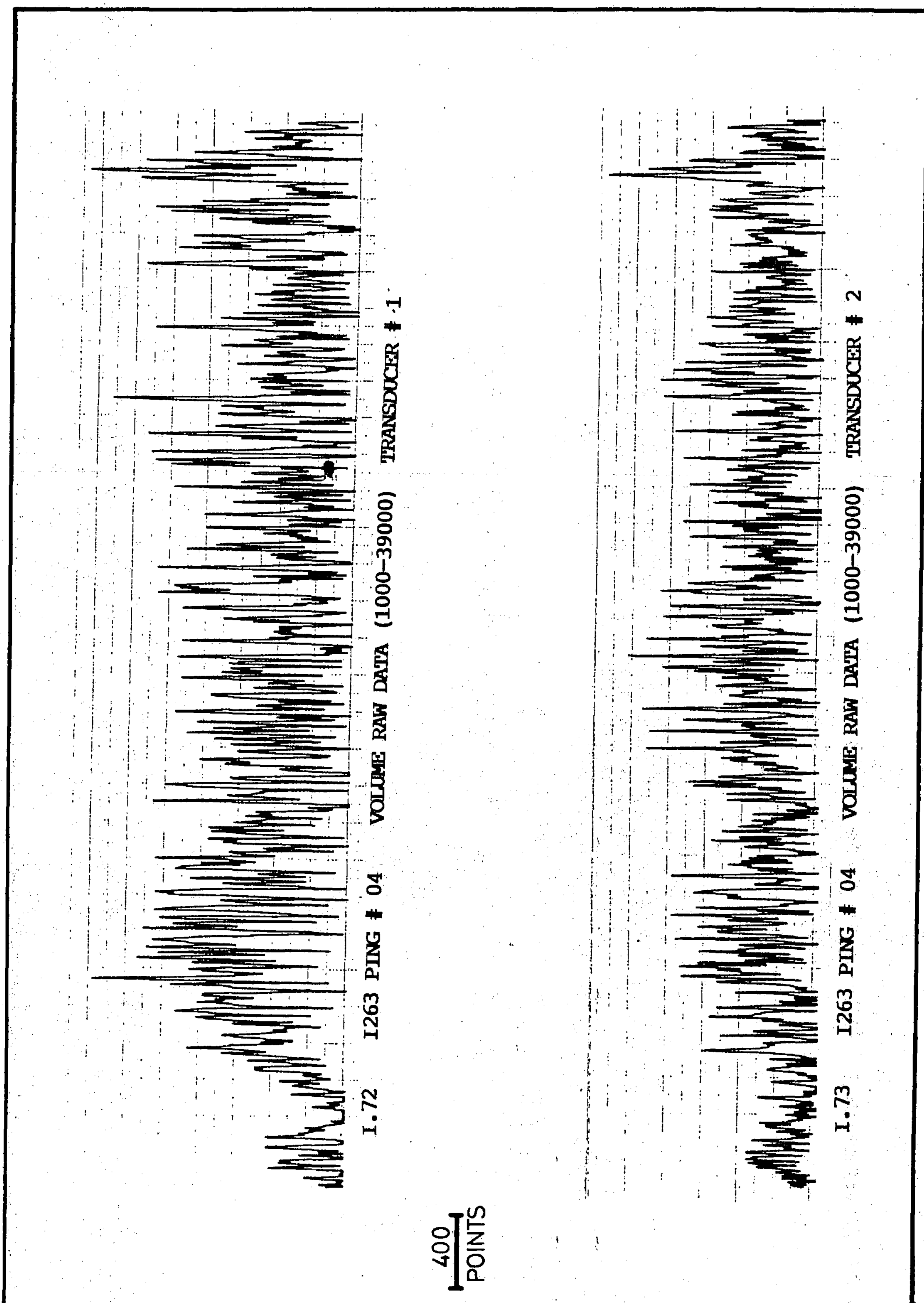
I.72 I263 PING # 04 VOLUME RAW DATA (1000–39000) TRANSDUCER # 1
I.73 I263 PING # 04 VOLUME RAW DATA (1000–39000) TRANSDUCER # 2
400 POINTS

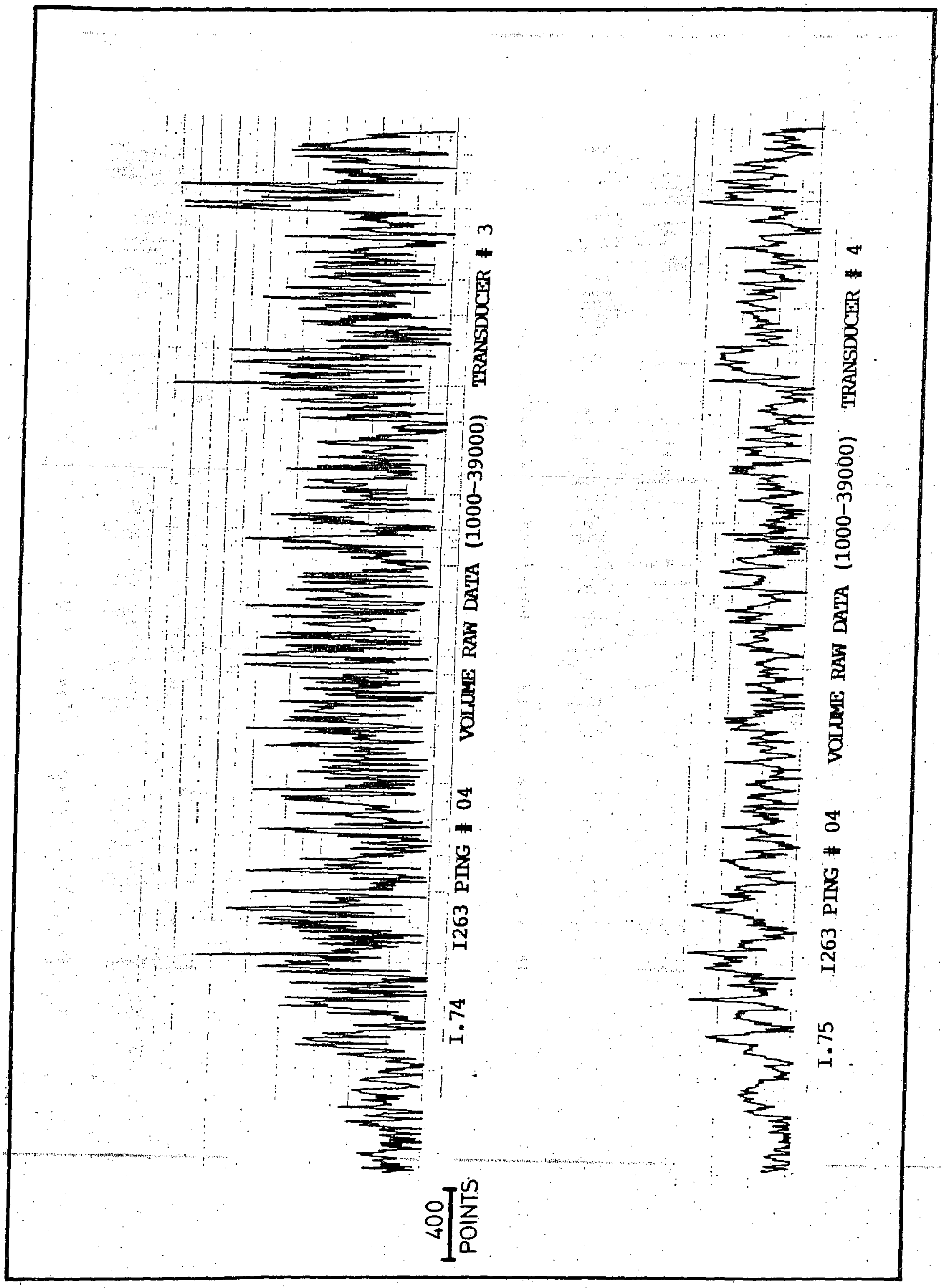
I.74 I263 PING # 04 VOLUME RAW DATA (1000-39000) TRANSDUCER # 3
I.75 I263 PING # 04 VOLUME RAW DATA (1000-39000) TRANSDUCER # 4
400 POINTS

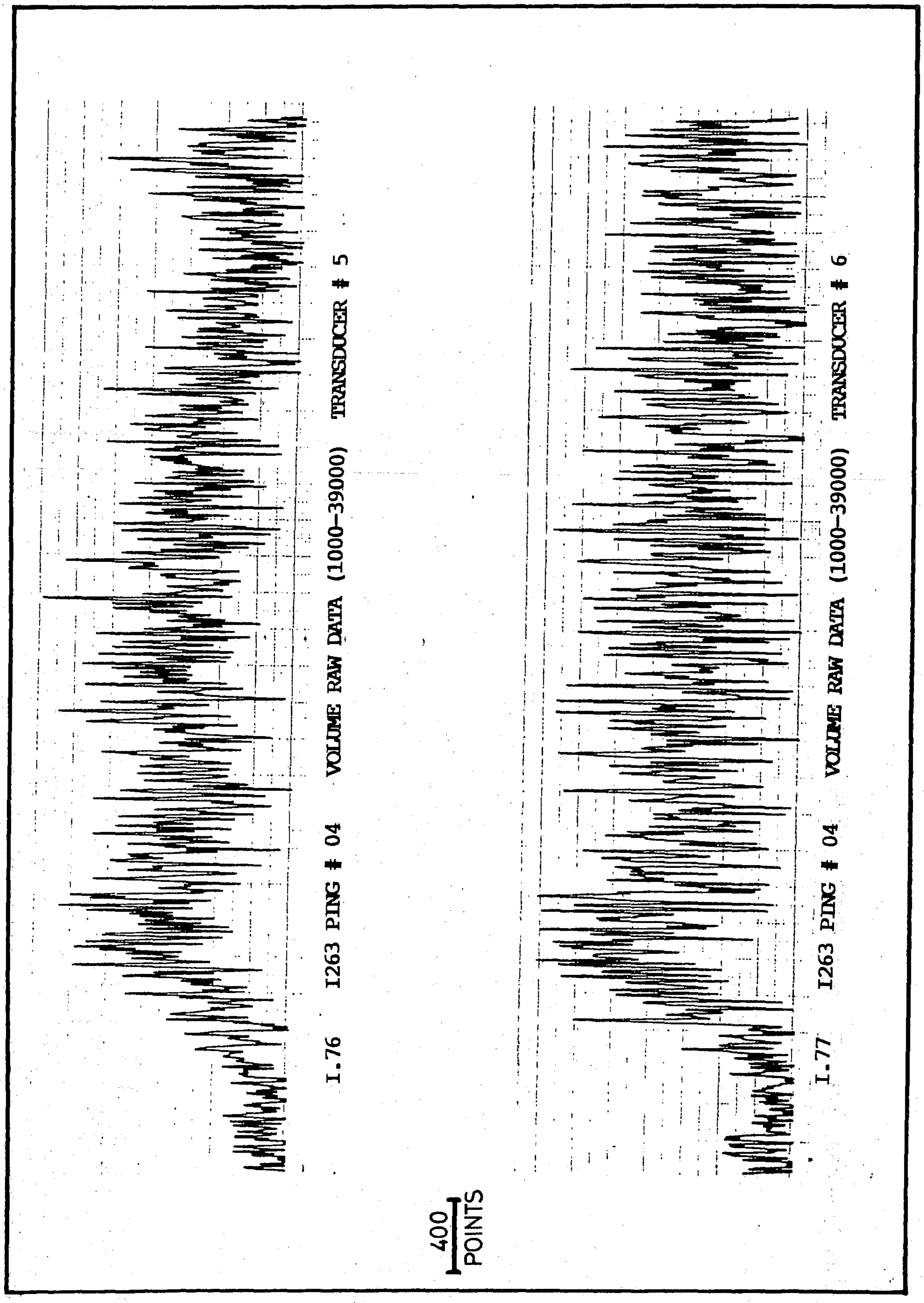
I.76 I263 PING # 04 VOLUME RAW DATA (1000-39000) TRANSDUCER # 5
I.77 I263 PING # 04 VOLUME RAW DATA (1000-39000) TRANSDUCER # 6
400 POINTS

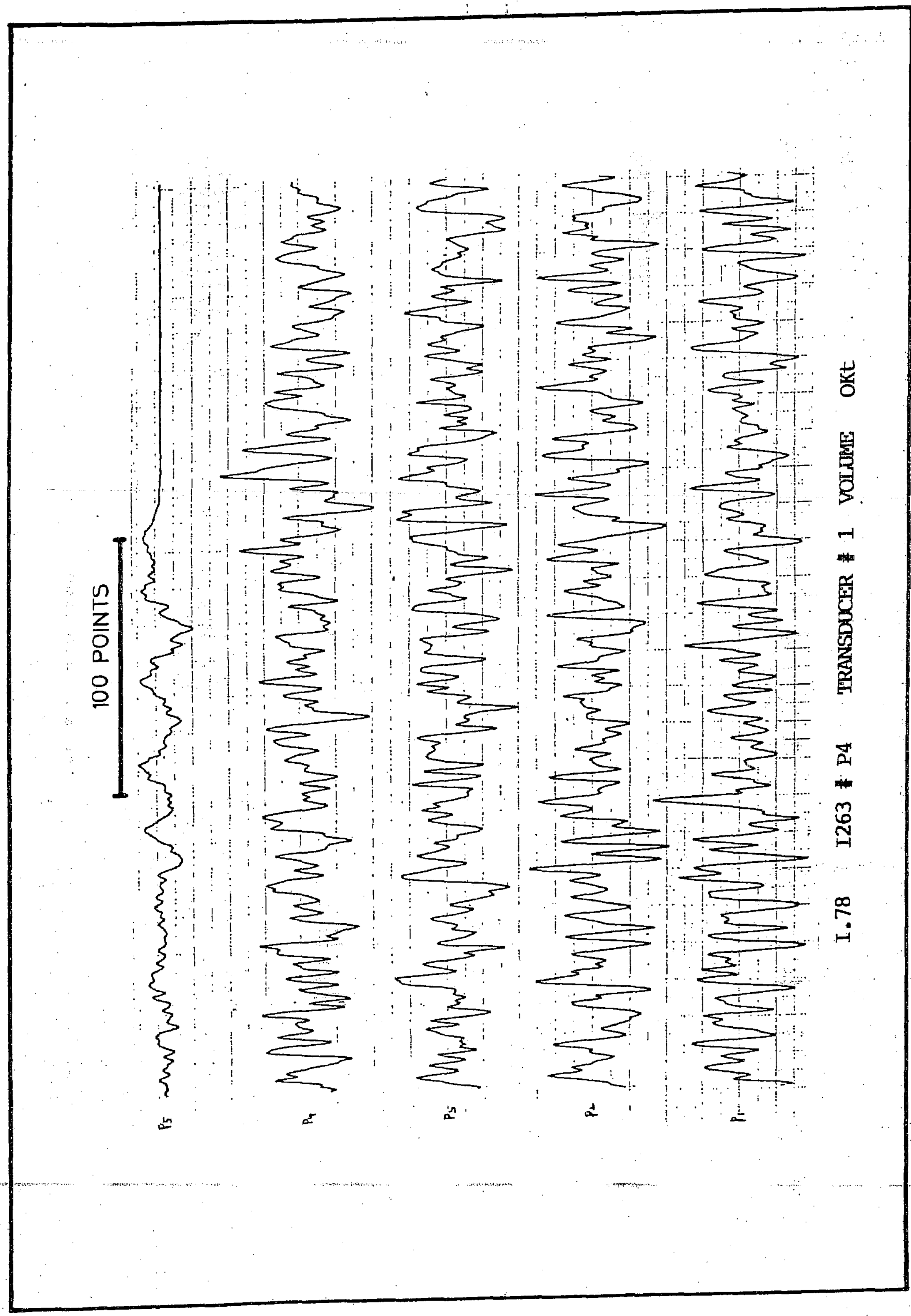
100 POINTS
I.78 I263 # P4 TRANSDUCER # 1 VOLUME OKt

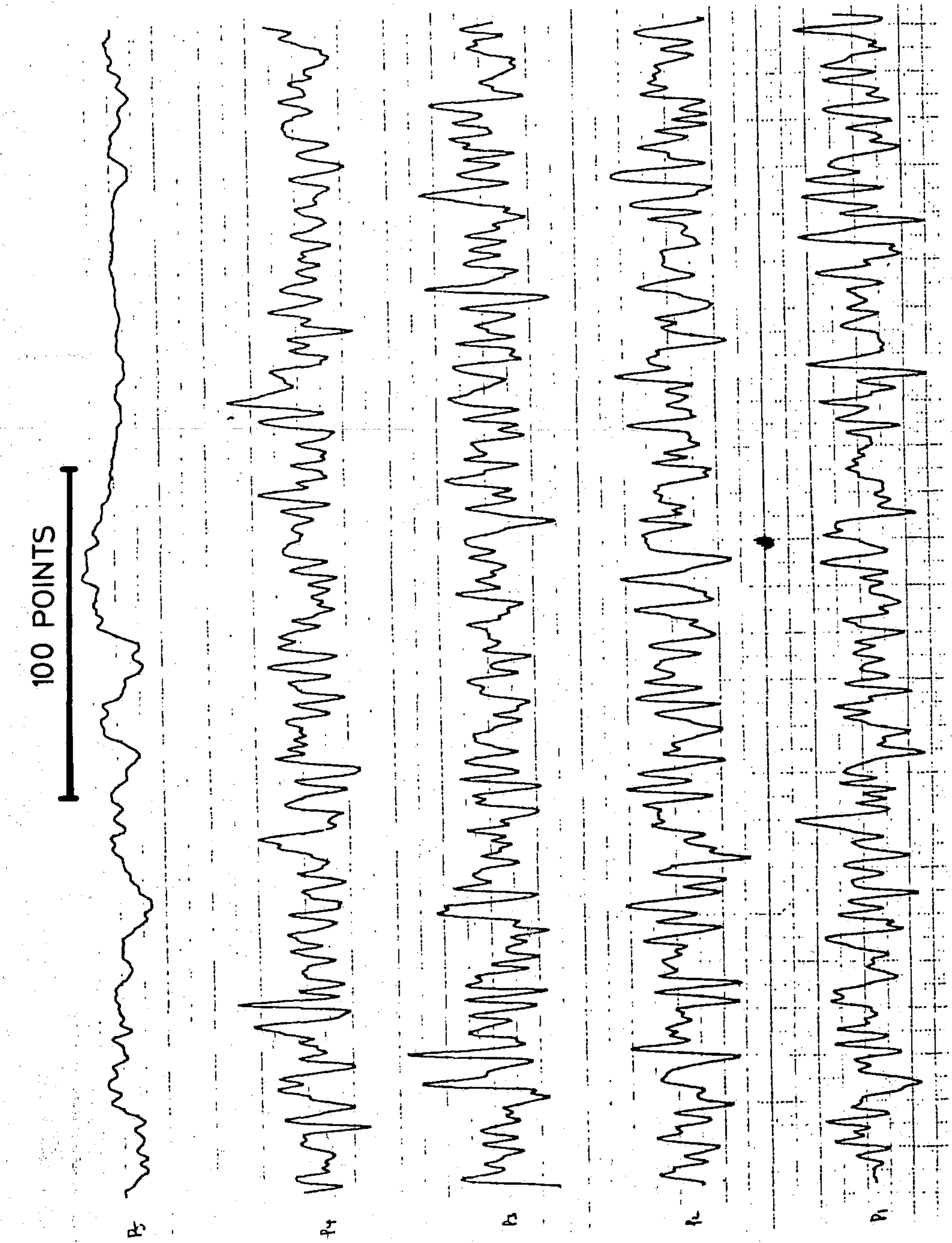

I.79 I263 # P4 TRANSDUCER # 2 VOLUME OKt

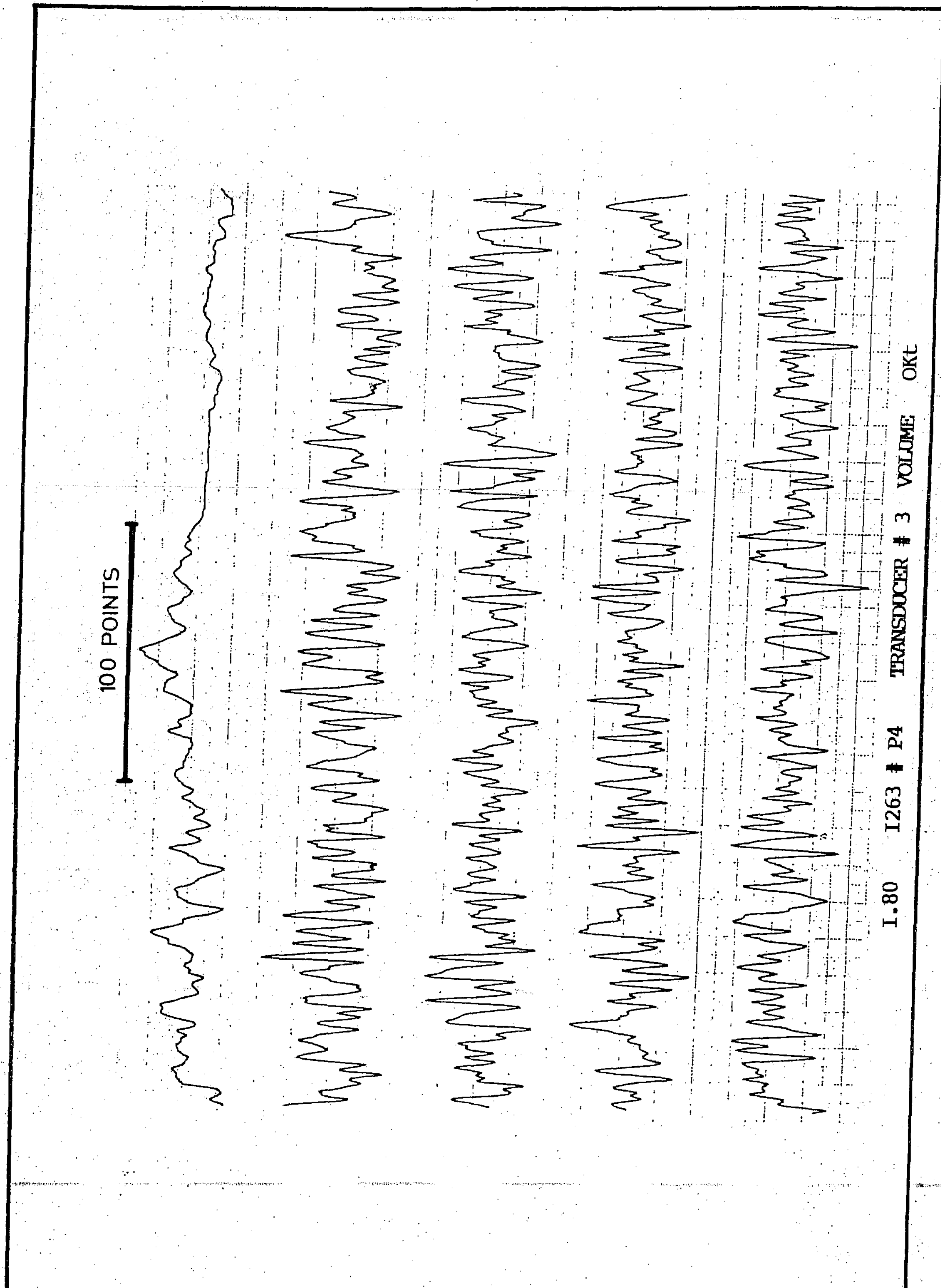
100 POINTS
I.80 I263 # P4 TRANSDUCER # 3 VOLUME OKt

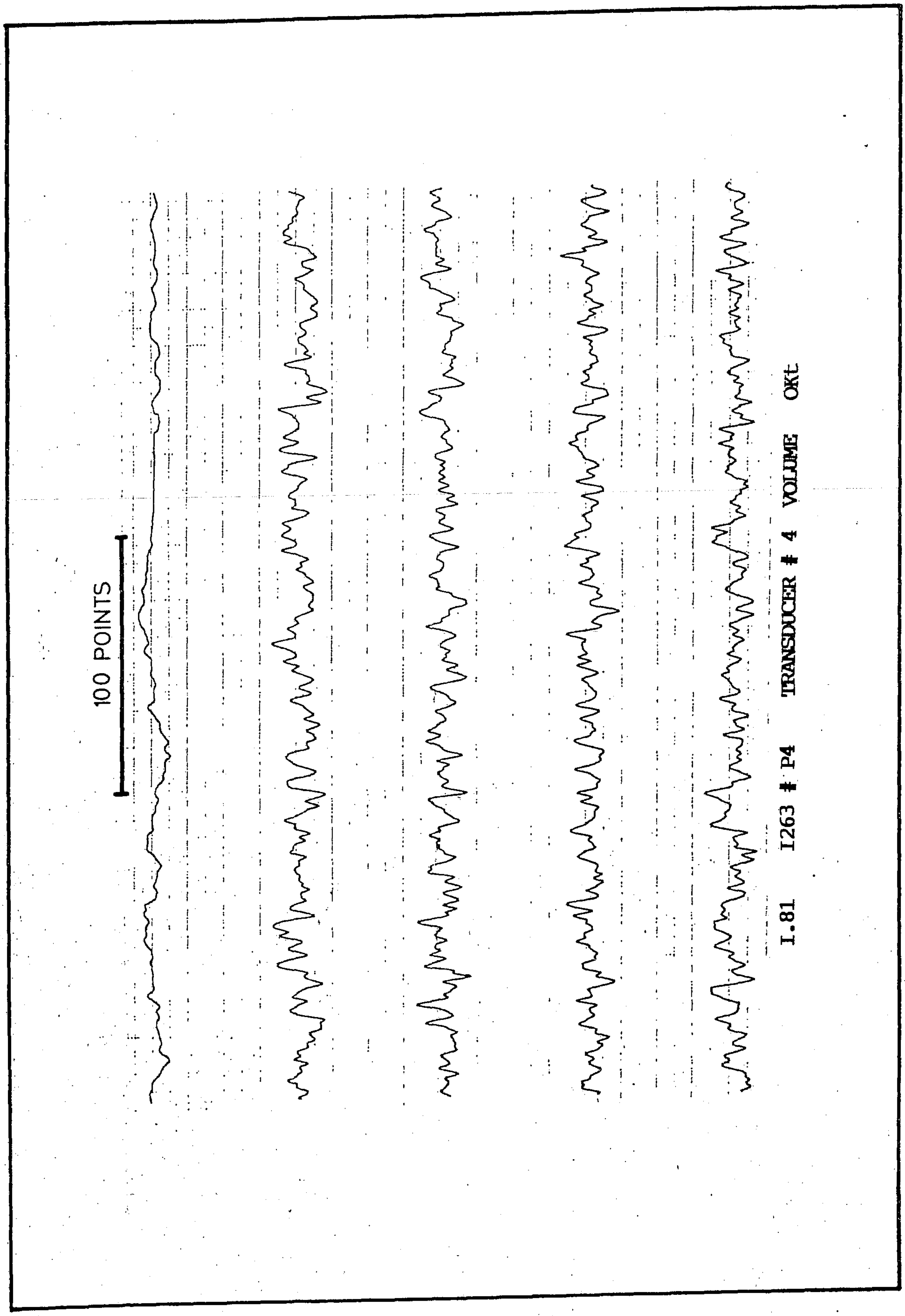
100 POINTS
I.81 I263 # P4 TRANSDUCER # 4 VOLUME OKt

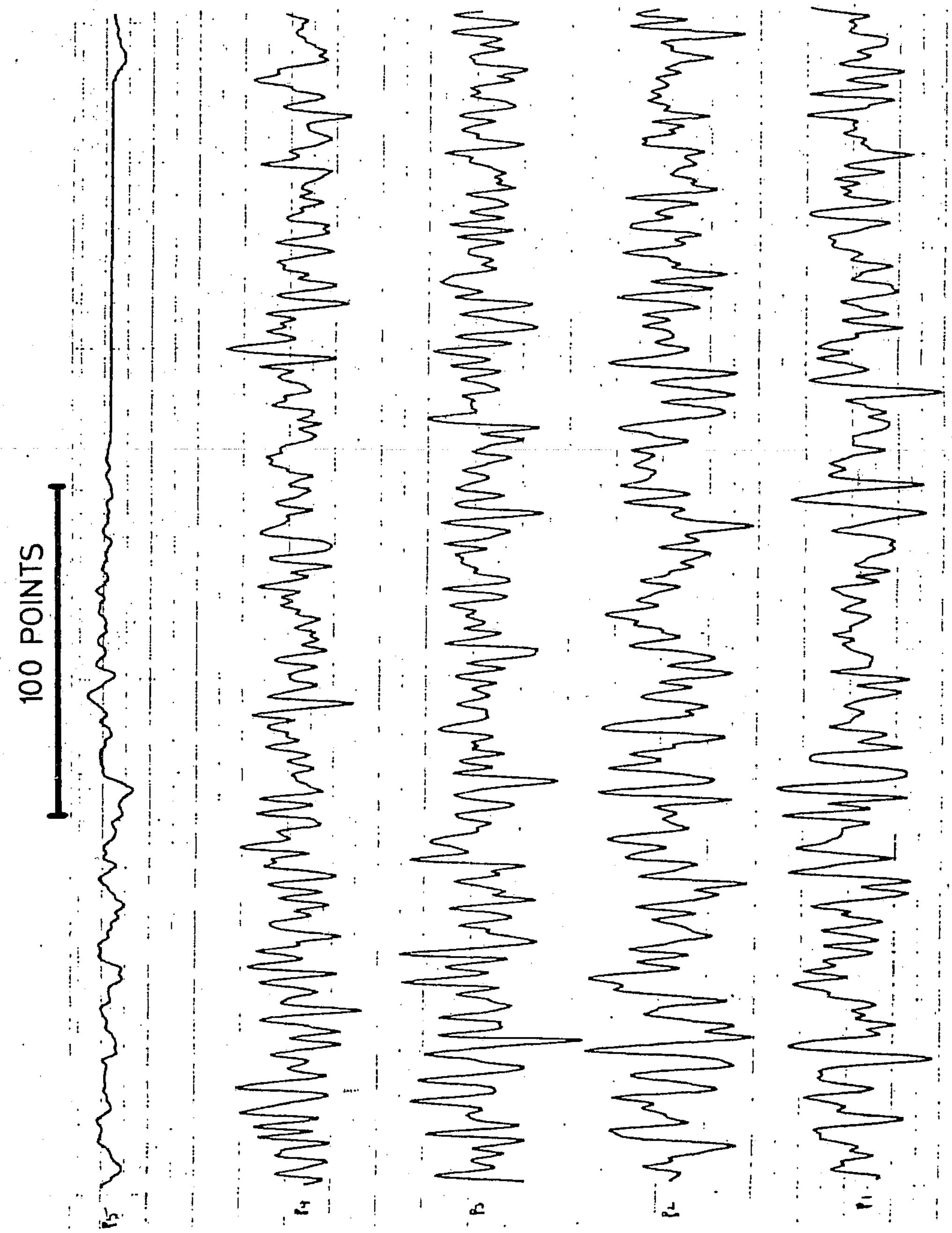

I.82 I263 # P4 TRANSDUCER # 5 VOLUME OKt

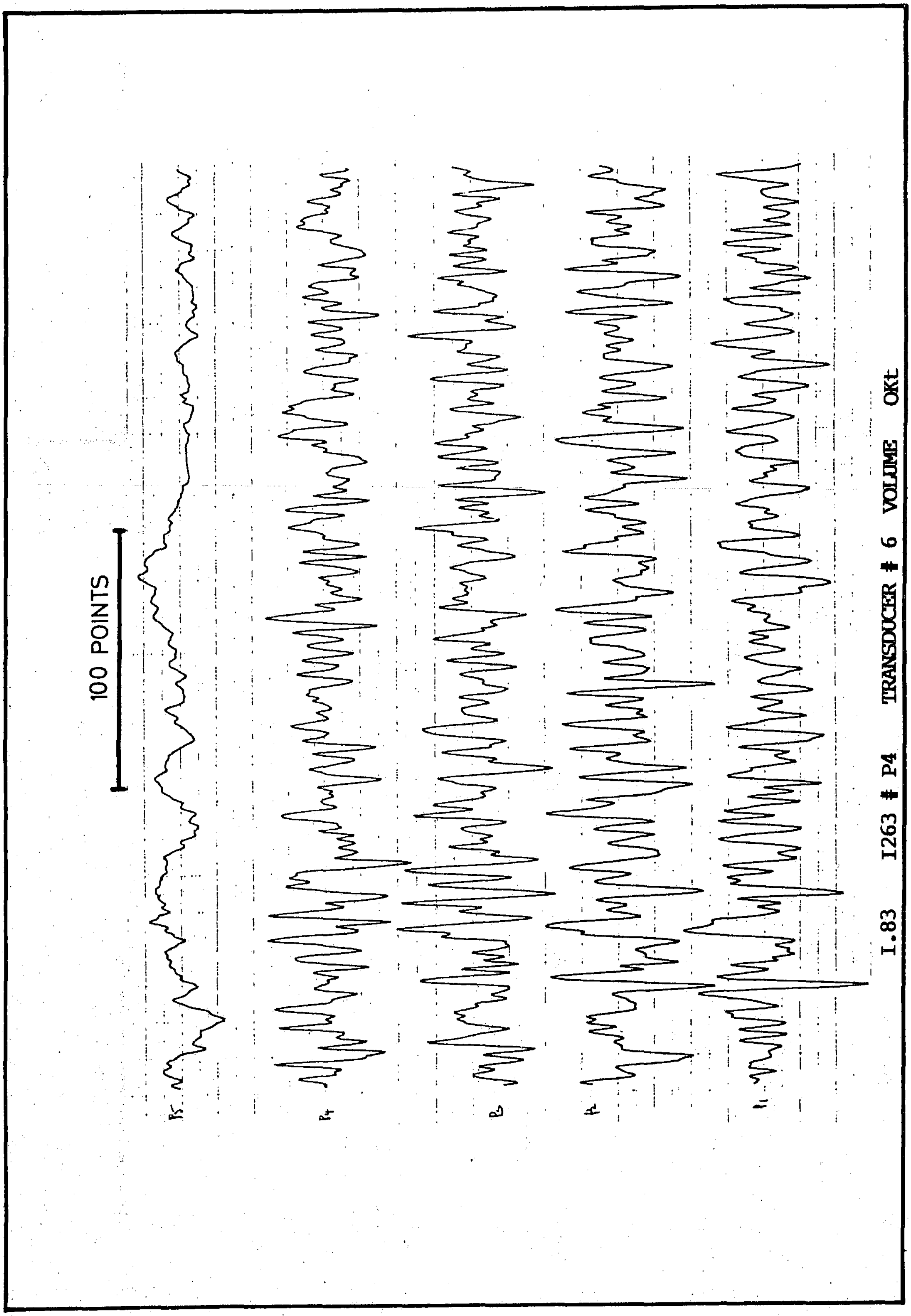
100 POINTS
I.83 I263 # P4 TRANSDUCER # 6 VOLUME OKt

P1&2, P2&3, P3&4, P4&5 160 POINTS

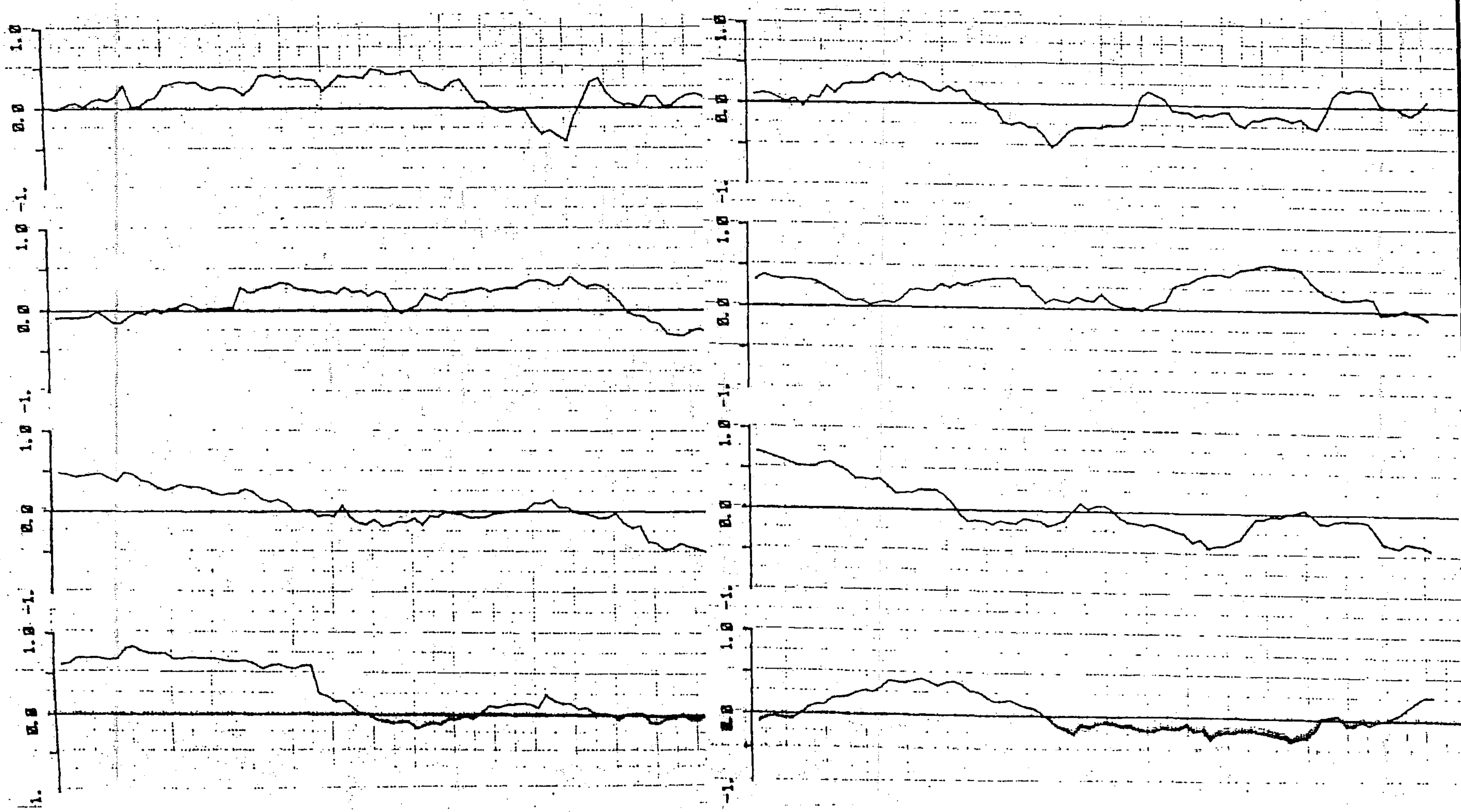

I.84 I263 PING # 4 VOLUME RETURN TRANSDUCER #1

I.85 I263 PING # 4 VOLUME RETURN TRANSDUCER #2

P1&2, P2&3, P3&4, P4&5 160 POINTS

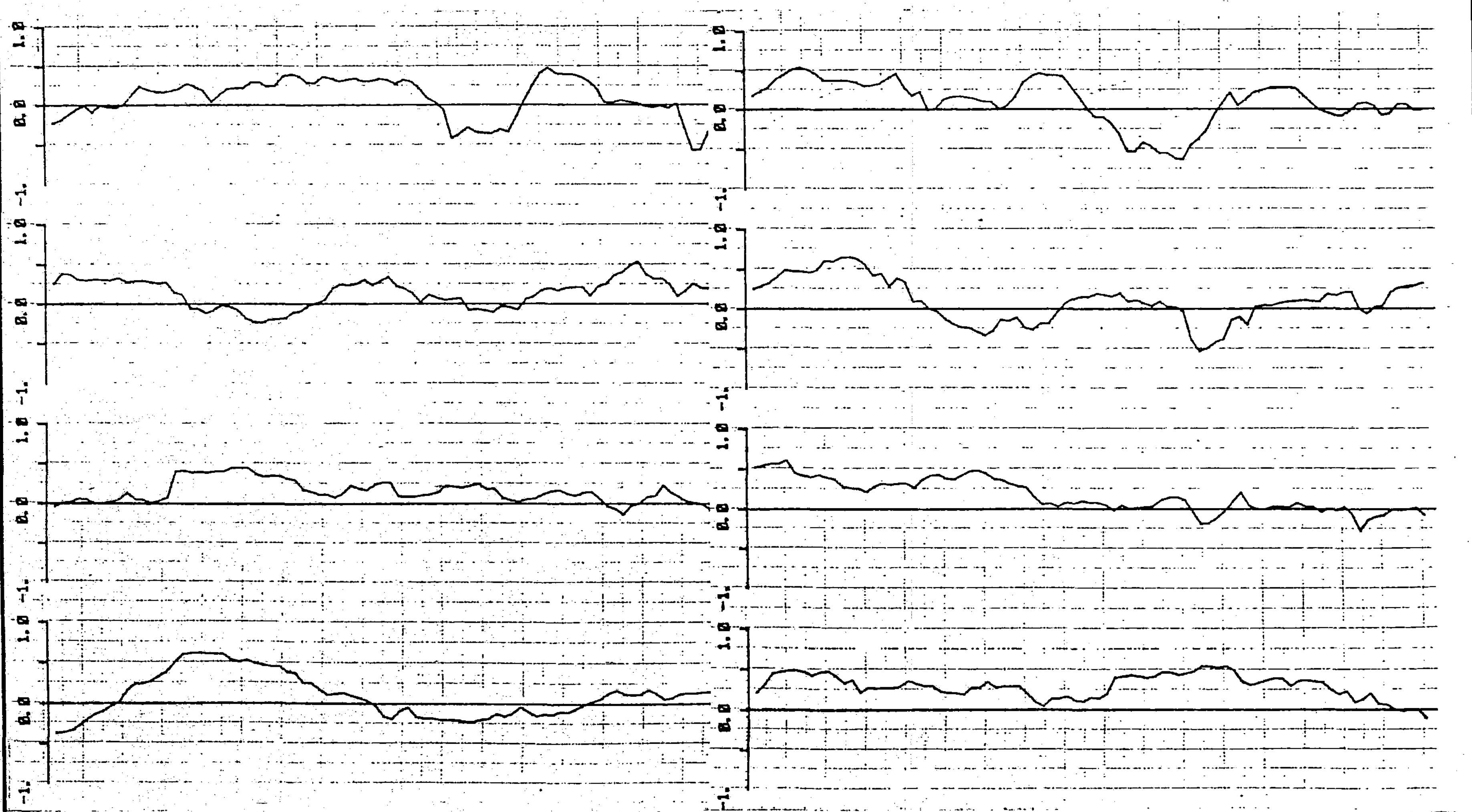

I.86 I263 PING # 4 VOLUME RETURN TRANSDUCER #3 I.87 I263 PING # 4 VOLUME RETURN TRANSDUCER #4

P1&2, P2&3, P3&4, P4&5 160 POINTS

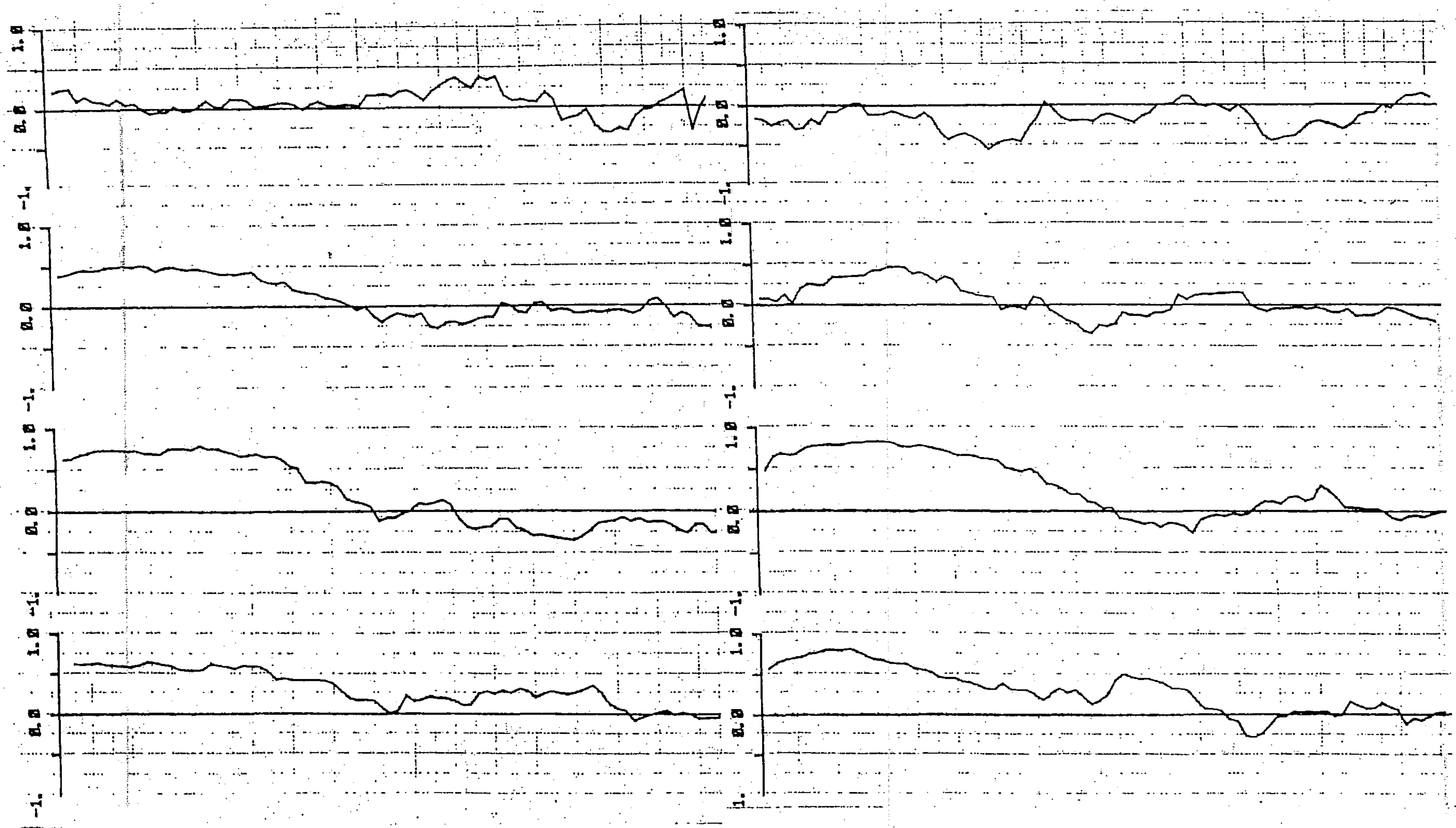

I.88 I263 PING # 4 VOLUME RETURN TRANSDUCER #5

I.89 I263 PING # 4 VOLUME RETURN TRANSDUCER #6

PI&2, P2&3, P3&4, P4&5 160 POINTS

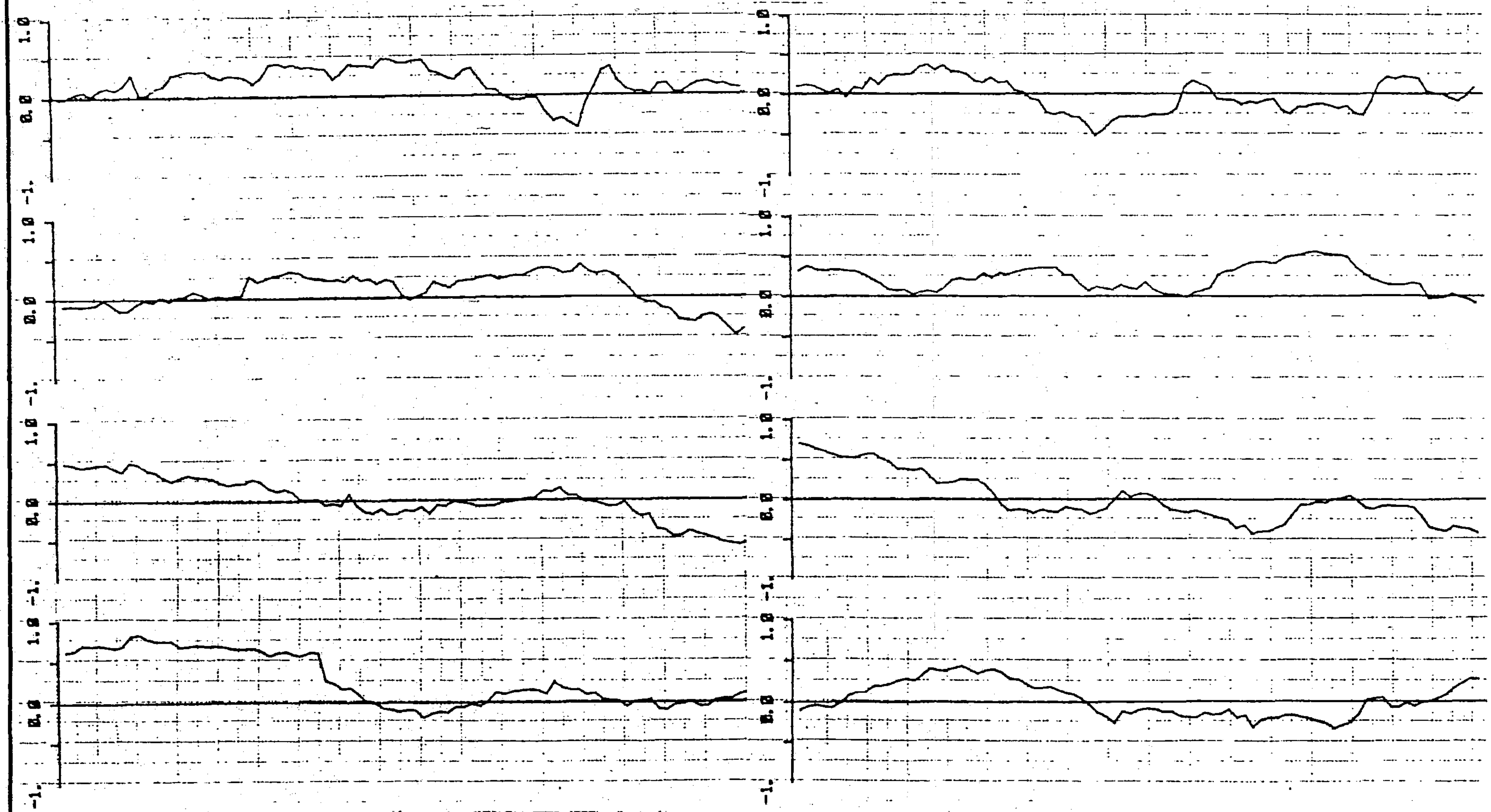

I.90 I263 PING # 4 VOLUME RETURN TRANSDUCER #1

I.91 I263 PING # 4 VOLUME RETURN TRANSDUCER #2

P1&2, P2&3, P3&4, P4&5 160 POINTS

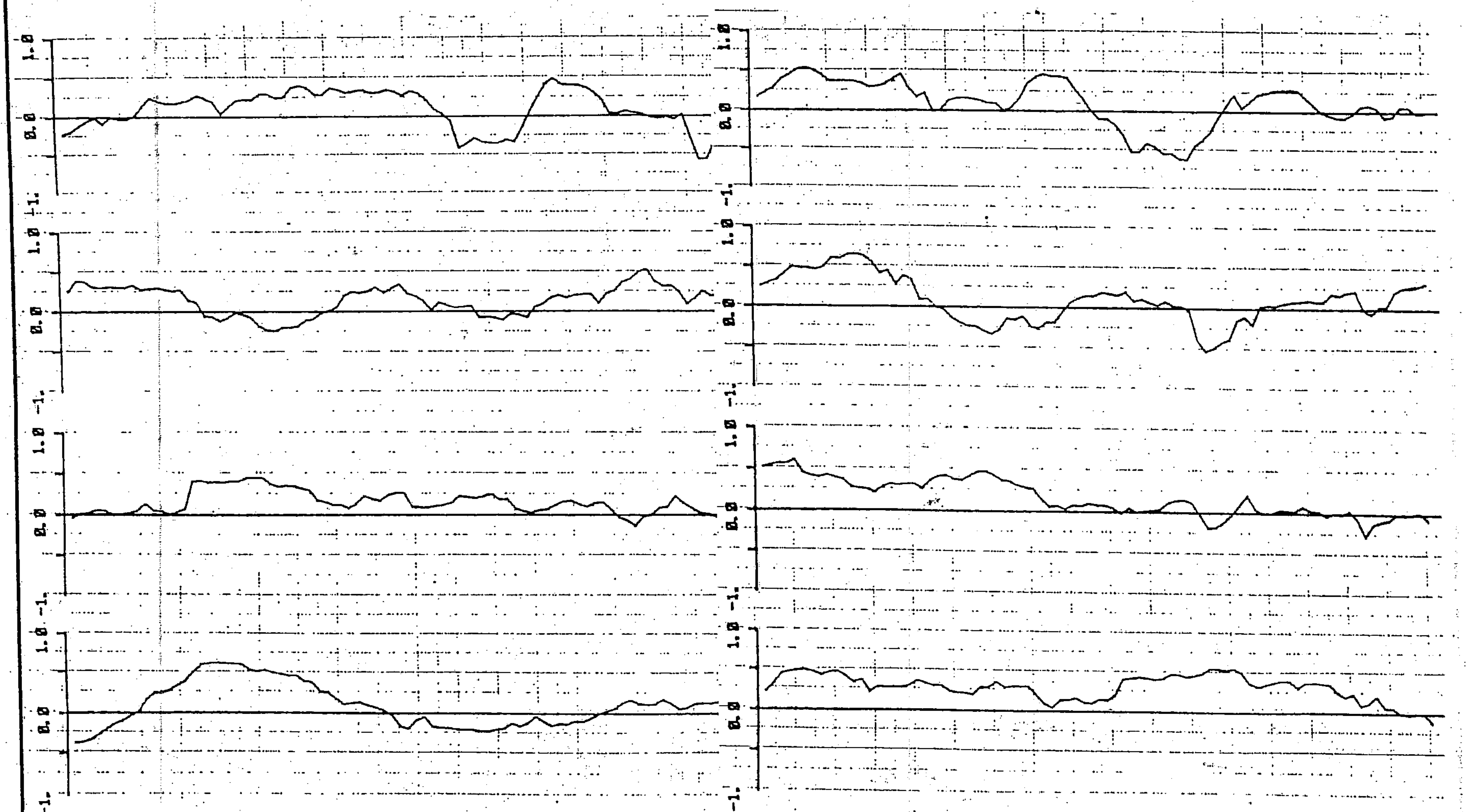

I.92 I263 PING # 4 VOLUME RETURN TRANSDUCER #3 I.93 I263 PING # 4 VOLUME RETURN TRANSDUCER #4

P17&2, P2&3, P3&4, P4&5 160 POINTS

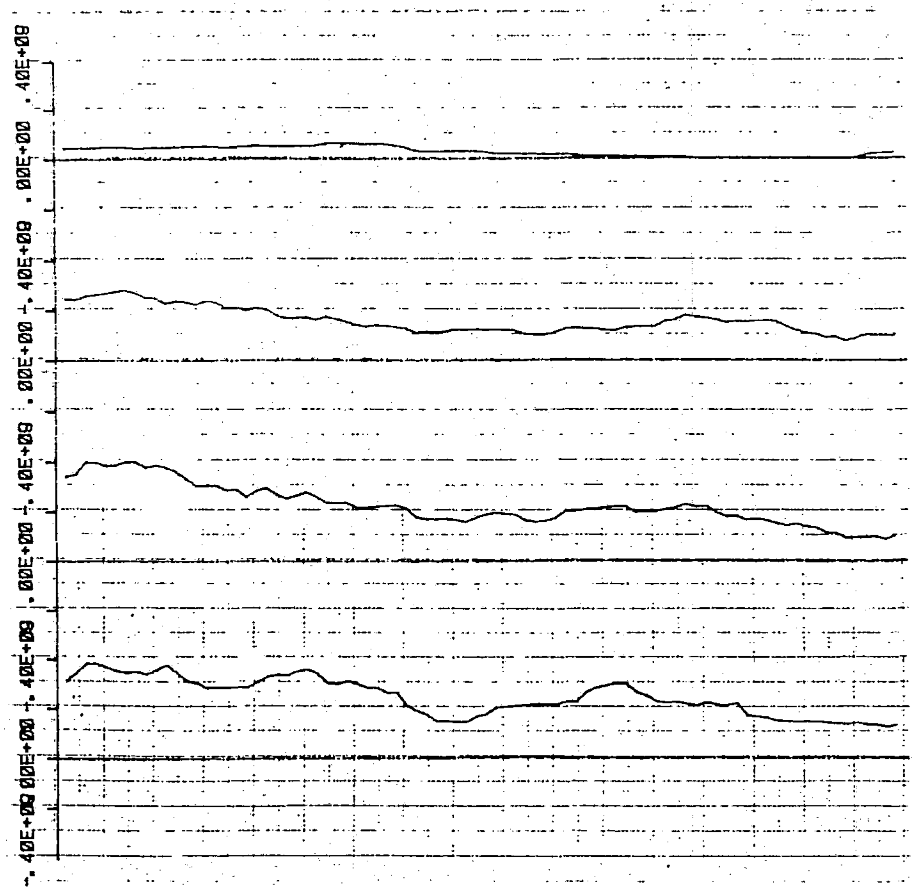

I.94   I263 PING # 4 VOLUME RETURN TRANSDUCER #5

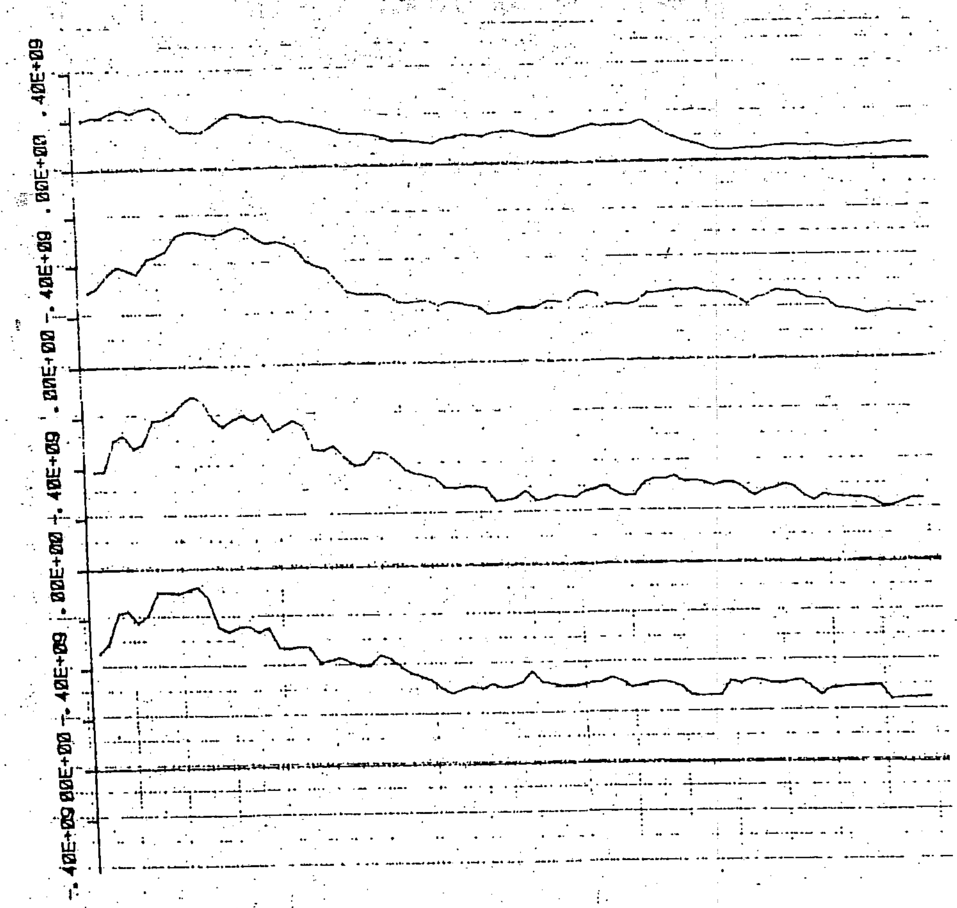

I.95 I263 PING # 4 TRANSDUCER #6 P1&2, P2&3, P3&4, P4&5 "DENOMINATOR"